RICE UNIVERSITY
Houston, Texas

Final Report

A FUNDAMENTAL STUDY OF SUBLIMATION THROUGH A POROUS SURFACE

Prepared For
NASA Manned Spacecraft Center
Houston, Texas

Contract NAS 9-7969

FINAL REPORT

A FUNDAMENTAL STUDY OF SUBLIMATION

THROUGH A POROUS SURFACE

Contract NAS 9-7969

Prepared for

NASA Manned Spacecraft Center
Houston, Texas

by
Rice University
Houston, Texas

Alan J. Chapman
Principal Investigator
July 30, 1971

TABLE OF CONTENTS

LIST OF TABLES AND FIGURES

NOMENCLATURE

A_j area of jth segment ft^2

c_p specific heat of heater fluid, BTU/lb$_m$-°R

D pore diameter, ft.

ℓ melting interface location within a pore, ft.

g_o acceleration of gravity, ft/hr^2

G_z^+ reciprocal Graetz number, dimensionless

h heat transfer coefficient, BTU/hr-ft^2-°F

I ice thickness in the water chamber, ft.

k thermal conductivity, BTU/hr-ft-°R

k_{pe} equivalent conductivity of plate filled with water, BTU/hr-ft-°R

L distance from plate outlet to position at triple point pressure, ft.

m number of pore diameters in a plate

$\dot{m}$ mass flow rate in a pore, #$_m$/sec.

$\dot{M}$ total mass flux, #$_m$/sec.

n number of pores per unit area of a given diameter

N_u Nusselt number, dimemsionless,

P_a ambient pressure (vacuum chamber pressure), psf

P_r Prandtl number, dimemsionless,

P porosity, void fraction

q heat flux, BTU/hr-ft^2

R_a Rayleigh number, dimensionless,

S sublimation interface location within a pore, ft.

t time, sec.

T absolute temperatute, °R

T_f freezing point temperature, °R

T_{hf} heater fluid bulk temperature, °R

T_o heater plate temperature, °R

T_p porous plate entrance temperature, °R

U thermal conductance, BTU/hr-ft^2-°R

$\dot{W}$ mass flow rate of heater fluid, lb$_m$/hr.

α thermal diffusivity, ft^2/hr.

δ thickness of water chamber, ft.

ΔH_f latent heat of fusion BTU/lb$_m$

ΔH_s latent heat of sublimation BTU/lb$_m$

Θ porous plate thickness, ft.

λ mean free path, ft.

μ dynamic viscosity, #$_m$/hr-ft.

ρ density, #$_m$/ft^3

σ surface tension, #/ft.

Subscripts

e evaporation

f fusion

I ice

ℓ liquid

mm mixed mode

p porpous plate

s sublimation

tp triple point

w water

SUMMARY

The principal modes of operation for a porous plate
sublimator-evaporator are defined and analyzed. This
includes analysis of the sublimation mode, evaporation
mode, mixed mode, and a newly hypothesized cyclic sublimation
mode. The physical properties which govern the operation of
each mode are investigated and analytical expressions are
derived to allow prediction of operating modes and tempera-
tures. These equations are derived by relating the heat and
mass flow relations. For the mass flow through the porous
plate to be expressed explicitly, simplifying assumptions
were made concerning the porous structure of the porous
plate. The plate is assumed to consist of a known number of
pores of known size.

Because of the pressure and temperature range involved
and the small size of the pores, the flow through the porous
plate is in the free molecular regime. This allows the
pressure drop through a pore to related to the mass flow and
pore size by the Knudsen equation.

An experimental investigation was performed to verify
and aid in the development of the mode models. This investi-
gation utilized uniformly heated modular units. A description
of the apparatus used and test procedure used for these modular
units is presented. The experimental results at various heat
flux rates are presented and good correlation with predicted
values is indicated.

The verified analyses are then incorporated into a
performance analysis scheme applicable to sublimator units

heated by a circulating fluid loop - a situation typical
of current application. An additional test program was
carried out for such fluid-heated systems, and the experi-
mental results discussed. Again, good agreement with the
theoretical predictions is obtained.

INTRODUCTION

Porous-plate boiler-sublimators have been used as heat rejection devices for spacecraft systems. The basic concept is that of providing a heat sink by evaporating or subliming an expendable substance into the vacuum of space. Carry-over of the expendable material to space is prevented by imposing a porous plate of suitable pressure drop characteristics between the expendable supply and space. Present practice uses water as the expendable and it is either evaporated, or frozen and subsequently sublimed, through the porous surface. The heat to be rejected is transferred to the water by the cooling of a circulating coolant stream. These basic elements of a boiler-sublimator are illustrated in the schematic sketch of Fig. 1.

Three basic modes of operation of such devices have been hypothesized. The <u>sublimation</u> mode is that in which an ice layer forms on the inside surface of the porous plate (the liquid being supplied to that side) and sublimation occurs at the ice-plate interface. For sufficiently low external back pressures and heat rejection loads, the pressure drop of the vapor flowing through the porous plate is low enough that the pressure at the inner plate surface is below the triple point -- resulting in sublimation of the ice at that interface. The thickness of the ice layer formed is dependent upon the heat rejection rate and the pressure drop of the vapor flowing through the plate. The supply water freezes at the water-ice interface at the same rate at which sublimation occurs, producing a "flow" of ice between the liquid phses and the porous plate.

At higher heat rejection rates and at higher back pressures, it is possible that pressures throughout the water feed and porous plate system will be above the triple point pressure, and no ice will form. For appropriate feed pressures and porous plate characteristics, the liquid will be retained at some location within the plate. Cooling is then provided by evaporation of the liquid, and the heat rejection

is regulated by the liquid and vapor pressure-drops in the plate. This mode of operation is termed the evaporation mode.

When the evaporative mode exists, or when conditions are favorable for its existence, feed pressures of the expendable water may inadvertantly be applied which exceed the water retaining capabilities of the plate pores. In such instances liquid breakthrough may occur in which unevaporated liquid is carried over to space, representing a loss of cooling capacity.

A mixed mode of operation of a sublimator has been hypothesized (Reference 1). In this mode it is theorized that the random distribution of pore size and shape found in commercially available porous plates causes a transition to the evaporative mode in certain pores (the smaller ones first), as the heat load increases, while other portions remained covered by ice as in the sublimation mode. Thus a mixture of the evaporative and sublimative mechanisms may occur. It is further hypothesized that the average effect produced is that of a mean plate temperature at, essentially, the triple point temperature. The work reported herein indicates that such a mixed mode is unlikely to occur in practice and that a more realistic model is provided by the cyclic mode proposed here for the first time.

The mixed mode described above can occur only when the porous plate material is non-wetting and, hence those pores operating in the evaporative mode restrain the liquid at the upstream interface. However, most commercially available porous plate materials are wetted by water. In this instance when the vapor pressure drop through a pore is greater than the triple point pressure, water will enter the pore. The water will flow into the capillary to the point at which the pressure drop through the remainder of the pore is below the triple point pressure -- at which time it will freeze. The ice thus formed will then sublime and receed back into the pore until the pressure rises above the triple point end the resulting liquid begins, again, to flow toward the low

pressure end and the entire cycle repeated. This process of the water flowing part way into the pore, freezing, subliming back, melting, and flowing again has been named the cyclic mode and is analysed in some detail in this work. This cyclic model proposed here is verified by the experimental work also reported herein and explains the "constant" porous plate temperature previously observed in sublimators operating at the higher heat flux ranges and erroneously identified as the "mixed mode."

The work described in subsequent portions of this report is divided into two main phases. The first phase, described in Part A considers a uni-dimensional model of a sublimator -- one in which the heat source is considered to be a surface of uniform temperature and heat flux rather than the fluid heated source depicted in Figure 1. By this means, one may direct attention to the basic physical mechanisms taking place without the additional problem of longitudinal temperature gradients. All physically possible sublimation-evaporation modes are described, analysed, and reduced to working formulas. Wetting and non-wetting plates are considered as are plates with uniform pore sizes and non-uniform pore sizes. Those modes which are then likely to occur in practice are then scrutinized experimentally by a series of modular, electrically heated, tests, and certain conclusions drawn.

Subsequently, in Part B, the verified analyses of the uni-formly heated units of Part A are incorporated into an analysis which represents a prototype sublimator system in which the heat source is a circulating coolant -- introducing longitudinal temperature gradients. An additional test program for such systems is described and the results discussed.

PART A

Modular, Uniformly Heated, Sublimator Units

The physical setup for a functioning sublimator is shown
in Figure 1. The heated surface between the coolant and water will
have a longitudinal temperature gradient since the temperature of the
coolant will be reduced as it flows through the sublimator. The
behavior of a functioning system can be understood only if the basic
local heat transfer mechanism is known. Hence, in the analysis which
follows, the heat source is represented as a heated plate which is
assumed to have a constant temperature in steady state operation. The
heat flux into this surface is then constant over the whole surface
and assumed to be of known value. The physical models which result
from these assumptions and which are subsequently analyzed are shown in
Figures 2 and 3. These figures show the system operating in the subli-
mation and evaporation modes. In each, it is assumed that the heat
flow is one dimemsional across the water plenum and is uniform over
the whole area of the plate. This means that it is assumed there are
no convective currents in the water layer.

First, porous plates in which it is assumed that the pores
are all of the same size are considered and then plates in which the
pore size is non-uniform are studied. In both instances the pores are
presumed to be circular in cross section and perfectly straight.

I. Analysis for a Plate with Uniform Sized Pores

The number of pores per unit area, n, and the diameter of the pores, D, are taken as known quantities. Because of the uniformity of the pore size and heat source temperature, it is assumed that each pore carries the same mass flow rate of vapor. The thermal conductivities of the water and the plate matrix are taken as independent of temperature. The object of the analysis which follows is to relate, for all possible operational modes, the temperatures of the porous and heater plates to the imposed heat load.

Sublimation Mode

For low heat loads and ambient pressures, the pressure drop across the porous plate may be below the triple point pressures of water since the vapor flow rate through a capillary is small. Thus ice is formed on the upstream side of the plate as suggested in Figure 2. This is a characteristic of the sublimation mode. In this mode, heat is transferred across the water and ice layer; then is rejected as the ice sublimates. In steady state operation, water freezes at the water-ice interface at the same rate as the ice sublimates. Thus the total effect is a glacier like flow of ice toward the plate with the ice thickness remaining constant. The temperature at which the ice sublimates is the equilibrium temperature for sublimation corresponding to the pressure build-up from the vapor flow through the pores.

The equations relating the mass and heat flow rates are

$$q_c = \dot{M} \, \Delta H_s \tag{1}$$

and

$$q_c = q_b + \dot{M} \, \Delta H_f \tag{2}$$

For a given heat flow rate $(q_a = q_b)$, the mass rate of flow per unit area can be calculated from (1) and (2), namely

$$\dot{M} = q_b / (\Delta H_s - \Delta H_f) \tag{3}$$

The mass flow through a pore can then be calculated from

$$\dot{m} = \dot{M} / n \tag{4}$$

At the triple point pressure and temperature, the mean free molecular path for water vapor is 6.95×10^{-6} meters. This has been calculated using the kinetic theory relation from Reference 4, namely

$$\lambda = \frac{\mu}{P} \sqrt{\frac{\pi R T}{2 g_o}} \tag{5}$$

For most applications, the diameters of the pores in the porous plate will be from 0.5 to 10 microns. Thus the flow at triple point properties or below may be treated as <u>free molecular</u>.

Kinetic theory analysis has resulted in the so-called Knudsen equation for free molecular flow through a capillary. This equation is (Reference 4)

$$\Delta p = p - p_a = \frac{6 \dot{m} \, \theta}{D^3} \sqrt{\frac{R T}{2 \pi g_o}} \tag{6}$$

The Knudsen equation is used to calculate the pressure at the sublimation interface which is at the entrance to the porous plate. From pressure-temperature equilibrium data for sublimation of water, the temperature at the sublimation interface can be calculated for the known pressure. For the sublimation mode to exist, the pressure at the entrance to the porous plate must be less than the triple point pressure. The sublimation temperature T_s corresponding to this pressure will then be less than the freezing point temperature.

Assuming that the conductivities are constant across the water and ice layer, the heat conduction relation across the ice layer can be written

$$q_a = \frac{k_I}{L} (T_f - T_s) \tag{7}$$

Combining (1) and (2) gives

$$q_c = q_b / \left(1 - \frac{\Delta H_f}{\Delta H_s}\right) \tag{8}$$

Equating (7) and (8) results in the relation

$$I = \frac{k_I}{q_b}(T_f - T_s)\left(1 - \frac{\Delta H_f}{\Delta H_s}\right) \qquad (9)$$

The equation governing heat conduction across the water layer is given by

$$q_b = \frac{k_w}{L}(T_0 - T_f) \qquad (10)$$

Using the relation $L = \delta - I$, this can be solved for T_0, the temperature of the heat source, to obtain

$$T_0 = T_f + \frac{1}{k_w}(q_b \delta - q_b I) \qquad (11)$$

Equation (9) can be used to eliminate $q_b I$ and thus obtain

$$T_0 = T_f + \frac{1}{k_w}\left[q_b \delta - k_I(T_f - T_s)\left(1 - \frac{\Delta H_f}{\Delta H_s}\right)\right] \qquad (12)$$

One criteria which is used to compare porous plates operating in a sublimator under steady state conditions is the heater plate temperature at a given heat flux. For a porous plate with known physical properties (thickness, pore diameter and number of pores per unit area), Equation (12) can be used to calculate the heater plate temperature at a given heat flux. Thus the plate separation (δ) and plate properties can be chosen such that T_0 is at a desired level for a given heat flux. This equation can also be used to give the temperature at heat fluxes away from the design value as long as the system operates in the sublimation mode.

A sublimator is usually designed so that it will not completely freeze at low heat fluxes. If this happens the structural integrity of the unit can be endangered by the expansion of the ice. Equation (9) can be used to obtain the ice layer thickness in a sublimator operating in the sublimation mode. The heat flux at which the unit will be filled with ice can thus be calculated and a minimum safe operating condition established. It should be pointed out again that the sublimation temperature T_s in all of these equations is obtained using sublimation temperature-pressure data and the pressure calculated from (6).

Thus this temperature is a function of the pore properties of the plate and the heat flux.

As the heat flux increases, T_s increases toward the freezing point, and thus the ice layer thickness decreases. The layer disappears when the triple point temperature and pressure is reached at the entrance to the porous plate. The system then enters either the evaporation or cyclic mode as described later.

It is interesting to note that the heat transferred in the sublimation mode depends on the physical properties of the plate (thickness, diameter of pores, and number of pores per unit area) but not on the thermal properties of the plate. This is true because the heat is transferred to the water vapor by the phase change which occurs before the porous plate is reached.

Evaporation Mode

1. Hydrophobic

If the heat flow rate is large enough for the pressure drop across the plate to be greater than the triple point pressure and the water is retained behind the plate, the heat is transferred by evaporation. When the plate materials is non-wetting, the water is constrained behind the plate by surface tension unless the water pressure is greater than the breakthrough value. Thus the relation between heat and mass flow is given by

$$q_b = q_a = \dot{M} \, \Delta H_e \qquad (13)$$

For a given heat flow rate, the mass flow can be calculated and thus the pressure drop through the plate can be calculated from (6). The evaporation temperature T_e can then be calculated from equilibrium temperature-pressure evaporation data. The heater surface temperature can then be calculated using the conduction equation, namely

$$q_b = \frac{k_w}{\delta} (T_o - T_e) \qquad (14)$$

This gives

$$T_o = g_b \frac{\delta}{k_w} + T_e \qquad (15)$$

For a system operating in the evaporative mode, the temperature at the plate entrance will be above the freezing point. The temperature, as stated above can be obtained using (6) for a specified system with known porous plate properties carrying a given heat flux. The temperature of the heated surface must be high enough to allow the heat load to be conducted across the water layer. Equation (15) allows this heater surface temperature to be calculated. The heater surface temperature must be below a certain value or else heat cannot be transferred from the circulating coolant to the water. Thus the above equation can be used to check if an evaporation system is compatable with the circulating coolant part of the heat rejection system.

In actual application, it is undesirable to have a system operating in the evaporative mode due to the increased possibility of breakthrough. This exists because the water must be restrained by surface tension only. In the sublimation mode, the ice layer blocks the pores and prevents breakthrough.

2. Hydrophilic

If the ambient pressure is above the triple point pressure, the water in the porous plate will not freeze. When the plate material is hydrophilic, the water will be constrained at the downstream end of the plate by surface tension unless the water pressure is too high. Breakthrough occurs when the water pressure is above a certain value, and this phenomenon will be analyzed in a later section.

In this mode, the temperature of evaporation can be obtained from equilibrium pressure-temperature evaporation data using the ambient pressure as the evaporation pressure.

The equivalent conductivity of the water-filled plate is given by

$$k_{pe} = k_w P + k_p (1 - P) \qquad (16)$$

This equation is a commonly used representation for the conductivity of a porous material filled with a liquid and was

obtained from References 1 and 9.

The equivalent conductance of the water layer and plate is then expressed as

$$\frac{1}{u} = \frac{\delta}{k_w} + \frac{\theta}{k_{p+e}}$$ (17)

The heat conduction equation gives

$$q_b = u(T_0 - T_e)$$ (18)

This equation can be combined with (17) and solved for the heater plate temperature to obtain

$$T_0 = T_e + q_b\left[\frac{\delta}{k_w} + \frac{\theta}{k_w P + k_p(1-P)}\right]$$ (19)

In this mode the heater surface is seen to depend upon the physical properties of the porous plate, plate separation and heat flux as before. Dependence on the thermal conductivity of the porous plate also exists for this mode of operation because the phase change takes place inside the porous plate. The plate material helps to conduct the heat to the interface where the change of phase occurs.

Given the physical configuration of a sublimator-evaporator and the properties of the porous plate, equations (6) and (19) can be used to predict the operating temperatures of the system for a specified heat flux. These temperatures can be used to judge if the configuration and plate satisfy the requirements of the heat rejection rejection device needed for a certain mission.

Once again it should be pointed out that the evaporation mode is not a desirable mode due to the increased likelihood of breakthrough. For space flight applications it is important to keep the weight of a sublimation unit as low as possible. Thus it is important to get full heat rejection from the water in the sublimation. If breakthrough occurs, either the heat rejection requirements will be unfulfilled or extra weight must be added to the vehicle in the form of extra water. Both of these are very undesirable situations.

Other Modes

For the case of a plate with uniform pore size the "mixed" mode is not possible. The "cyclic" mode proposed here is of such signifigance that it is treated separately in section A.III.

II. Analysis for a Plate with Different Sized Pores

In the analysis of the sublimation and evaporation modes
of operation for a porous plate with variation in pore size presented
here, it is assumed that the number of pores and diameter of each
size is known. The heat flux carried by a pore is assumed to be
proportional to the cross-sectional area of the pore (the area
perpendicular to the direction of heat flow). This is reasonable
since the heat flux is uniform. Because the pores are rather evenly
spaced in most plates, the heat load carried by a pore would be
proportional to its area. Thus, if one pore has twice the area of
another, it will carry twice the heat flux as the other. In this
analysis, m distinct pore sizes will be considered.

Sublimation Mode

The analysis is much the same as for a plate with pores
of one size only. For sufficiently low heat loads, the pressure
drop across the porous plate is below the triple point pressure in
pores of all sizes and thus ice is formed on the upstream side of
the plate. This ice sublimes through the plate with the result that
heat is rejected due to the latent heat of sublimation. For steady
state operation, the supply water freezes at the water-ice interface
at the same at which sublimation occurs. Thus the ice flows between
the water and the porous plate.

The mass flow rate will be made up of the flow rates through
pores of sizes D_1 to D_m, thus

$$\dot{M} = \dot{M}_1 + \dot{M}_2 + \cdots + \dot{M}_m = \sum_{i=1}^{m} \dot{M}_i \tag{20}$$

It can be seen from the sublimation properties given in
Table 2 that the heat of sublimation changes very little with
temperature variations from -40 to 32°F. The sublimation temperature
differences between pores of various sizes will be small for a plate
operating in this mode. Thus it is assumed that the heat of sublimation

is the same for each sized pore. Using this, the relations governing
heat flux and mass flow can be written

$$q_c = \dot{M} \Delta H_s = \Delta H_s \sum_{i=1}^{m} \dot{M}_i \tag{21}$$

and

$$q_c = q_b + \Delta H_f \sum_{i=1}^{m} \dot{M}_i \tag{22}$$

Combining these last two equations gives

$$\dot{M} = q_b / (\Delta H_s - \Delta H_f) \tag{23}$$

Since the number of pores n_i of diameter D_i is known,
using the assumption that heat flow and thus mass flow through a pore
is proportional to the square of the diameter gives the system of
equations

$$\dot{M}_2 = \frac{n_2 D_2^2}{n_1 D_1^2} \dot{M}_1, \quad \dot{M}_3 = \frac{n_3 D_3^2}{n_1 D_1^2} \dot{M}_1, \quad \cdots, \quad \dot{M}_m = \frac{n_m D_m^2}{n_1 D_1^2} \dot{M}_1 \tag{24}$$

These equations can be combined with (23) to obtain

$$\dot{M}_1 = \frac{q_b}{\sum \frac{n_i D_i^2}{n_1 D_1^2}} \cdot \frac{1}{(\Delta H_s - \Delta H_f)} \tag{25}$$

Thus (24) and (25) combine to give the values of the
total mass flow through each size of pore. The mass flow through
each individual pore of size D_i is then given by

$$m_i = \frac{\dot{M}_i}{n_i} \tag{26}$$

The pressure drop across the plate in each pore size
D_i can be calculated from a form of the Knudsen equation given
below.

$$\Delta P_i = P_i - P_a = \frac{6 m_i Q}{D_i^3} \sqrt{\frac{RT}{2\pi g_o}} \tag{27}$$

This equation gives the pressures P_i at the sublimation
point for each pore size since the ambient pressure is known

(vacuum in outer space). From sublimation pressure-temperature data the sublimation temperature T_s can be calculated corresponding to each P_i.

Using the method described above, the temperature at the entrance to each of the pores can be calculated. Since the pore sizes will be randomly mixed over the plate surface, the effective temperature at the porous plate entrance will be some average of all the pore temperatures. Because a large pore rejects more heat and covers a larger fraction of total area of the porous surface than a small pore, the temperature of the large pore should be weighted more in the temperature calculation. The weighting factor which will be used here is the area of a pore divided by the area of all pores. Using this factor, the effective plate temperature is given by

$$T_s = \frac{\sum_i n_i \frac{\pi}{4} D_i^2 T_{si}}{\sum_i n_i \frac{\pi}{4} D_i^2} = \frac{\sum_i n_i D_i^2 T_{si}}{\sum_i n_i D_i^2} \qquad (28)$$

From this point on, the calculation for heater plate temperature T_o and the ice thickness I are the same as when there was only one pore size. The relations given by (9) and (12) are

$$I = \frac{k_I}{q_b} (T_f - T_s)\left(1 - \frac{\Delta H_f}{\Delta H_s}\right) \qquad (29)$$

and

$$T_o = T_f + \frac{1}{k_{ew}}\left[q_a S - k_I \left(1 - \frac{\Delta H_f}{\Delta H_s}\right)(T_f - T_s)\right] \qquad (30)$$

Using the above equations, the performance parameters can be predicted for a given porous plate and sublimator configuration. At a given heat flux, (24), (25) and (26) give the mass flow through the pores of different sizes and (27) relates this mass flow to the pressure drop in each pore. These pressure drops can be related to temperatures, and using (28) the porous plate temperature can be obtained. The above two equations can then be used to calculate the ice thickness in the water chamber and temperature of the heater

surface. This approach can be used to select properties of a porous plate to give a desired heater plate temperature and insure that the sublimator does not freeze at a specified heat load.

Evaporation Mode

1. Hydrophobic

When the plate material is non-wetting, the water is constrained behind the plate by surface tension for water pressures below the breakthrough level. If the heat flow is large enough for the pressure drop in the pores of all sizes to be greater than the triple point pressure, no ice will be present and the heat will be transferred by evaporation. This is basically the same method that the Lister bag uses to keep water cool in dry climates.

The heat of evaporation changes slowly with increasing temperature. Over the range of temperature encountered in the operation of an evaporator, it can be assumed constant. This assumption allows the heat flux and mass flow equation to be given by

$$q_b = q_a = \Delta H_e \sum_{i=1}^{m} \dot{M}_i \tag{31}$$

Combined with relations given by (24), this gives

$$\dot{M}_1 = \frac{q_b}{\Delta H_e} \frac{1}{\sum_i \frac{n_i D_i^a}{n_1 D_1^a}} \tag{32}$$

All of the mass flow rates $\dot{M}_i$ can then be calculated from (24). Using the relations given by (26) and (27), the mass flow and pressure drop through each pore size can be calculated. For a known ambient pressure, the pressure at the evaporation interface in each pore is given. These pressures P_i give the evaporation temperatures T_{e_i} from the evaporation data in Table 3.

The same weighting factor is used in this mode as was used in the sublimation mode to calculate the effective temperature. The expression is given by

$$T_e = \frac{\sum_i n_i D_i^2 T_{ei}}{\sum_i n_i D_i^2} \tag{33}$$

The heater plate temperature is expressed by

$$T_o = q_a \frac{\delta}{k_w} + T_e \tag{34}$$

For a given heat flux, the effective evaporation
temperature of a porous plate is determined by the physical properties
of the plate. The heater plate temperature can be calculated using
(34) when the plate separation distance is specified. Because the
vapor must pass completely through the plate in this mode, the pressure
drop can become very large for large values of heat flux. Under these
conditions, the evaporation temperature can become too high to allow
the evaporator to function as an effective heat rejection device. The
non-wetting characteristic of the plate requires the water to remain
behind the plate and, thus, causes the evaporation temperature to be
high. This hydrophobic characteristic, however, does increase the
breakthrough resistance of the plate.

2. Hydrophilic

If the ambient pressure is above the triple point pressure,
the water will not freeze in the system and the heat will be transferred
by evaporation. For a hydrophilic plate, water will be constrained
at the downstream end of the pores if the water pressure is below the
breakthrough pressure. The evaporation temperature T_{ei} is thus the
same for all pores and can be calculated from equilibrium liquid-vapor
data using the ambient pressure.

The equivalent conductivity of the plate can be expressed
as

$$k_{pe} = k_w P + k_p (1 - P) \tag{35}$$

The equivalent conductance of the water layer and plate
system is given by

$$\frac{1}{u} = \frac{\delta}{k_w} + \frac{\Theta}{k_{pe}} \tag{36}$$

The temperature of the heater plate is then given by the following expression

$$T_0 = T_e + q_b \left[\frac{\delta}{k_w} + \frac{\theta}{k_w \mathcal{P} + k_p (1 - \mathcal{P})} \right] \qquad (37)$$

These relations allow the operating temperatures of a given sublimator to be evaluated at a specified heat flux and ambient pressure. These calculations can be used in a design operation to obtain desired plate properties for specified temperatures.

If the ambient pressure is maintained just above the triple point pressure, the evaporation temperature will be near the freezing point. This is a relatively low sink temperature and should allow the evaporator to operate effectively. Since the water is at the downstream end of the porous plate, however, the water pressure must be kept steady and low to prevent breakthrough.

Mixed Mode

The mixed mode is a special case of operation where some pores are operating in the evaporation mode and the rest in the sublimation mode. For this to occur, the water must not enter the plate. Thus the plate material must be hydrophobic. If this were not true, water would enter the pores, freeze, and initiate the cyclic mode. The mixed mode can occur because there are pores of different sizes. At an appropriate heat load, some pores will operate in the evaporation mode (one such pore having diameter D_1) and some in the sublimation mode (one of these having diameter D_2). Such a case will occur for some intermediate heat flow rate between that for pure evaporation and that for pure sublimation. The water is confined behing the plate by surface tension. for pores in the evaporation mode when the water pressure is below the breakthrough level.

If it is assumed that $\Delta H_e = \Delta H_S - \Delta H_f$ is constant, the mass flow rate for a given heat flow rate is given by

$$\dot{M} = q_b / \Delta H_e \qquad (38)$$

Using (20) and (24) gives

$$\dot{M}_1 = \frac{q_b}{\Delta H_e \sum_i \frac{n_i D_i^2}{n_1 D_1^2}} \tag{39}$$

Knowing $\dot{M}_1$, (24) can be used to give all of the $\dot{M}_i$'s.
The pressure p_i and temperature can then be calculated using (27)
and equilibrium pressure-temperature data. For pressures above the
triple point, evaporation data is used, and for pressures below the
reiple point, sublimation data is used. If mixed mode exists, some
of the temperatures will be above and some below the freezing point.

Consider pores of diameter D_1 and D_2. Since $T_1 > T_f$
and $T_2 < T_f$, then $p_1 > p_2$ because the temperature increases with the
pressure. From (27) we see that $D_1 < D_2$. Thus it is seen that the
larger pores will be the last to lose their ice. This is fortunate
since the large pores will tend to breakthrough first and the ice at
the entrance tends to prevent it.

For mixed mode, the ice coverning the pores must be
confined to the pore areas only and thus can be assumed fairly
thin. Using this knowledge, it can be assumed that there will be a
small temperature drop across the ice portion. The effective
temperature of the plate at the entrance will be given by

$$T_{mm} = \frac{\sum_i n_i D_i^2 T_i}{\sum_i n_i D_i^2} \tag{40}$$

For the physical situation of mixed mode to exist, T_{mm}
must be essentially equal to the freezing point temperature.

The heater plate temperature will be given by

$$T_o = q_b \frac{\delta}{k_w} + T_{mm} \tag{41}$$

The above analysis can be used to calculate the temperatures
governing the operation of a sublimator with a porous plate of known
properties. As stated above, the temperature of the porous plate in
this mode is essentially equal to the freezing point temperature. The
heater plate temperature, as seen in (41), thus depends directly on the

plate separation.

As stated earlier, the mixed mode can occur only with porous plates which are non-wetting. In the test program, all of the plates were hydrophilic. Thus the mixed mode was not encountered in actual operation. The existence of this mode, however, seems possible when a hydrophobic porous plate is used.

Because some of the pores operate in the evaporation mode, the danger of breakthrough is increased. This situation always exists when the evaporative mode is present. If the plate is hydrophilic, the water behind the pores when the evaporation mode is initiated will enter the plate and the cyclic mode will be initiated.

III. The Cyclic Sublimation Mode

In the foregoing analysis of porous plates with different sized pores, the range of operating loads between that which produces the sublimation mode and that which produces the evaporative mode was investigated only for the case in which the plate is hydrophobic -- leading to the "mixed mode". However, most commercially produced plates are hydrophillic, and in the load range being discussed water may enter the pores. This will lead to a entirely different set of phenomena which will be called here the "cyclic mode".

The cyclic sublimation mode occurs when the plate material is hydrophilic and the heat flow rate is such that no ice can exist behind the porous plate. Under these conditions water will enter the pores, freeze and then sublimate from the down stream end of the pores. As sublimation occurs, the ice-vapor interface will recede and the pressure drop increases. The interface will recede until the vapor pressure at the interface surpasses the triple point pressure or until the ice is all sublimed. If the first of these events occurs, the ice remaining in the pore will melt. The water will then be free to re-enter the pore and freeze again. Thus it is seen that the process repeats. For this reason it is termed the cyclic mode.

Although a cyclic process occurs within the pores, the system as a whole operates in an equilibrium condition when the heat flux is constant. The porous plate appears to have a constant temperature over the entire surface at the water interface.

The initial efforts to describe this mode of operation consisted of an attempt to consider one pore at a time. The mathematical description of this model is presented in Appendix II. The pores were assumed to fill completely and freeze, thus being exposed to low temperatures at the downstream end. Different pore sizes, it was thought, would have different cyclic periords. The effective temperature of the plate would consist of a sum of many time varying temperatures in the different pores and could possibly remain constant.

For each pore to act independently, it had to be assumed that the plate material was essentially a perfect insulator. If not, the plate conductivity would not allow the large temperature gradients necessary to satisfy the model. In actual operation, the porous plates are often nickel and have a high value of conductivity. Thus the initial model did not fully represent the physical situation.

This led to the model that assumes that the plate operates in a cyclic mode but only over a small distance as shown in Figure 5. If the cyclic process occurred over a large distance, the sublimation pressure variation between the extreme positions of the ice-vapor interface would also be large. This is true since the pressure drop increases linearly with the length of the unfilled pore. The large pressure variation would produce a large temperature variation also. If the pores operate independently, the large temperature drop would not be allowed because of the high conductivity of the plate material. If the interfaces in all of the pores move uniformily, the temperature of the porous plate would vary with time. However, from experimental observations, the porous plate is known to operate under seemingly steady state conditions. Thus the assumption that the cyclic process occurs only over a small distance is justified. The ice layer within the plate is located such that the pressure drop caused by mass flow through the remainder of the pore is equal to the triple point pressure.

The ice layer is presumed thin and is located at the same depth in all of the pores. This assumption is required by the relatively high conductivity of the plate material which tends to diminish any lateral temperature gradients. Pores of different size will thus have ice layers at equal distances from the plate surface. The ice cyclically sublimes about this fixed point. The temperature is assumed to be constant at any given depth over the whole plate. This assumption is justified since the heat flux into the porous plate is uniform and the plate material tends to diminish lateral temperature variations. Heat is conducted one-dimensionally through the plate and water to the point where the cyclic mechanism occurs and is then carried away by

means of the latent heat of sublimation.

The assumption of no lateral gradients within the plate appears to represent the physical situation well since the conductivity of the porous plate material is often quite high.

The temperature drop in the plate up to the cyclic point is such that the given heat flow is maintained. The temperature drop in the plate beyond this point is zero.

To calculate the distance L where the triple point pressure is reached, a modification of the Knudsen equation is used. This relation comes directly from (27) and is given below.

$$\dot{m}_i = \frac{D_i^3}{6L} \sqrt{\frac{2\pi g_o}{RT_f}} (P_{tp} - P_a) \tag{42}$$

From this equation, it is noted that the mass flow through a pore must be proportional to the cube of the diameter for the cyclic point to be the same in all pores. This requirement is different from the assumption made in earlier sections where the mass flow was assumed proportional to the square of the diameter. The change of phase inside of the porous plate in the cyclic mode is the cause of this difference.

The total mass flow is related to the heat flux by the relation

$$q_b = \dot{M}(\Delta H_s - \Delta H_f) \tag{43}$$

The total mass flow consists of the sum of the individual pore mass flows. This is represented mathematically by

$$\dot{M} = \sum_{i=1}^{m} n_i \dot{m}_i \tag{44}$$

As stated above, the distance from the outer edge at which the cyclic mechanism occurs is assumed virtually constant. Since all of the quantities on the right hand side of (42) are constant except D_i, (42) and (44) can be combined to give

$$\dot{M} = \frac{1}{6L} \sqrt{\frac{2\pi g_o}{RT_f}} (P_{tp} - P_a) \sum_i n_i D_i^3 \tag{45}$$

The expressions for $\dot{M}$ from (43) and (45) can be equated to give

$$\frac{q_b}{\Delta H_s - \Delta H_f} = \frac{1}{6L} \sqrt{\frac{2\pi g_o}{RT_f}} (P_{tp} - P_a) \sum_i n_i D_i^3 \quad (46)$$

This can be solved for L to obtain

$$L = \frac{\Delta H_s - \Delta H_f}{6 q_b} \sqrt{\frac{2\pi g_o}{RT_f}} (P_{tp} - P_a) \sum_i n_i D_i^3 \quad (47)$$

With this distance known, the heat conduction equation can be used to relate the temperature at the plate entrance to the heat flux. This expression takes the form

$$q_b = k_{pe} \frac{T_p - T_f}{\Theta - L} \quad (48)$$

Since the layer of ice which sublimated cyclically is assumed to be very thin, the equivalent conductivity in this part of the plate can be expressed as in (16), namely

$$k_{pe} = k_w P + k_p (1 - P) \quad (49)$$

This equation can be used in (48) to give

$$T_p = q_b \frac{\Theta - L}{k_w P + (1 - P) k_p} + T_f \quad (50)$$

The temperature of the heater surface is then given by

$$T_o = q_b \frac{S}{k_w} + T_p \quad (51)$$

The assumption that the cyclic process occurs over a small distance has allowed the temperature of the ice layer to be approximated by the freezing point temperature.

If a hydrophilic porous plate with known physical properties is being used to reject a heat flux such that the pressure drop through the plate is greater than the triple point pressure, the system will operate in the cyclic sublimation mode. This, of course, will be true only if the ambient pressure is sufficiently low. For a plate operating

in this mode at a specified heat flux, (47) can be used to locate the position of the ice layer in the plate. With this position known, (50) and (51) can be applied to obtain the temperatures of the porous plate and heater surfaces. These temperatures, in turn, can be used to evaluate the possible application of this porous plate in a mission which would require rejection of the specified heat flux. It should be noted that the cyclic model hypothesized here, while simple in concept, has the deficiency of requiring an infinite heat load to locate the ice layer at the downstream plate surface.

The equations developed above may also be used to predict desired properties in a porous plate to satisfy given temperature requirements such as a heater surface temperature below a specified value.

It should be pointed out that the temperature of the heater plate can be reduced by decreasing the heat flux. This can be decreased by making the sublimator surface area larger. This however, adds weight to the total system and possibly violates the weight constraint. A trade-off between these two requirements is usually necessitated. The heat flux is increased by decreasing the sublimator area until the heater plate reaches its maximum value at which the system will function. This is done at the peak heat load to be encountered on the mission. Possibilities of breakthrough at the peak heat load and freeze-up at the minimum heat load must also be considered in this sizing process.

IV. Experimental Program

An experimental program was devised and carried out to verify the models described in the foregoing sections. Since the porous plates actually tested were hydrophillic, only those mechanisms in which the water wets the plate were examined.

The basic experimental apparatus consisted of a vacuum system to simulate the conditions of outer space, an electrical system to provide a known heat load, a water feed system to supply a known mass flow of water to be sublimed, and a test module with a porous plate. A schematic of these various systems is shown in Figure 6. Photographs of the apparatus are shown in Figures 19-22.

Vacuum System

The vacuum chamber consisted of a 18" diameter, 30" high bell jar above a stainless steel base plate. The plate was fitted with ports allowing thermocouple leads, power leads, and water lines to enter the vacuum chamber.

A 4" vacuum line connected the chamber to the liquid nitrogen trap. This trap was manufactured by the Rice machine shop and has 9 sq. ft. of freezing surface with a volume of 0.285 cubic ft. to hold liquid and gaseous nitrogen. The manifold which contains the nitrogen was designed to insure contact of the water vapor produced by the sublimation process with the freezing surface as the vapor flows through the trap.

The pressure in the system was measured using thermo-couple gages (Bendix Vacuum #TGC-100) with a range from 0 to 1000 microns. Two gages were used, one located in the vacuum line just below the base plate and the other between the cold trap and the vacuum pump. A 2" line connected the trap with the vacuum pump (Welch 1497B).

Electrical System

The power source for the electrical system consisted of a power stat with a 60 cycle, 115 volt input and a 0-140, 0-8 amp. output. A Weston Model 433 ammeter, with two scales for accuracy was used to measure the current and a Triplett Model 630-plk combination meter, with 5 scales, was used to measure the voltage. The voltage drop across the test module and the current through it determine the power input.

Water System

The water reservoir was a stainless steel closed cylinder (6" diameter, 12" tall) having lines with micro-needle valves connecting the top with the vacuum line and the outside. These controls allowed the pressure above the water to be controlled accurately, and thus the pressure in the test sample was controlled.

The water line carried the water to a 0.45μ absolute filter (Gelman #12505) and then through one of two flow meters (Fischer and Porter Model #10A1338) which measured the flow rate in cc/min. Connection lines of stainless steel and polyprophelene and valves of stainless steel were used to keep corrosion out of the water since any particles could block pores in the porous plate and reduce the plates ability to pass water.

The water line connected the flow meters with the test sample inside the vacuum system through the base plate. A pressure tap from the test module connected with an external gage (Crosby ASO-10854) to give the water pressure inside the water chamber. As mentioned before, this pressure was controlled by controlling the pressure above the water in the reservoir.

Test Module

A cutaway diagram of the test module is shown in Figure 7. The heater plate was a 1/8" thick copperplate to give a uniform temperature and insure one dimensional heat flow. This plate was heated

by a nichrome resistance heater placed directly under it. The initial heater module was made using 0.425 ohm/ft Nichrome wire as the heating element and Micart (a phenolic material) as insulation. The wire was layed in grooves cut in the phenolic material. Sauereisen cement was used to hold the wire in the groove and provide a media for conduction to the copper plate. The copper plate was attached to the insulation and heating element using RTV silicon rubber. Because of the temperature limitation on the phenolic material, this heater unit had a maximum output of 3200 BTU/hr-ft^2. This heater was used in all the tests which were run.

For breakthrough testing, it was desirable to have a heater with a higher power output. A second heating module was made using 1.1 ohm/ft Nichrome wire as the element and Transite (a cement and asbestos material) as insulation. This module was made in the same manner as the previous one and could withstand much higher temperatures. Breakthrough tests were run with heat fluxes up to 8000 BTU/hr-ft^2 using this heater unit. The unit could withstand the maximum output of the power supply (10,700 BTU/hr-ft^2), but the temperature limitation of 150 °F on the plastic spacer prohibited fluxes above 8000 BTU/hr-ft^2. It should be pointed out that both heater units gave essentially the same data in the sublimation testing.

The spacer square which separated the porous and heater plates was made of plexiglass. This substance is advantageous since it can be polished on the edges to allow the water chamber to be viewed during operation. The plastic has desirable insulation properties to maintain one dimensional heat flow and cut down on heat losses.

The porous plate fitted into a groove in the plexiglass spacer and was held in place by a phenolic frame which is bolted to the insulation material below the copper heater plate.

The water inlet and water pressure tap to the water chamber were connected using #18 stainless steel hypodermic needles which were epoxied into holes drilled through the plexiglass spacers.

Temperatures of the heater and porous plates were measured

using copper-constantan thermocouples. Three thermocouples were mounted in the copper plate to detect non-uniformity in the heating. To measure the temperature at the plate water interface, the thermocouples were soldered in holes drilled almost through the plate from the back side. The thermocouple to measure the porous plate temperature was welded to the plate surface on the water side. Forty gage thermocouple wire was used to reduce the error, and the lead wires came through the plexiglass spacer.

The thermocouples were connected to a continuous recorder so that steady state conditions could be easily verified.

Test Procedure

The test procedure involved taking heater plate and porous plate temperatures, vacuum and water plenum pressures, water flow rate, and ice thickness data for various heat flow rates.

A test was initiated by allowing liquid nitrogen to enter the cold trap to reduce the temperature of its freezing area. The vacuum pump was then started and the bell jar chamber was evacuated to a pressure below 300μ of Hg absolute. During this process, the pressure above the water in the reservoir was reduced (i.e., 5 in. Hg absolute or less). The valves on the water system were then opened and water was allowed to enter the test sample. Since the pressure in the reservoir had been reduced, the pressure differential from the water chamber to the evacuated bell jar was reduced and the chances for breakthrough were reduced.

The system was allowed to run a short time to cool the test module and then the powerstat was set at the desired initial input. For each heating rate, 30 to 45 minutes time lapse is allowed for the cooling system to reach steady state. The condition of steady state was determined to exist when the temperatures of the heater and porous plates no longer varied with time.

When equilibrium conditions were reached, the data was taken and then the power was increased to a higher setting.

The sublimation testing was done with the water pressure in the chamber between 2.0 and 3.0 psia. In the initial tests, this pressure was difficult to maintain at a steady level due to in leaks in the water line and vapor locks at the water filter. Since the water flows at a pressure of 3 psia or less, the dissolved air in the water tended to collect at the 0.45 filter and choked the flow. The initial filter had a small area and was easily choked. In the later tests, a cartridge filter with several square feet of filter area was used and the problem was solved.

During the sublimation tests, the pressure in the vacuum chamber was maintained below 100μ. It is important that this pressure be maintained at a low value to realistically represent the vacuum of space.

The shut down procedure consisted of turning off the power supply, closing the water inlet valve, and opening the bypass valve around the filter to prevent damage by backflow. The vacuum chamber was then slowly returned to atmospheric conditions. After each run, a drain was opened at the bottom of the cold trap to remove the accumulated water. Dry air was then blown through the cold trap to help dry it.

Breakthrough data was taken in much the same way. Steady state operation was obtained at a given heat input and then the water pressure in the water plenum was increased slowly until uncontrolled breakthrough occured. Since this caused a large amount of ice to form above the porous plate, a breakthrough test terminated a run. Thus the breakthrough data was taken only for the highest power setting in a standard run. The pressure in the water plenum was increased by slightly opening the micrometer needle valve to allow air to enter the water reservoir.

Bubble tests were also run on the porous plates to give information about the pore sizes. The test procedure and apparatus are described in Appendix I.

V. Results, Correlation, and Conclusions

Experimental tests were run to verify the analysis presented in the earlier sections of this report. The porous plates used were hydrophilic. Thus all modes presented in the analysis were not encountered. These include the evaporation and mixed modes. The analysis which is checked by these experiments is that for the pure sublimation mode and the cyclic sublimation mode. The temperatures of the porous and heater plates are the important quantities which determine the usefulness of a system operating at a given heat flux. These temperatures, for the pure sublimation mode, are determined using (6) and (12) for a plate with uniform pores and (27), (28) and (30) for a plate with different size pores. For the cyclic sublimation mode, Equations (50) and (51) give the desired temperatures. The experimental data collected were compared with the predictions given by these equations.

Tests were run on ten porous plates of sintered nickel wire mesh (Rigimesh) produced by Aircraft Porous Media, Inc. Because of the manufacturing process, these plates have pores of more uniform size and straighter path than plates made of sintered spheres. Since the physical model which was analyzed in the earlier sections consisted of straight pores of known size, the Rigimesh plates were desired for testing. The plates as received were rated by the maximum pore size. This rating was done by the manufacturer.

The plates were trimmed to size, measured for thickness and area, and weighed. With these quantities known, the porosity of each plate was determined.

Bubble tests were run on each plate to determine the maximum pore size and to gain more insight about pore size distribution. Using alcohol as the wetting agent, the air pressure behind the plate was increased gradually until the first air bubble comes through the plate. Since alcohol forms a contact angle of nearly

zero with most surfaces, including nickel, the pressure to break the first bubble through the plate is dependent only upon the surface tension and the pore size. Thus an equivalent maximum pore size can be calculated for the initial bubble point.

The test can be continued by further increasing the pressure to note the bubble points of the next larger pores. For the test samples, the pore size distribution was rather uniform and thus, a slight increase in pressure from the initial bubble point caused many pores to break through. To bypass the problem of keeping count of each bubble point, the pressure was increased until about 50% of the surface was covered with bubbles. The pressure at this point can be related to an equivalent pore diameter which will be near the median size. This method of determining a median pore size leaves much to be desired but no better direct methods appear to be available. A suggested alternate method for actual design purposes is given in the final conclusions of this report.

Tests were run on each test plate and the equivalent diameters are presented in Table 1. Included is the thickness, porosity, spacer width, and manufacturers specified maximum pore size for each plate. The plates ranged in thickness from 0.0175 to 0.0496 inches, in porosity from 0.071 to 0.313, and in maximum pore size from 4.69 to 17.9 microns.

The rankings of the plates by increasing porosity and increasing maximum pore size correspond almost exactly with only two interchanges being the difference. This is as expected, since all plates are made from a varying number of layers of the same wire mesh. The reduction in pore size is obtained by rolling the layers with increasing pressure and thus reducing the porosity.

One criteria which may be used to compare plates operating in a steady state condition is the heater plate temperature at a given heat flux. Since this temperature varies with changing plate separation, however, a better comparison may be gained by considering the tempera-

tures of the porous plates for a given heat flux. This temperature should not change with varying plate separation.

Tests were run on the porous plates with heat flux variations from 300 to 3000 BTU/hr-ft^2. The experimental results, heater and porous plate temperatures versus heat flux, are shown in Figures 8-16. Plates 9 and 10 were tested but no valid data was obtained since both plates had excessive breakthrough over most of the heat flux range.

In each figure the lower solid line indicated the theoretically predicted temperature for the porous plate. The X on the line indicated the heat flux at which, theoretically, the pure sublimation mode ends and the cyclic sublimation mode begins. At heating rates below this changeover value, the system operates in the sublimation mode and the sublimation temperature is obtained using Equation (6) and Table 2. The porous plate temperature for operation in the cyclic mode is determined from (50). The temperature of a porous plate was calculated assuming that the plate had pores with a diameter equal to the median diameter. The total number of pores per unit area was obtained by dividing the porosity by the area of one pore.

For the plates with small median pore diameters, the theoretical porous plate temperatures given by Equation (50), of heat fluxes, varies little from 32°F. These calculations were done using the equations governing the cyclic sublimation mode from Section IV. This approach was used in all cases when the theoretical pressure drop through the plate was above the triple point pressure since nickel is hydrophilic. Thus water should enter the plate to the depth such that the pressure drop equals the triple point pressure, freeze, and oscillate about that point. The experimentally measured porous plate temperatures are close to the predicted values, but in all cases are slightly lower.

The plates with higher porosities and larger pores have lower pressure drops through the plates for given heating rates. Thus the maximum heat flux at which ice can be present behind the

porous plate increases with increasing porosity and pore size. When
the pore properties of a plate are represented by pores of only one
size, the theoretical temperature and ice thickness change rapidly
with decreasing heat flux once the heat flux in below that which gives
triple point pressure drop through the plate. The sharp theoretical
drop off in temperature which results when the sublimation mode sets
in is particularly apparent in Figures 13 and 14. The experimental
temperature in these cases dropped much more slowly with decreasing
 heat flux. This slower decrease is easily explained by the fact
that the plate is really made up of a statistical distribution of
pore sizes. The actual temperature is thus a statistical average
due to a variety of pore sizes, many smaller than the median. This
variety in size causes the total change in temperature with changing
heat flux to be much less pronounced. At the higher heat fluxes,
the experimental porous plate temperatures agree quite well with the
theoretically precisted valves.

In each of Figures 8 - 16, the upper solid lines represent
the theoretically predicted heater plate temperatures. Figure 8
shows the theoretical prediction given by Equations (3) and (51) as
compared with the experimental data collected for Plate 1. The
discrepancy is rather obvious. The source of this error lies in the
basic assumption that a sublimator is most likely to operated in the
zero-gravity environment of space. This assumption leads to the
corresponding assumption that conduction is the only mechanism by
which heat is exchanged between the heater plate and the porous
plate -- indeed, this was the basis of Equation (30) and (51). The
laboratory tests, however, were performed in a 1-g environment with
the heater plate facing upward. Thus, the expendable water layer
was heated from below -- a configuration leading to an unstable free
convection situation. Verification that free convection leads to
the discrepancy shown in Figure 8 was performed in two ways.

Although the original design of the apparatus did not con-

veniently accommodate it, the test module was mounted in an upside-
down configuration and the test repeated. The liquid layer would
be heated from above and not subject to free convection effects.
The test results are again compared with the thoretical prediction
in Figure 9, and the close correspondence is readily apparent.

In order to continue using the test apparatus in the
original design configuration (heated from below) it was decided to
attempt to account for the free convection effect by use of existing
correlations. Reference 5 reports on an empirical study of free
convection in a liquid layer between two plates, heated from below.
Good experimental agreement, for a number of different liquids, was
obtained with the following relation for the Nusselt number:

$$Nu = 0.069 \ R_a^{1/3} \ P_r^{0.074} \tag{52}$$

The Rayleigh number is based on the plate spacing and the liquid
properties are evaluated at the mean temperature.

When the free convection mechanism is coupled with the
conductive mechanism given by Equations (30) and (51) the curved
line of Figure 9 is obtained. Good agreement is seen to occur with
the data collected in the original configuration. The remaining
tests, shown in Figures 10 - 16, were conducted in the "up" configu-
ration, and Equation (52) was used, along with (30) and (51), to
predict the heater plate temperatures. The good agreement between
theory and experiment leads to the conclusion that the analyses
presented for the sublimation and cyclic modes are valid representations
of the mechanisms taking place in a functioning sublimator.

The effect of free convection in ground testing deserves
additional emphasis. Consider, as an example, Plate 1, (Figure 9)
operating at a heat flux of 1200 BTU/hr-ft^2. With free convection
present, a heater plate temperature of about 65°F was measured --
resulting in a temperature difference of 33°F across the water layer.
In the zero-gravity of space this same temperature difference will
maintain a heat flux of only 620 BTU/hr-ft^2 -- approximately 50% of

the ground-based value! Alternatively, a temperature difference of
58° (heater plate at 90°F) would be required to maintain the 1200
BTU/hr-ft^2 flux, a fact having a profound influence on the rest of
the heat rejection system!

It is noted that the porous plates operate essentially at
32°F over a wide heating flux range. The difference in operation of
the various plates in the range is thus negligible. If the tempera-
tures of the porous and heater plates is to be reduced in operation
at a given heat flux, a plate with large enough porosity and pore
size must be chosen so that ice will be present behind the porous
plate. The limitation to the pore size is brought about by the
breakthrough phenomenon.

The temperature which the heating surface will have in a
given sublimator operating at a specified heat flux is determined
by the porous plate used. This temperature thus determines which
porpous plates are desirable. It is usually required to keep the
temperature as low as possible since this makes the transfer of heat
from the circulating coolant to the water less of a problem. To
maintain a low heater plate temperature, it is desirable to have
ice in the water chamber. A low heater plate temperature will then be
required to maintain a given heat flux since the distance from the
heater plate to the point of a freezing temperature is reduced. Thus
the sublimator should be designed for the pure sublimator mode. The
heat flux at which the sublimation mode theoretically vanishes is in-
dicated by X in Figures 8-15. The sublimation mode exhibits no break-
through problems since the ice forms a physical barrier to prevent
the escape of the water. Since the ice thickness can increase rapidly
with decreasing heat flux, care must be used to prevent complete
freezing of the sublimator at heat fluxes below the design value.

In all the analysis presented in this report, it has been
assumed that the pores in a plate are straight. This is not the case
in most porous plates. It seems possible that a tortuosity factor
might be added to all of the pressure drop equations to correct the

crookedness of the path length of a pore to some equivalent straight,
longer pore. This factor would always be greater than unity and
would have to be determined for each plate. With such a factor in-
cluded, the analysis presented could be applied to plates with more
random paths.

The breakthrough properties of some of the plates was in-
vestigated using the method described under the experimental procedure
section. At a given heat flow rate, the water pressure in the water
plenum was increased gradually. The test was terminated if the water
pressure reached atmospheric pressure and breakthrough had not occured.

Tests were run on seven of the porous samples. These plates
had a range in maximum pore size from 4.69 to 12.8 μ. The tests on
these plates did indicate some basic trends. However, exact conclusions
are diffucult to obtain due to the varied results from sone of the tests.

The water pressure at which uncontrolled breakthrough occurred
depended upon the initial condition of a plate. A porous plate which
was dry before the test usually exhibited breakthrough at a lower
pressure than it would have had it been wetted from a previous break-
through run. The test data on the plates was not always repeatable.

A typical run was that on plate number 4. The plate has a
maximum pore diameter of 9.70 μ. Equilibrium conditions were reach-
ed with an input heat load of 3040 BTU/hr-ft^2 and a water pressure of
2 psia. The water pressure was gradually increased. At a value just
above 3 psia, self-healing breakthrough started to occur. Water
broke through the plate over a small area and immediately froze. The
pore was blocked by the ice and, thus, the breakthrough at this point
ceased. This phenomenon occurred over several areas of the plate
regularly. Air bubbles in the water chamber seemed to aid this pro-
cess when the air passed through the porous plate.

This intermittent process occurred as the pressure in the
chamber was increased to 11.5 psia. At that pressure, uncontrolled
breakthrough occurred. Water passed through the plate in a steady
stream and froze quickly when it reached the vacuum chamber. This

water formed a mound which covered the test plate and continued to grow until the water supply was shut off.

The breakthrough pressure for the various plates tended to decrease with increasing heat flux and pore diameter. This is illustrated in Figure 17. This graph shows breakthrough pressure versus pore diameter with heat flux as a parameter. The dashed line is the theoretical breakthrough point for water, with no heat flux, calculated from

$$\Delta P = \frac{4\sigma}{D} \tag{53}$$

The data obtained tends to indicate that the water retention properties of the plates, at a given heating rate, increase much more rapidly with decreasing pore size than the theoretical curve for water. This is as expected, since the ice in the pores would enhance the breakthrough resistance.

The data roughly suggests that the breakthrough point is determined by a series of curves, one curve for each heating rate.

It should be pointed out that no uncontrolled breakthrough was experienced by the plates with maximum pore size of 8.66μ or less, even when the heat flux was at a maximum of 8000 BTU/hr-ft^2.

From these tests it may be concluded that if the maximum pore size is less than 9μ, the breakthrough problem should be minimized.

It should be pointed out that the ice inside a plate is certainly important in preventing breakthrough. After the small pore plates did not breakthrough, the pressure in the vacuum chamber was raised above the triple point and all of the plates broke through almost immediately. Since no ice could be present at the higher pressure, it seems certain that ice had been the restraining force preventing breakthrough.

VI. Summary Of Typical Performance and Design Calculations

It would appear useful at this point to summarize the methods of carrying out calculations for porous plate sublimators heated with a uniform heat source. Both performance and design calculations are of interest. In all that follows, it if presumed that the porous plate in question is hydrophillic. Thus, only the sublimation and cyclic modes of operation are possible.

Performance Calculation

With the median pore size and number of pores known for each plate, the mode of operation can be predicted for a given heat flux $(q_a = q_b)$. The mass flow of water is given by

$$\dot{M} = q_b / (\Delta H_s - \Delta H_f) \tag{3}$$

The flow through a pore is then given using

$$\dot{m} = \dot{M}/n \tag{4}$$

Since the pore diameter and plate thickness is known, (6) gives

$$p - p_a = \frac{6 \dot{m} \theta}{D^3} \sqrt{\frac{RT}{2\pi g_0}} \tag{6}$$

If the pressure calculated from this equation is greater than the triple point pressure, the cyclic sublimation mode exists. This will be considered later. If the pressure is less than 0.0886 psia, data from Table 2 is used to find the corresponding sublimation temperature T_s.

The ice thickness and heater plate temperature are then given by

$$I = \frac{k_I}{q_b} (T_f - T_s) \left(1 - \frac{\Delta H_f}{\Delta H_s}\right) \tag{9}$$

and

$$T_0 = T_f + \frac{1}{k_w}\left[q_b \delta - k_3(T_f - T_s)\left(1 - \frac{\Delta H_f}{\Delta H_s}\right)\right] \quad (12)$$

Thus the mode of operation and the important parameters governing this mode have been calculated.

If the pressure had been greater than 0.0886 psia, operation would have been in the cyclic mode.

The distance from the outer edge of the plate to the ice layer within the plate is

$$L = \frac{\Delta H_s - \Delta H_f}{6 q_b} \sqrt{\frac{2\pi g_o}{R T_f}} (P_{ep} - P_a) \sum_{i=1}^{m} n_i D_i^3 \quad (47)$$

The equivalent conductivity can be calculated using

$$k_{pe} = k_w P + k_p (1 - P) \quad (49)$$

The temperatures of the porous plate and heater surface are then given by

$$T_p = \frac{\theta - L}{k_{pe}} q_b + T_f \quad (50)$$

and

$$T_0 = \frac{\delta}{k_w} q_b + T_p \quad (51)$$

Thus again the operating mode and temperatures can be calculated. The above calculations have the restriction that the water pressure is maintained at a reasonable value (5 psia or less) and that the maximum pore size is less than 10 microns. The above mentioned restrictions insure that the possibility of breakthrough is minimized.

These equations apply for performance in space. If it is desired to predict the performance on the ground, Equation (52) must be used to calculate the heater plate temperature in sublimators which will have free convection.

Design Problem

In a given sublimator, the plate properties, water pressure, and heater plate temperature are known. Can the heat flux and mode be predicted? The answer is yes and the approach is given below.

The problem can be solved iteratively. The heat flux is guessed and the problem is handled as outlined in the first of this section. For each guess at the heat flux, the mode and heater plate temperature can be calculated. If the calculated value of the plate temperature does not equal the given value, the heat flux guess is adjusted in the appropriate direction and the process is repeated. Increasing the heat flux always increases the heater plate temperature.

PART B

Prototype, Fluid-Heated, Sublimator Units

The entire disscussion, analysis, and experimental verifica-
tion of Part A has been devoted to a simplified uni-dimensional model
of a sublimator -- that in which the heat source is represented as an
iso-thermal surface of uniform heat flux. A model more representative
of actual, functioning, sublimator units is that depicted in Figure 1.
In this instance the heat to be rejected is brought to the sublimator
by a circulating "coolant". (The term "coolant" is used here in the
relative sense -- this stream being a coolant to the heat generating
devices interior to the spacecraft being cooled by the sublimator).
To avoid future confusion and to maintain consistency with the term-
inology of "heater plate" in Part A dealing with the uniformly heated
modular units, the circulating fluid will be referred to as the heater
fluid in the remainder of this report although this is somewhat incon-
sistent with usual terminology dealing with spacecraft thermal control
systems.

I. Application of the Modular Unit Analysis to Performance Calculations
of Fluid-Heated Sublimators

Since the temperature of the heater fluid decreases as it
passes through the sublimator, it is apparent that the relations developed
for the uniform heater plate modules cannot be applied to a fluid-
heated unit without modification. The basic assumption made in the
development of the following analysis is that the relations obtained
for the uniformly heated units may be applied locally over a section
of suitable length in the fluid-heated unit. On this basis, the
sublimator is modeled as a series of discrete segments, each being a
uniform heater unit, as suggested in Figure 23.

The following assumptions are implicit in this basic model:
1. Conduction along the porous plate is negligible.
2. Conduction along the heater plate is negligible.

3. Conduction in the water layer, parallel to
the direction of the heater fluid flow, is negligible.

4. Axial conduction in the heater fluid is neglibeble.

Assumptions 1, 2, and 3 are justified by the fact that
temperature gradients along the sublimator (parallel to the heater fluid
flow) are typically quite small compared to the gradients over the unit
thickness. For example, the experimental units tested here were approx-
imately 25 times as long as thick. A typical temperature drop over the
thickness was 50°F, while a temperature drop in the heater fluid of 7°F
was typical.

Assumption 4 has been found to be valid for Peclet numbers
above one hundred (Reference 12). This condition was satisfied in the
range of heat conditions studied.

In the tests performed on the fluid-heated units, the design
error noted for the uniform modulus was corrected. The units were
mounted facing downward in order that free convection effects in the
water layer could be ignored.

To predict the performance of a fluid-heated sublimator on
the basis of the model just described, a modification of the procedure
described in A.VI for the uniform heated unit can be used. The principal
difference in the method is that instead of calculating the heater
plate temperature, T_o, the temperature of the heater fluid, T_{hf}, is
calculated. Thus, an additional parameter, the heat transfer coefficient
between the heater fluid and the heater plate, becomes involved. Con-
sequently, it must be presumed that the geometrical and hydrodynamical
conditions of the heater fluid passage are sufficiently defined that
existing heat transfer correlations may be used to predict this heat
transfer coefficient. The particular correlation used for the units
tested here is discussed in detail later. It is sufficient at this
point to presume that this heat transfer coefficient, h, is calculable
as a function of longitudinal position along the heater fluid passage.

As noted earlier, the basic model used for the fluid-heated
unit is that of a series of uniform heater plate units. The inlet

temperature is taken as the fluid temperature of the first segment and the heater fluid temperatures of succeeding segments are obtained from heat and mass balance relations. Assuming that the overall unit geometry, the heater fluid flow rate and inlet temperature are known, the detail performance calculation procedure is then (refer, again, to the summary in A.VI):

1. Divide the sublimator into a number of longitudinal segments. Let the subscript j denote one such segment.

2. The heater fluid of the first segment is taken equal as equal to the unit inlet temperature and constant over the segment length.

3. An estimate is made for the heat flux in this segment, and the heat flux per pore is calculated.

4. Equations (3), (4), and (6) are used to calculate the pressure at the inside of the porous plate and the corresponding sublimation temperature (presuming the sublimation mode is in effect).

5. Equation (12) is used to calculate the heater plate temperature T_{oj}.

6. The estimated segment heat flux, q_{oj}, and the "known" value of segment heat transfer coefficient, h_j, are used to calculate the bulk heater fluid temperature of the segment, T_{hf_j}:

$$T_{hf_j} = T_{oj} + \frac{q_{oj}}{hj} \tag{54}$$

in which T_{oj} is the segment heater plate temperature found in step 5.

7. The calculated T_{hf_j} is compared with the known inlet temperature. The estimated segment heat flux is revised and the process repeated until a suitable agreement is obtained between these two temperatures.

8. The inlet temperature of the next segment is then calculated from

$$T_{hf_{j+1}} = T_{hf_j} - \frac{q_{o_j} A_j}{\hat{W} c_p} \tag{54}$$

in which $\hat{W}$ and c_p are the mass flow rate and specific heat of the heater fluid and A_j the heat transfer surface area of the segment.

9.   The above series of calculations is then repeated for the next segment, etc., down the length of the sublimator.

10.   As before, if the calculation of step 4 yields a pressure above the triple point, the cyclic mode is presumed to be in effect for the segment and Equation (51) is used in step 5 in place of Equation (12). The model proposed presumes, then, that part of the overall unit may be operating in the sublimation mode and part in the cyclic mode.

11.   The bulk temperature of the heater fluid calculated for the last segment may usually be taken as the outlet heater fluid temperature of the overall unit if a sufficiently large number of segments has been used. Otherwise the outlet temperature should be calculated as the inlet temperature of a hypothetical "next segment" after the last segment.

Figure 24 presents a flow diagram of the calculation procedure just outlined.

II. Experimental Program

The method described above enables the calculation of the
outlet temperature, the temperature profile along the porous plate,
and the temperature profile along the heater plate for a given heater
fluid inlet temperature and flow rate. In order to test the useful-
ness of this method, an experimental apparatus was designed and built
so that these quantities could be measured in an operating sublimator.
This apparatus consisted of the following elements:

1. a sublimator containing a porous plate
2. a system to supply water to the sublimator
3. a system to supply heater fluid to the sublimator
4. a vacuum system

A schematic diagram of the apparatus appears in Figure 25, and a
photograph appears in Figure 26.

Sublimator Module

The construction of the sublimator module is illustrated
in Figures 27 and 28. The main body of the module was constructed
of reinforced phenolic. The exposed porous plate surface was 2 inches
wide and 13 inches long. The water layer was approximately .25 inches
thick. The heater plate was made of stainless steel sheet .0625
inches thick. The heater fluid channel was approximately .09 inches
thick and 2 inches wide. An entry length was provided so that flow
in the heater fluid channel might be hydrodynamically developed at
the onset of cooling. The unit was of sandwich construction, held
together by 36 stainless steel bolts. The unit could be disassembled
in order to interchange porous plates.

Feedwater System

The feedwater system consisted of a stainless steel tank
connected to the vacuum system and to the sublimator. A line from
the top of the tank connected to the vacuum system so that the feed-
water pressure could be maintained at approximately 5 inches Hg

absolute. A line from the bottom of the tank was connected through a filter and flowmeter to a valve at the base plate of the vacuum chamber, and from there to the sublimator module. A mercury mano-meter was connected to the top of the tank to monitor the feedwater pressure.

Heater Fluid Supply System

The heater fluid system contained the following elements:

1. a pump and motor
2. a reservoir
3. a knife-type immersion heater located in the reservoir and controlled by a "powerstat"
4. needle valves for controlling the flow through the sublimator module and through the bypass loop which returned to the reservoir
5. two quick-acting valves arranged so that the effluent stream from the sublimator module might be either returned to the reservoir or diverted into a graduated vessel for the purpose of measuring the flow rate.

Vacuum System

The vacuum system was identical to that used in the modular unit tests described in A.IV.

Instrumentation

Copper-Constantan thermocouples were used to measure the temperatures at the points of interest. These were connected to a potentiometer through a rotary switch so that the voltages could be read in rapid sequence. Thermocouples were places in the inlet and outlet heater fluid streams and at four equally-spaced points along the flow axis centerline of both the heater plate and the porous plate. The thermocouples were attached to the heater plate and porous plate by arc welding.

Procedure

Tests were run on three different porous plates, each of which was operated under as wide as practical a range of heater fluid inlet temperatures. The properties of the three plates used are tabulated in Table 4. The pore diameters and plate thicknesses specified in ordering the plates from the manufacturer were chosen to coincide with plates used in the modular tests reported in Part A. These properties were chosen so as to span the range found to be useful in these tests. Bubble point tests on the plates indicated that their properties were not as specified, so that direct correlation with the earlier tests was not possible. The properties of the plates received did, however, fall within the useful range. In calculating the performance of the experimental sublimators, the porous plates were assumed to consist of circular pores of uniform size. This uniform size was taken to be that of a median pore as determined by bubble point tests as described in Part A.

The heater fluid inlet temperatures were limited to the range from 50°F to 120°F because of the difficulty of insulating the flow loop. In the tests on two of the plates, breakthrough was encountered in the upper portion of this range. This led to the conclusion that the upper temperature capability of the apparatus was adequate. There is little practical justification for the operation of a sublimator with low heater fluid inlet temperatures (near 32°F) so that the lower temperature capability of the apparatus was also judged adequate.

The range of heater fluid flow rates was also limited to some extent. At very low flow rates, it was difficult to maintain steady flow. At high flow rates, the heater fluid temperature drop was small, and therefore, the percent error in this quantity was large. An intermediate range of 20 to 30 pounds mass per hour was found to avoid these difficulties.

Both water and a water-glycol solution were used as the heater fluids in tests with each of the three plates. The properties

of the glycol solution are tabulated in Table 5.

A typical test run consisted of the following steps.

1. Coolant was fed in to the cold trap and the vacuum chamber was evacuated.

2. The valve at the top of the feedwater tank was opened to connect with the vacuum system until the tank pressure was below 5 inches Hg absolute.

3. The feedwater valve in the base plate was opened to introduce water above the porous plate.

4. After ice had formed in the water above the porous plate, the heater fluid pump was started and the flow rate was adjusted.

5. The powerstat was adjusted to give the desired heater fluid inlet temperature.

6. The thermocouple voltages were read and recorded.

7. The heater fluid flow rate was measured and recorded.

8. Steps 6 and 7 were repeated until it became apparent that steady state had been attained.

The only major problem encountered during the tests was with the reliability of the porous plate thermocouples. The weld was extremely brittle and fragile. In several cases, porous plate thermocouples became inoperative during the course of a test and were subsequently found to be broken. For this reason, the porous plate temperature data is not complete for all tests.

Even for the tests where porous plate temperature data were obtained, the reliability of this data is questionable. The problems inherent in obtaining a good thermal contact between the thermocouple junction and the porous plate were never completely overcome.

Heat Transfer Coefficient Determination

As discussed in the foregoing, the application of the performance calculation technique of section B.II necessitates

knowledge of the heat transfer coefficient at the wall separating the
heater fluid and the water reservoir. The passage through which the
heater fluid flowed was rectangular in cross section.

        The flow in the rectangular heater fluid channel was laminar
in all cases with Reynolds numbers near 200. The thermal entry region
in the heater fluid channel was typically 20% of the sublimator's work-
ing length, so that the variation of the heat transfer coefficient at
the heater fluid-heater plate interface was significant. An approximate
solution to the energy equation, due to M. Leveque (Regerence 12) yields
a dimensionless heat transfer coefficient as a function of a dimension-
less distance along the duct for hydrodynamically established flows near
the thermal entrance according to:

$$Nu = 0.98 G_z^+$$

(56)

This solution has been experimentally verified for the range of conditions
encountered in the tests.

        This relation was used until a limiting Nusselt number of
2.43 was reached and the Nusselt number was assumed constant at this
value after this point. This limiting value was taken from the solution
for thermally developed flow between parallel plates with one plate
insulated and the other at uniform temperature (Reference 13). The
assumed Nusselt-Graetz relation is plotted in Figure 29.

        All thermodynimic properties were assumed to be independent
of temperature except the heat capacity of the glycol solution used as
the heater fluid in some of the tests (see below). The variation of this
property was approximated by a linear function of temperature.

III. Experimental Results, Correlation, and Conclusions

Twenty-eight tests were performed on the experimental sublimator units -- providing a wide variety of combinations of the three porous plates, water or water-glycol heater fluid, and various inlet temperatures.

The experimental data obtained are shown in Figures 30 through 57. Also shown in these figures are the theoretical predictions provided by the calculation procedure outlined in section B.I coupled with the heat transfer correlation of Equation (56). These theoretical predictions were generated by the use of the FORTRAN computer program listed in. Fifteen sub-segments were used in the model described in section B.I.

The test results correlate well with the theoretical predictions. The porous plate and heater plate temperatures were observed to be generally higher than predicted. This was anticipated in light of similar observations in some of the previous tests on the electrically heated modular units. The explanation for this discrepancy is that the porous plates actually contain a spectrum of pore sizes rather than pores of uniform size as modeled. Many of the pores are smaller than the equivalent median diameter used in the calculations, and many are larger. As the heat flux is decreased, the smaller pores would tend to remain longer in cyclic mode operation (at the freezing point temperature) and thus exert a moderating influence on the temperature response of the porous plate to heat flux changes.

The high conductivity of the porous plate material precludes the possibility of significant temperature variations between pores so that the pores all operate in the same mode. Because of this, at a given moderate heat flux, small pores operate at a lower temperature than calculated while the largest pores operate at a higher temperature than calculated. The heat flux through the small pores is smaller than calculated and conversely for the large pores. Consequently the actual temperature response to heat flux changes is determined by the shape of

the pore size distribution.

It can be seen from the graphs, Figures 30 thru 57, that
the discrepancy between calculated and observed heater plate tempera-
tures is greatest for low heat flux (low heater fluid inlet temperature).
The effect of moderated porous plate temperature response becomes most
important at low heat flux. This is because the thickness of the ice
layer increases with decreasing porous plate temperature. The thermal
conductivity of ice is much greater than that of water. If the calcu-
lated porous plate temperature is lower than observed, the calculated
ice thickness will be greater than observed. Thus, at low heat flux,
any discrepancy between the calculated and actual porous plate tempera-
tures will lead to a greater discrepancy between the calculated and
actual heater plate temperatures.

The porous plate temperature data shows a poorer correlation
with predictions than does the other data. In some instances the
correlation is quite good, while in others it is quite bad. This is
though to be due to problems encountered in welding the thermocouple
junction to the porous plate as mentioned above.

In some tests the curvature of the observed heater plate
temperature plot is opposite to that of the calculated heater plate
temperature plot. This may have been caused by deficiencies in the
thermocouple circuits. However, repeated inspections failed to reveal
the exact cause of this difficulty.

It is concluded here that the method presented is adequate
to predict the performance of a fluid-heated porous plate sublimator.

It is suggested that the bubble point test described in
Reference 1 is not a good method of measuring the mean effective pore
diameter since results obtained by different operators varied greatly.
Instead, it was found that better correspondence of results could be
obtained if a modular unit test of the kind reported in section A.V
were performed and the experimental date used to infer a median pore
diameter by reversing the calculations of A.VI.

PART C

Program Summary and Conclusions

Based on the work described in this report, the following summarizing statements and conclusions may be drawn:

For Uniformly Heated Modular Units

1. The operation mode temperatures of a porous plate sublimator at a specified heat flux can be predicted by the analytical methods presented here if information concerning pore size and size distribution is available. Agreement with experimentally measured data was very good.

2. Plates with a maximum pore size less than 10 microns should be used to prevent breakthrough when the plates are hydrophilic.

3. It is important that a pressure well below the triple point be maintained outside the porousplate to insure the presence of ice in the sublimator or plate. This ice helps to prevent breakthrough. Arrangements to insure this should be made in the manifold design.

4. Porous plates with the highest porosity function the most efficiently as heat rejection devices.

5. Ground tests on sublimators with large temperature and distance between plates will perform differently than in space due to free convection heat transfer in the water chamber.

6. Hydrophilic plates which operate with no ice in the test chamber will remain essentially at 32°F over a wide range of heat flux.

7. The pure sublimation mode is the most desirable since it pro-
duces the lowest heater plate temperature. The low heater temperature
produces the greatest potential for heat transfer from the cooling
fluid.

8. The heater plate temperature can be kept low by making the water
layer thin. This also reduces the danger of rupture during freeze-up
since the distance of expansion is proportional to the layer thickness.

9. Hydrophobic plates are undesirable to reject extremely large heat
fluxes since the resulting evaporation mode would produce high porous
and heater plate temperatures.

For Fluid-Heated Units

1. The modes of operation of fluid-heated, prototype, sublimator
units are adequately protrayed by the mechanisms hypothesized for
the modular units, at least in the case of hydrophillic plates as
tested.

2. The performance of a fluid-heated sublimator is well predicted by
the calculation scheme devised herein if adequate knowledge of the
heat transfer coefficient is known for the circulating heater fluid
loop.

3. Uniformly heated modular tests are superior for establishing an
equivalent, median, uniform pore size in application of the perfor-
mance calculation scheme than are bubble point tests.

REFERENCES

1. Sangiovanni, J. J., and J. L. Hepner, Porous
    Plate Water Boiler Design Study-Final Report",
    Contract No. NAS-9-2294, Hamilton Standard
    Division, United Aircraft Corp., May, 1965.

2. Graumann, D. W., and G. R. Woods, "Research
    Study on Instrument Unit Thermal Conditioning
    Heat Sink Concepts - Annual Report", Contract
    No. NAS-8-11291, Airesearch Manufacturing
    Division, Garrett Corp., January, 1968.

3. Crank, J., "Two Methods for the Numerical
    Solution of Moving-Boundary in Diffusion and
    Heat Flow", Quart., J. Mech. and Applied Math.,
    V. 10, 220, 1957.

4. Kennard, E. H., Kinetic Theory of Gases, Mc Graw-
    Hill, New York, 1939.

5. Globe, S., and D. Dropkin, "Natural-Convection
    Heat Transfer in Liquids Confined by Two Hori-
    zontal Plates and Heated from Below", J. of Heat
    Transfer, February, 1959.

6. Loeb, L. B., Kinetic Theory of Gases, Dover,
    New York, 1961.

7. Keenan, J. H., F. G. Keyes, P. G. Hill, and J. G.
    Moore, Steam Tables, John Wiley, New York, 1969.

8. Dorsey, N. E., Properties of Ordinary Water Sub-
    stance, Reinhold, New York, 1940.

9. Dyer, D. F., "Transport Phenomena in Sublimation
    Dehydration", Ph. D. Thesis, Georgia Institute of
    Technology, 1965.

10. Chapman, A. J., Heat Transfer, Second Edition,
    Macmillan, New York, 1967.

11. Richmyer, R. D., and K. W. Morton, Difference
    Methods for Initial-Value Problems, Second Edition,
    Interscience, New York, 1967.

12. Muntjewerf, A. K., "Laminar Flow Heat Transfer in the Thermal Entrance Region of Flat and Profiled Ducts", Delft, Technische Hogeschool, Doctor in de Technische Wetenschappen Dissertation, 1969.

13. Kays, W. M., <u>Convective Heat and Mass Transfer</u>, McGraw Hill, New York, 1966.

TABLE 1

POROUS PLATE PROPERTIES - MODULAR TESTS

Plate Number	Nominal Diameter (μ)	Maximum Diameter (μ)	Median Diameter (μ)	Plate Thickness (in.)	Porosity (void fraction)	Spacer Width (in.)
1	4.0	8.66	4.84	0.0466	0.105	0.214
2	5.0	4.69	2.50	0.0454	0.078	0.214
3	6.0	7.53	5.02	0.0496	0.071	0.214
4	7.0	9.70	5.62	0.0384	0.119	0.236
5	8.0	8.10	6.13	0.0402	0.097	0.236
6	9.0	11.3	6.12	0.0303	0.135	0.237
7	10.0	11.15	6.91	0.0358	0.141	0.236
8	12.0	12.8	7.20	0.0223	0.156	0.246
9	14.0	15.4	8.70	0.0307	0.234	0.236
10	16.0	17.9	9.66	0.0175	0.313	0.246

TABLE 2

SUBLIMATION DATA

Temperature °F	Pressure psia	BTU/#m
32	0.0886	1218.7
30	0.0808	1218.9
25	0.0641	1219.1
20	0.0505	1219.4
15	0.0396	1219.7
10	0.0309	1219.9
5	0.0240	1220.1
0	0.0185	1220.2
-5	0.0142	1220.3
-10	0.0109	1220.4
-15	0.0082	1220.5
-20	0.0062	1220.6
-25	0.0046	1220.6
-30	0.0035	1220.6
-35	0.0026	1220.6
-40	0.0019	1220.6

TABLE 3

EVAPORATION DATA

Temperature °F	Pressure psia	BTU/#m
32	0.0886	1075.4
35	0.0999	1073.7
40	0.1217	1070.9
45	0.14748	1068.1
50	0.17803	1065.2
55	0.2140	1062.4
60	0.2563	1059.6

TABLE 4

POROUS PLATE PROPERTIES - FLUID HEATED UNIT TESTS

Porous Plate Designation	Pore Diameter (microns)	Pore Density (pores/ft.^{2})	Plate Thickness (in.)	Void Fraction
A	6.4	5.5×10^8	.025	.19
B	8.8	4.5×10^8	.057	.30
C	6.3	12.0×10^8	.072	.40

Material: Sintered Nickel Wire Mesh

Manufactured: Aircraft Porous Media Inc.

TABLE 5

SPECIFICATIONS AND PROPERTIES OF

ETHYLENE GLYCOL-WATER SOLUTION

1. Density   67.5 lbm./ft.^{3}

2. Sodium Nitrite   .10 to .25% by weight

3. Sodium Benzoate   1.33 to 1.57% by weight

4. Water   36 to 38.5% by weight

5. Thermal Conductivity   .22 BTU/hr-ft-°F

6. Specific Heat Capacity   Approximately

                              .67 + .008T BTU/lbm.-°F

                              T in °F in the range of

                              T = 0°F to T = 100°F.

TABLE 6

TEST CONDITIONS - FLUID HEATED UNIT TESTS

Test	Porous Plate	Heater Fluid	Inlet Temperature (°F.)
1	A	Water	60
2	A	Water	75
3	A	Water	82
4	A	Water	86
5	A	Water	98
6	A	Glycol	58
7	A	Glycol	62
8	A	Glycol	70
9	A	Glycol	80
10	A	Glycol	100
11	A	Glycol	123
12	B	Water	60
13	B	Water	70
14	B	Glycol	61
15	B	Glycol	72
16	B	Glycol	80
17	C	Water	55
18	C	Water	58
19	C	Water	65
20	C	Water	70
21	C	Water	80

TEST CONDITIONS (CONTINUED)

Test	Porous Plate	Heater Fluid	Inlet Temperature (°F.)
22	C	Glycol	66
23	C	Glycol	71
24	C	Glycol	74
25	C	Glycol	81
26	C	Glycol	90
27	C	Glycol	98
28	C	Glycol	106
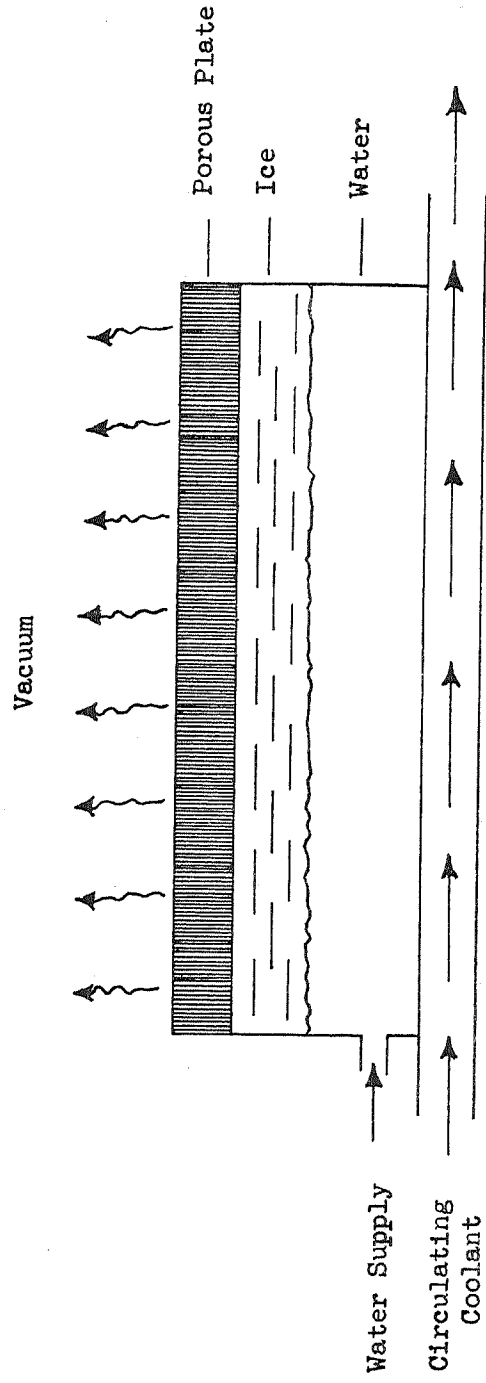
Figure 1

Schematic Diagram of a Porous Plate

Sublimator-Evaporator
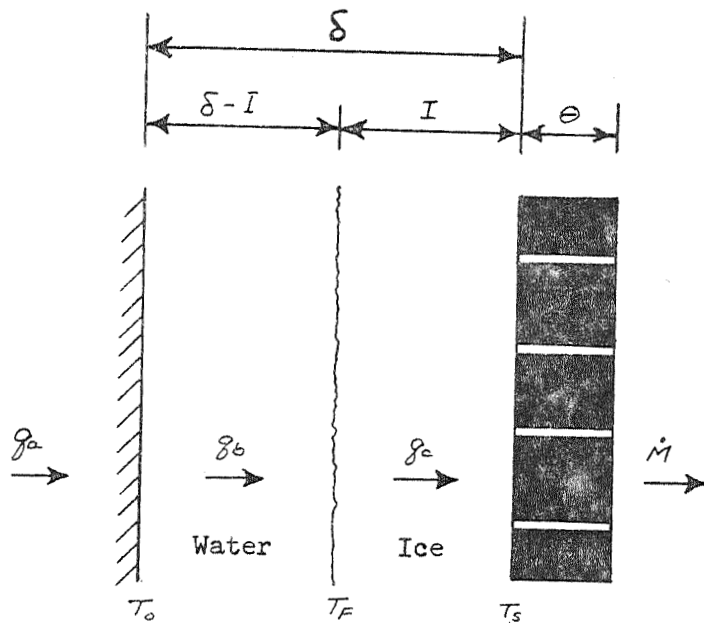
Figure 2

Sublimator operating in the Sublimation Mode
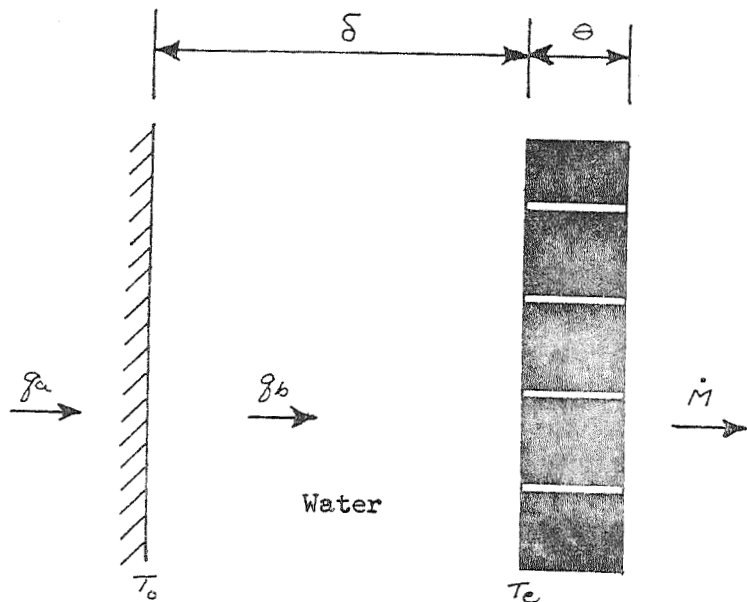
Figure 3

Sublimator operating in the Evaporation Mode
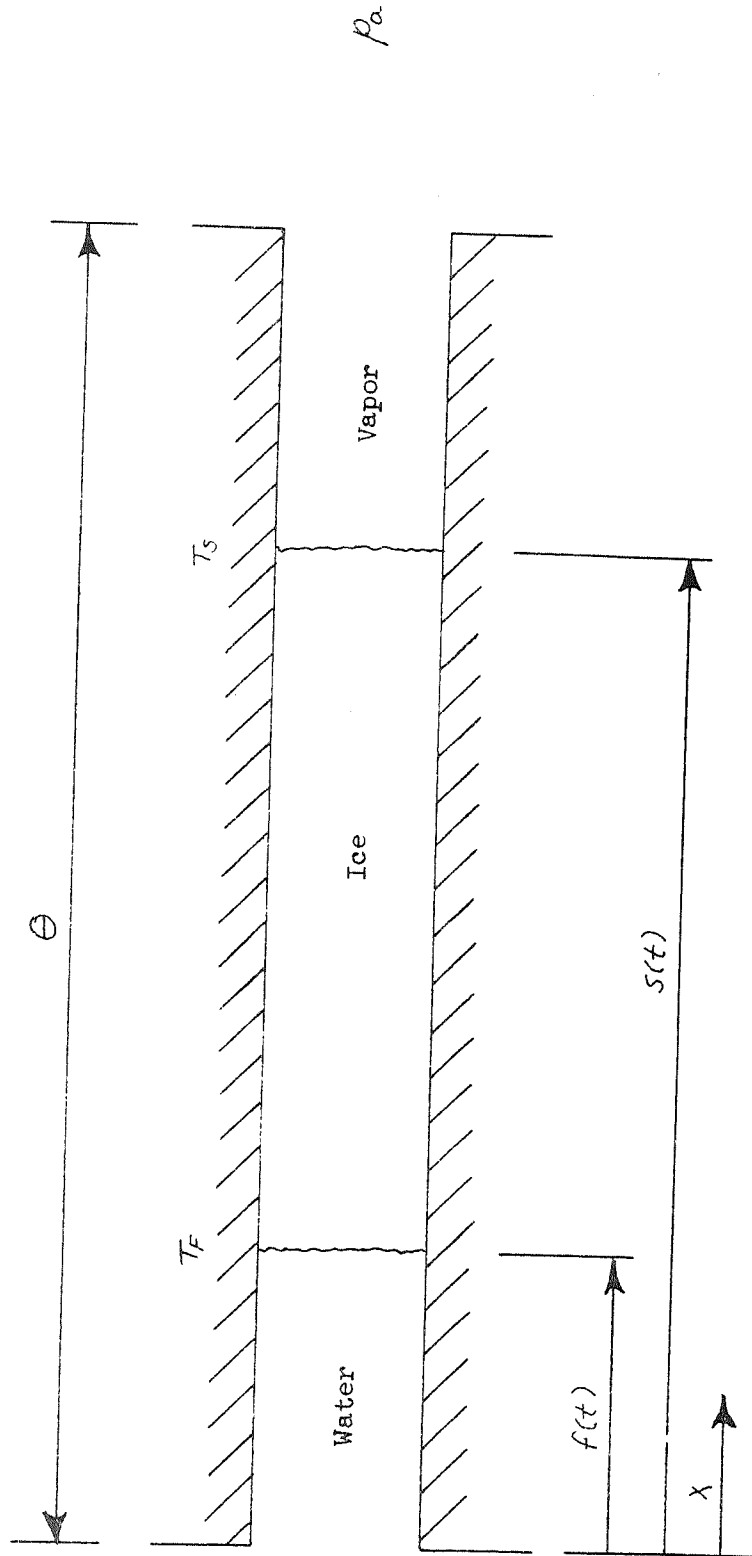
Figure 4

Initial Model of a Single Pore Operating in The Cyclic Mode
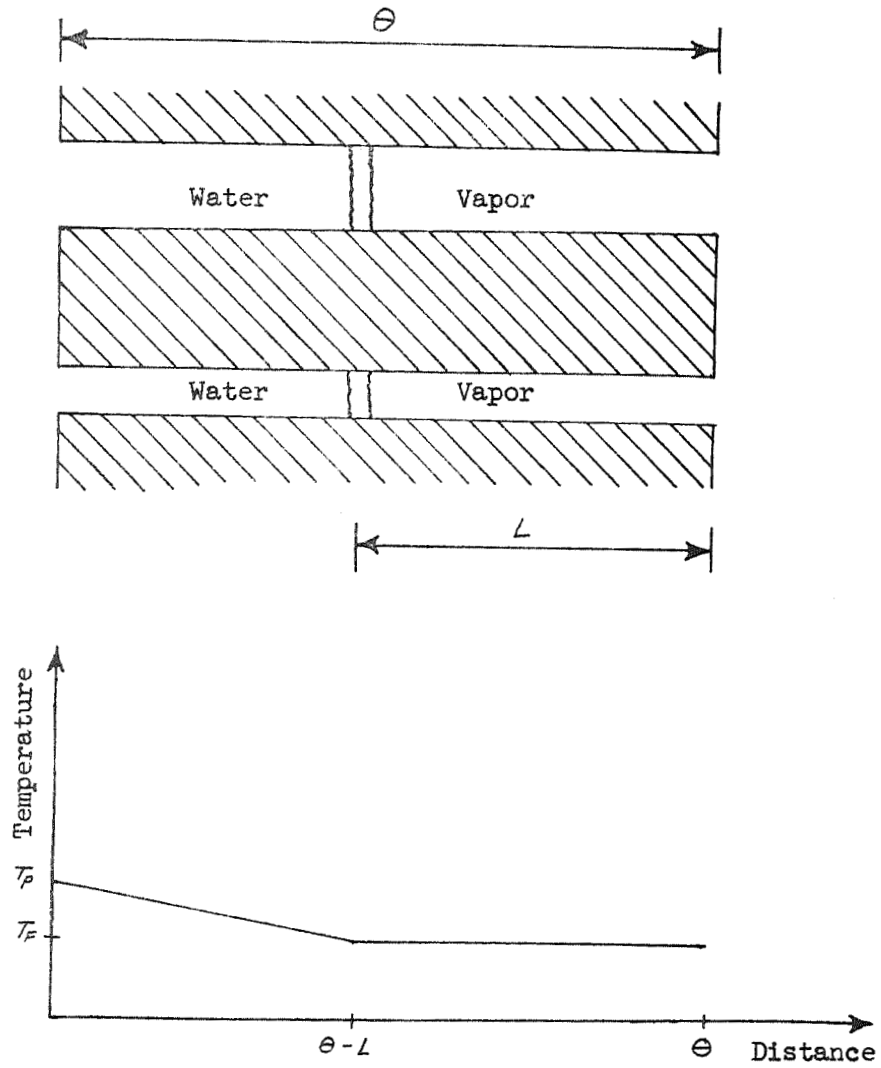
Figure 5

Two Pores Operating in the Cyclic Mode

Vacuum Pump

Vacuum Pressure Tap

Cold Trap

Vacuum Pressure Tap

Test Module

Water Chamber Pressure

Flow Meter

Filter $\frac{1}{2}$

Water Reservoir

A

V

P

Powerstat
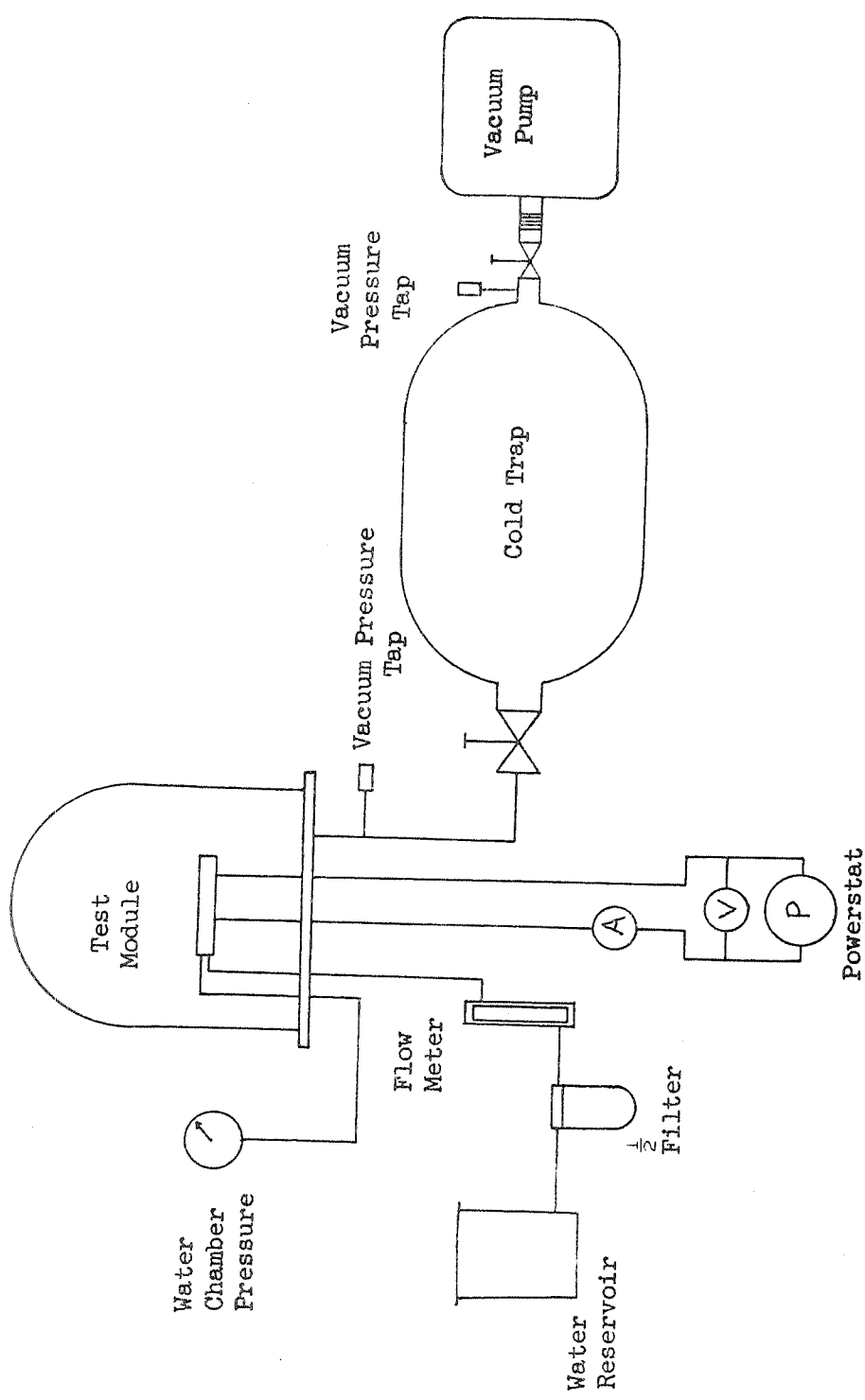
Figure 6

Schematic of the Test Apparatus

Porous Plate

Plexiglass

Pressure Tap

Nichrome Heater Wire

Water Chamber

Water Inlet

Copper Heater Plate

Insulation
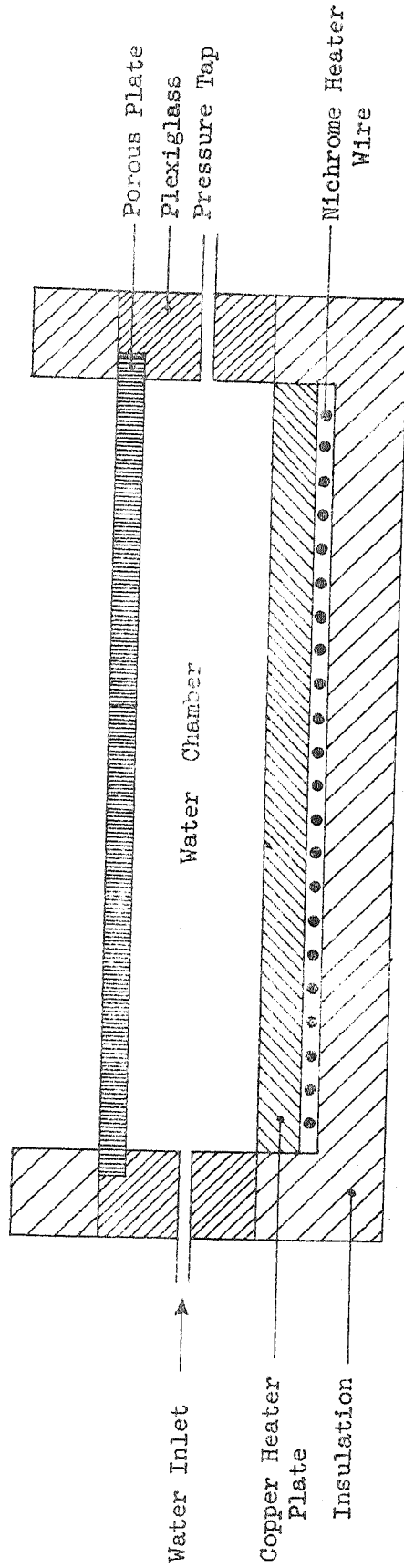
Figure 7

Cutaway Schematic of the Electrically Heated Test Module
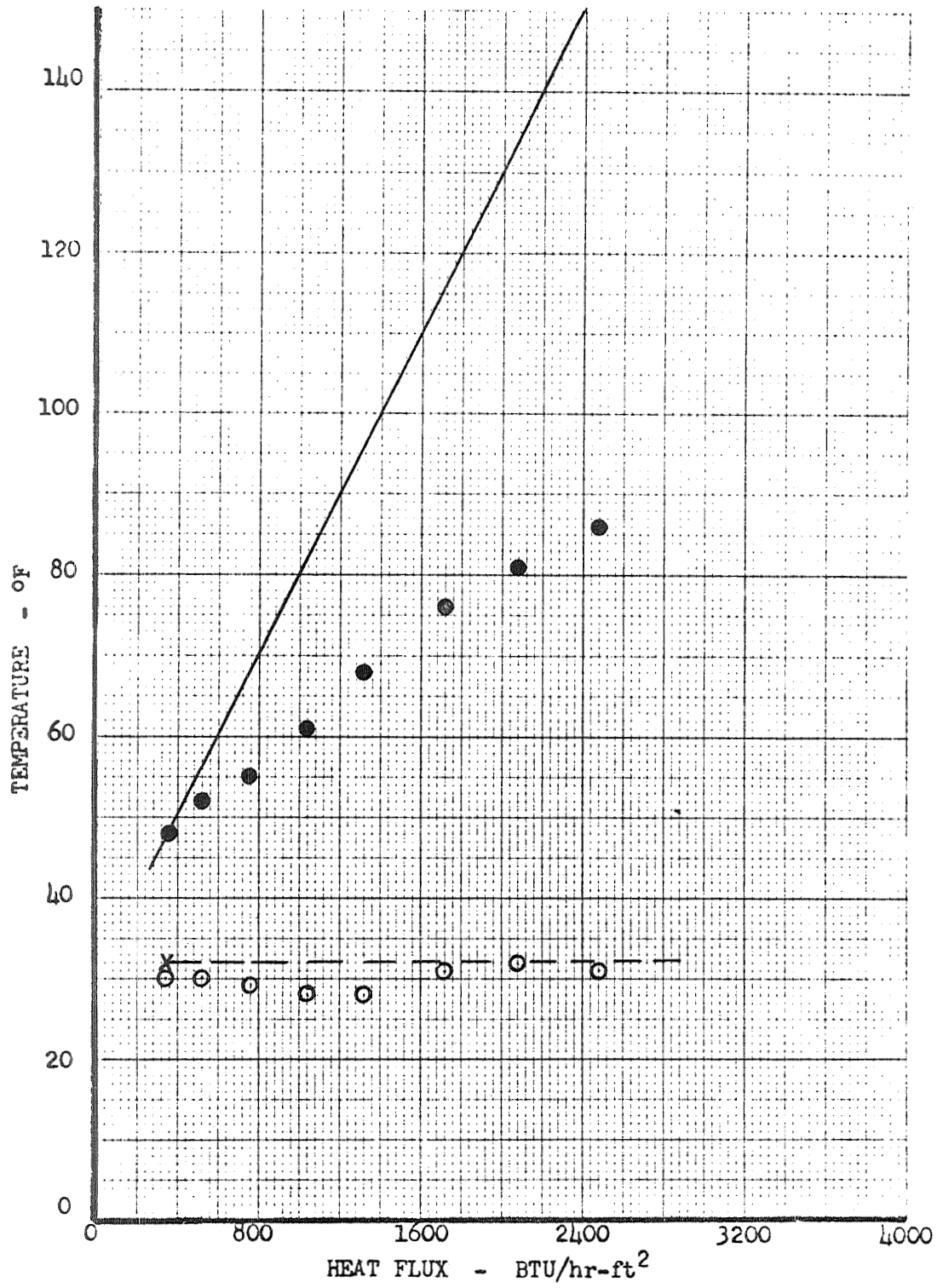
Figure 8

Porous Plate and Heater Plate Temperatures vs. Heat Flux for Plate 1
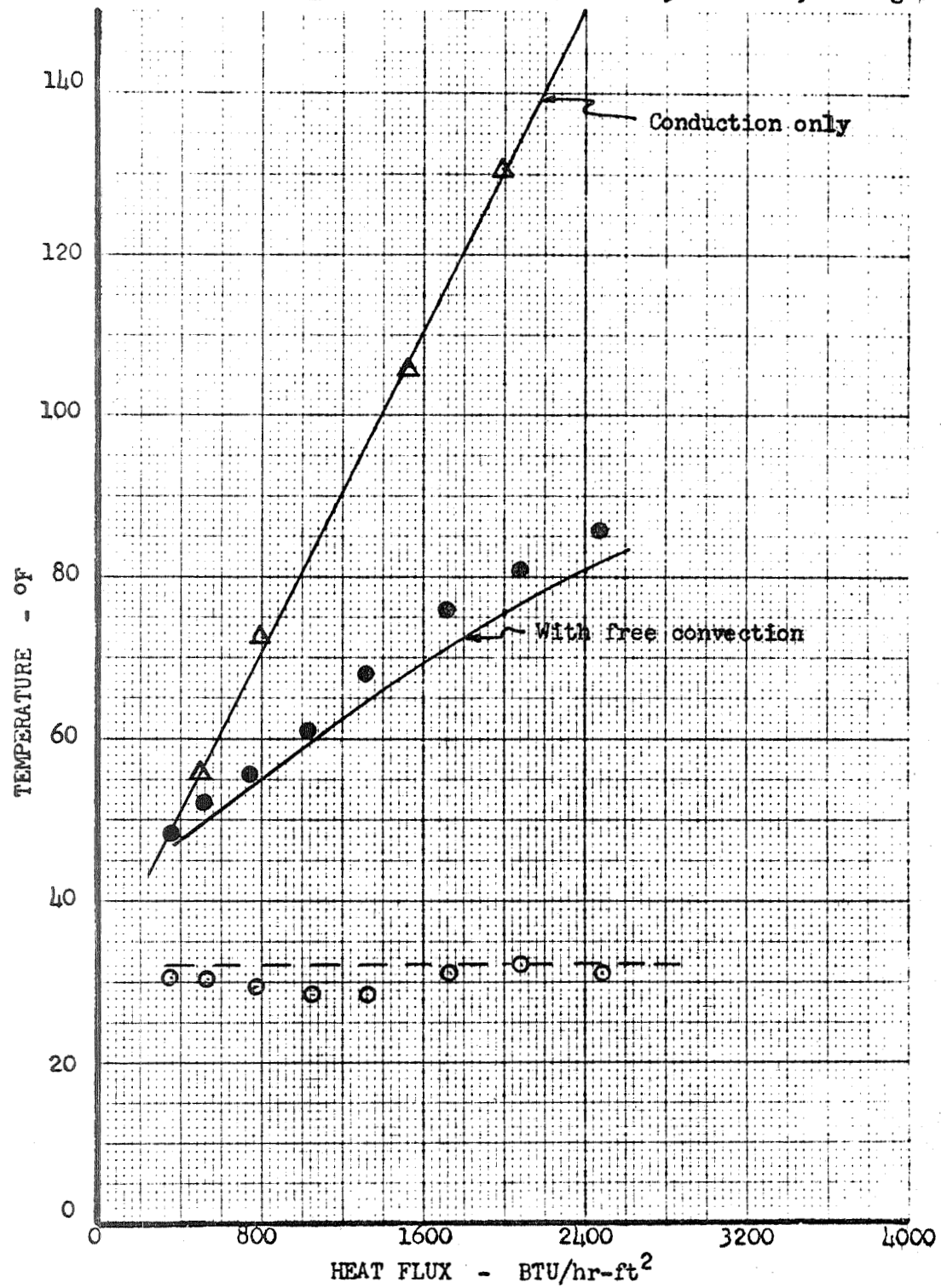
Figure 9

Porous Plate and Heater Plate Temperatures vs. Heat Flux for Plate 1
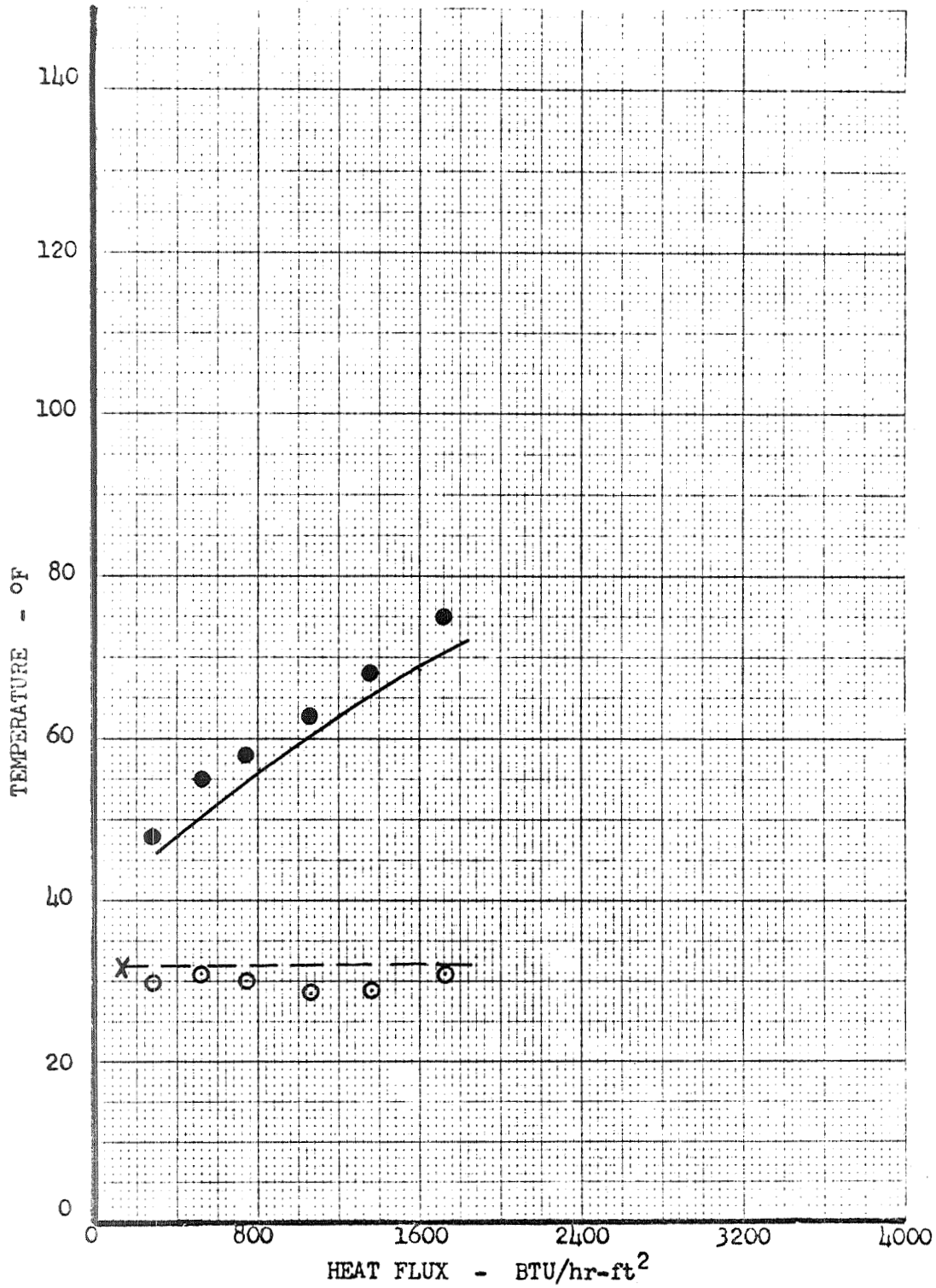
Figure 10

Porous Plate and Heater Plate Temperatures vs. Heat Flux for Plate 2
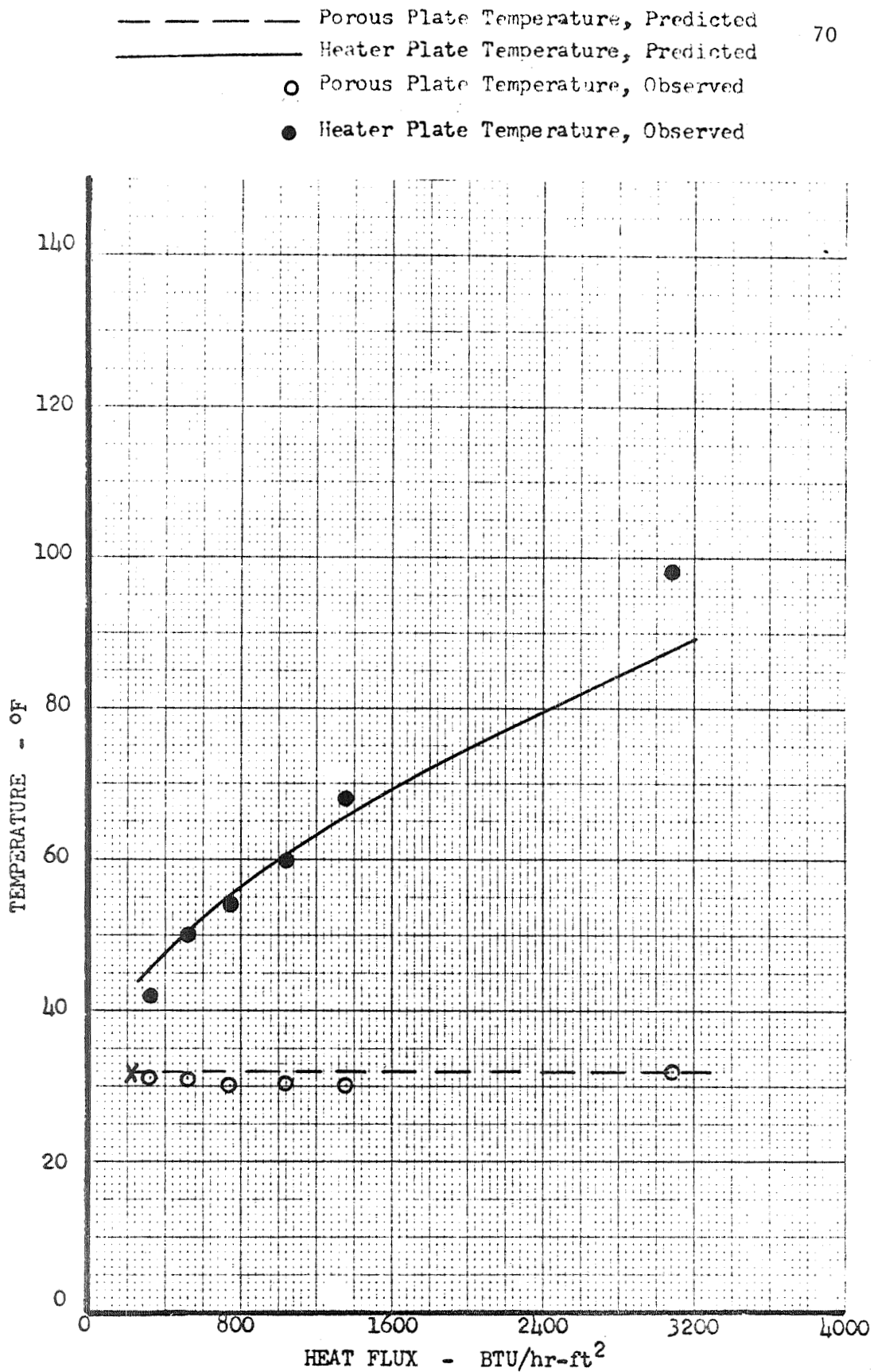
Figure 11

Porous Plate and Heater Plate Temperatures vs. Heat Flux for Plate 3

Porous Plate Temperature, Predicted

Heater Plate Temperature, Predicted

○ Porous Plate Temperature, Observed

● Heater Plate Temperature, Observed
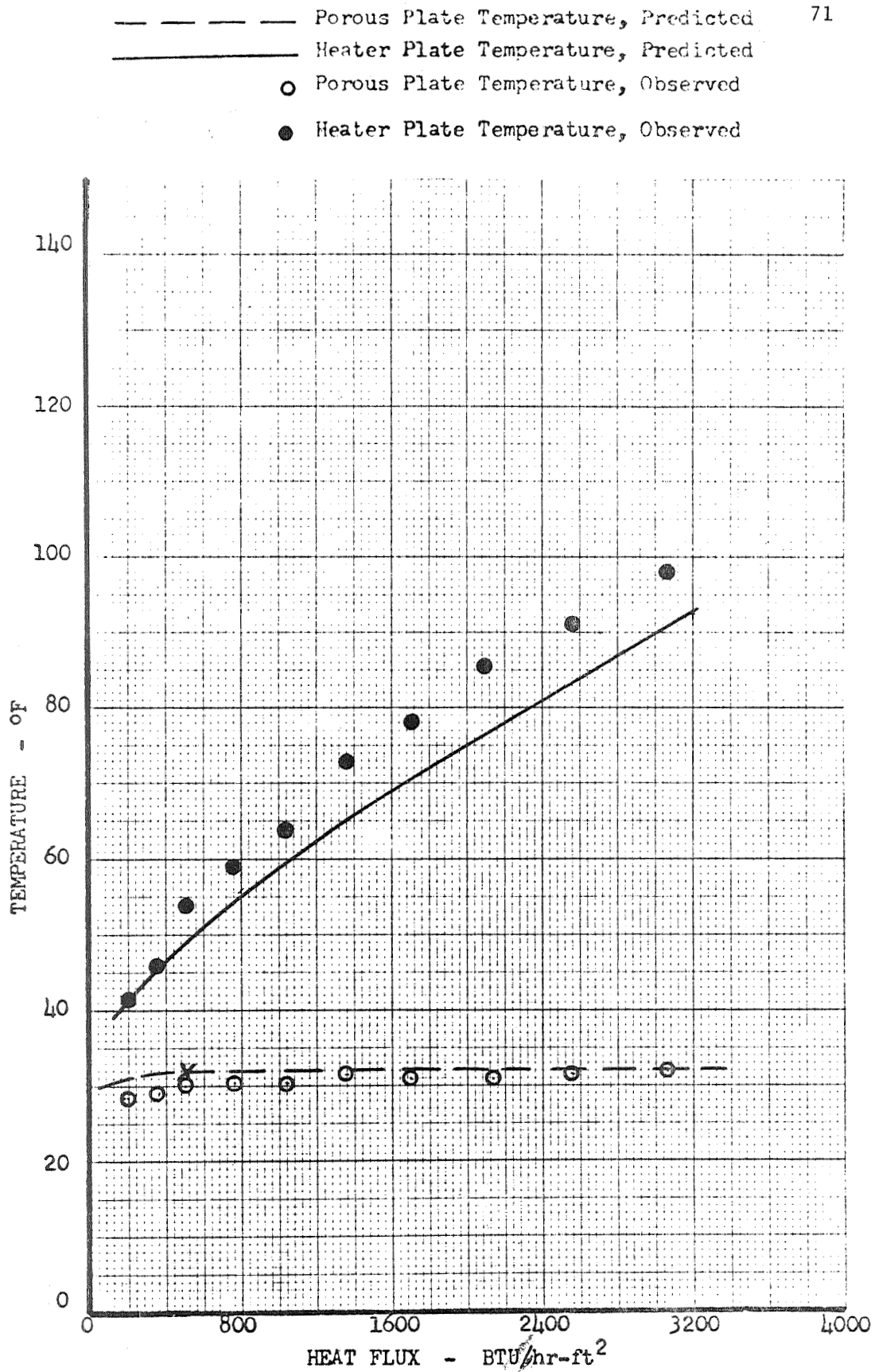
Figure 12

Porous Plate and Heater Plate Temperatures vs. Heat Flux for Plate 4
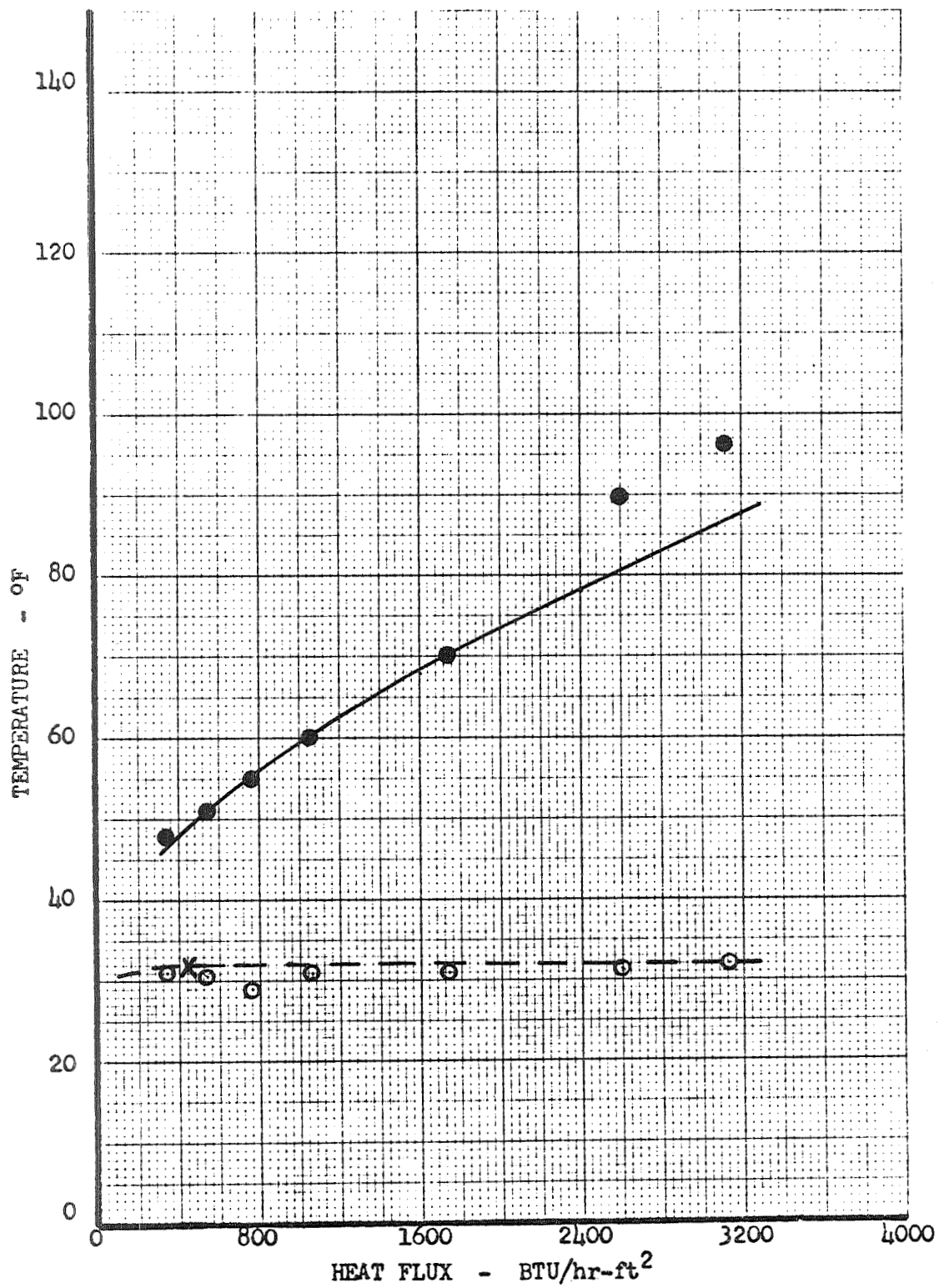
Figure 13

Porous Plate and Heater Plate Temperatures vs. Heat Flux for Plate 5
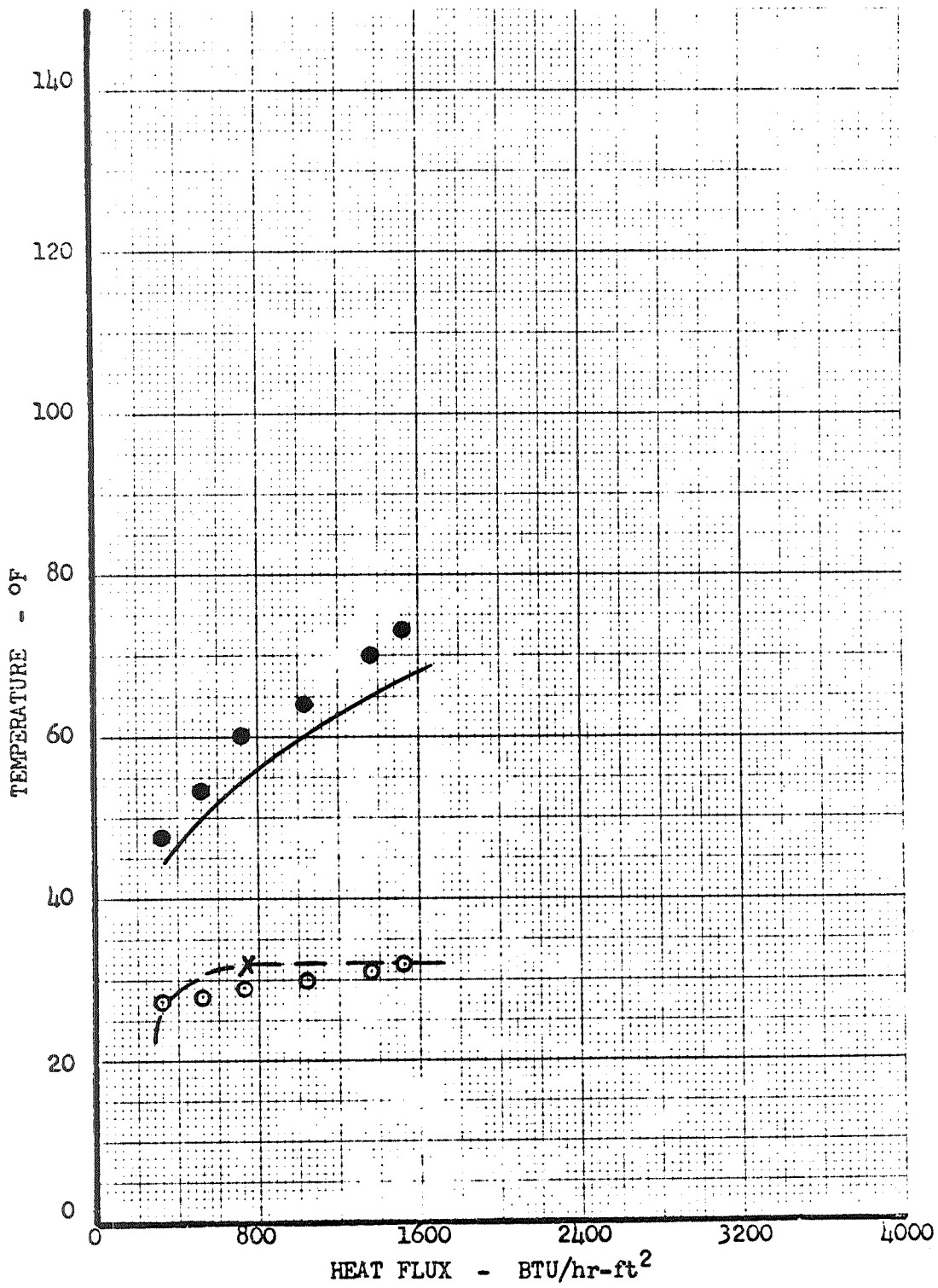
Figure 14

Porous Plate and Heater Plate Temperatures vs. Heat Flux for Plate 6
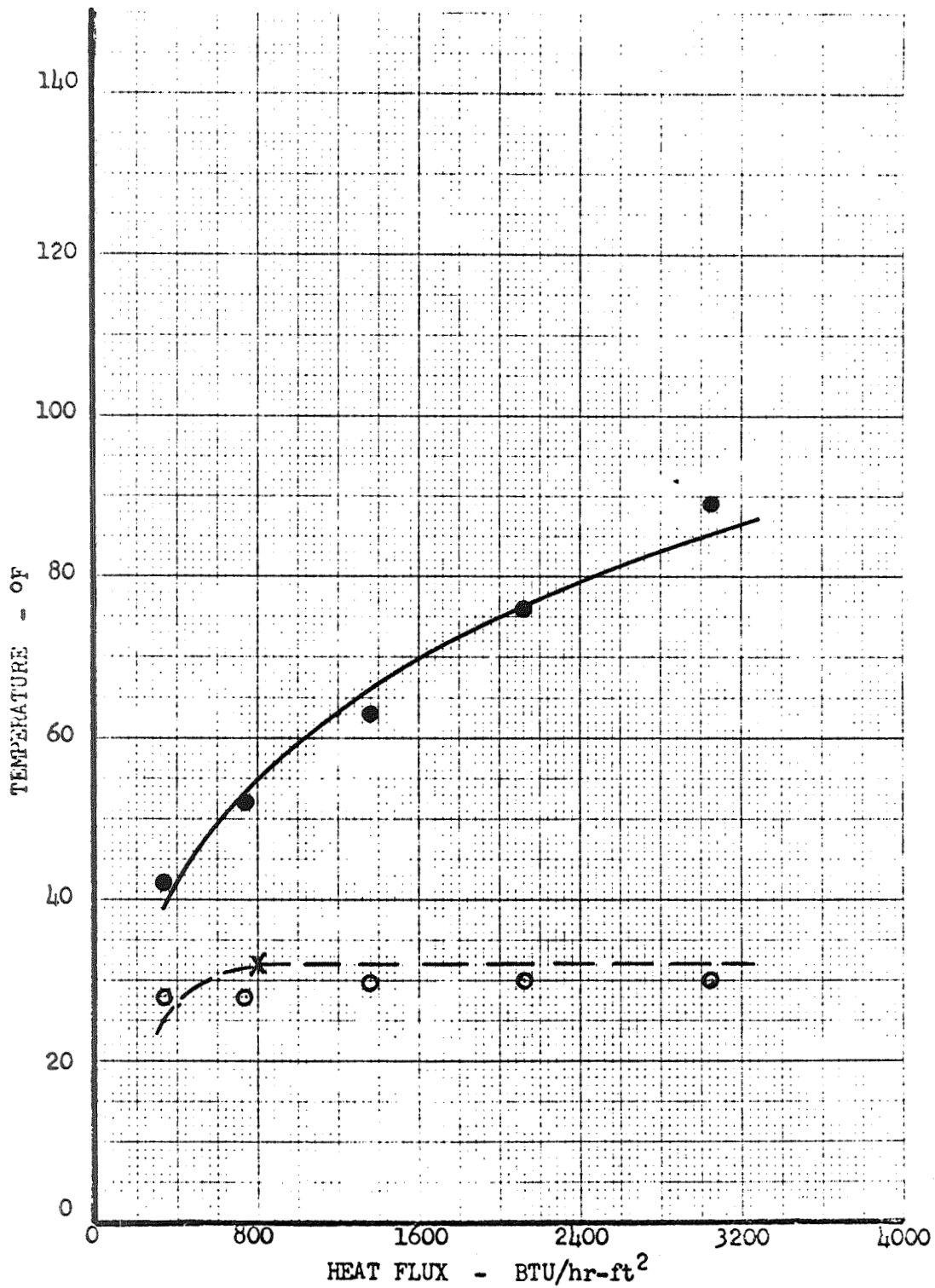
Figure 15

Porous Plate and Heater Plate Temperatures vs. Heat Flux for Plate 7
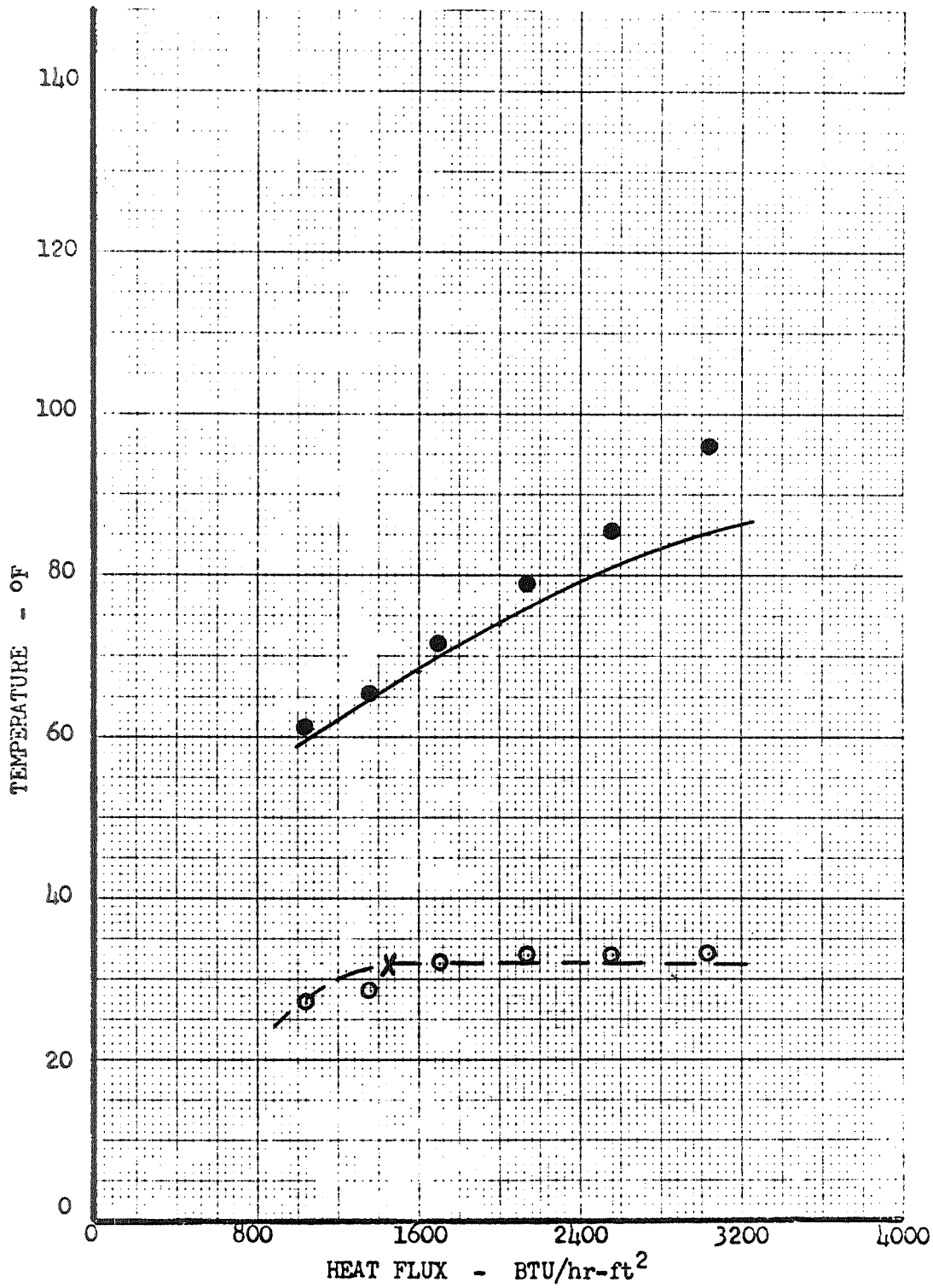
Figure 16

Porous Plate and Heater Plate Temperatures vs. Heat Flux for Plate 8

Legend (as shown on figure):

— Breakthrough, water with zero contact angle

○ Breakthrough, Heat flux 8160 BTU/hr-ft^2

● Breakthrough, Heat Flux 3040 BTU/hr-ft^2

△ Breakthrough, Heat flux 2120 BTU/hr-ft^2

X-axis: Pore Diameter, microns

Y-axis: Pressure Difference, psi
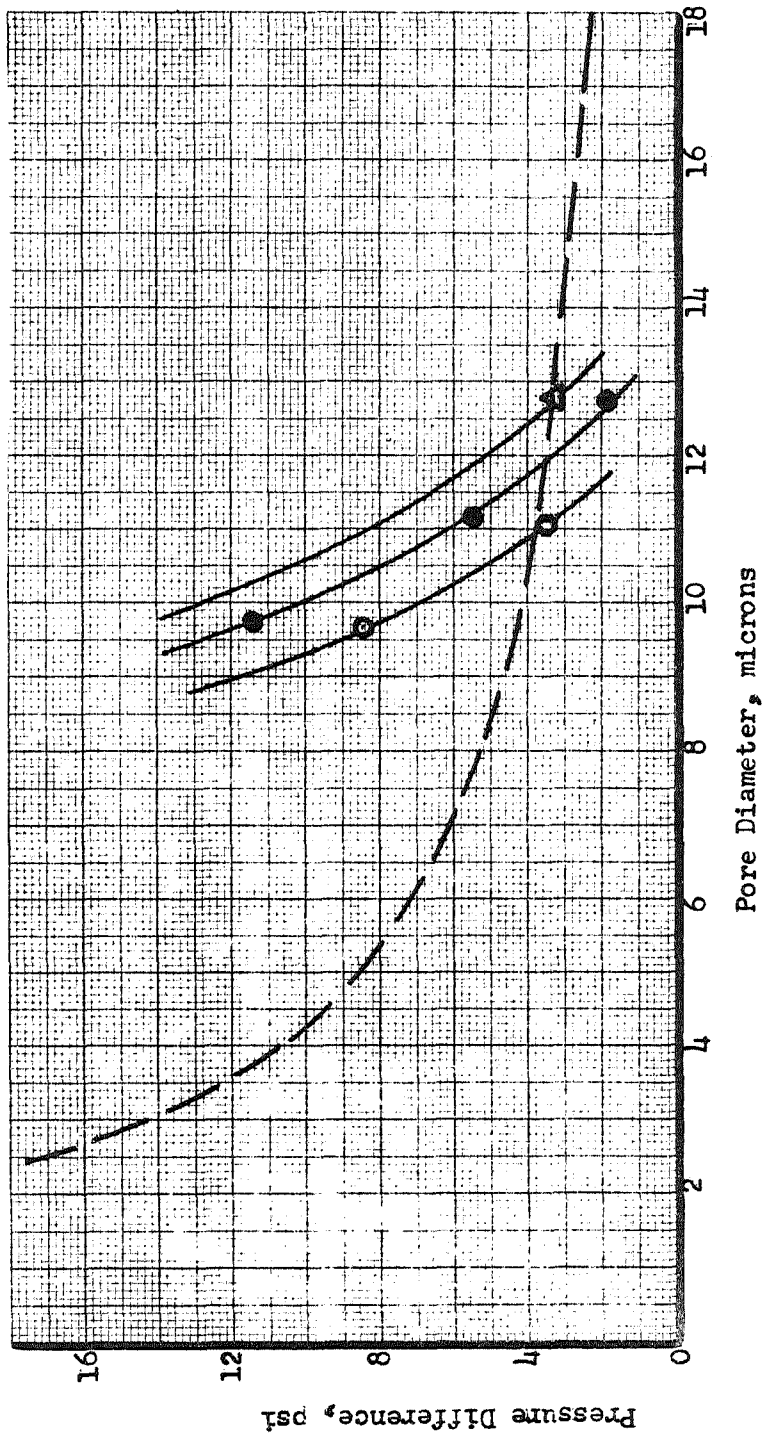
Figure 17

Breakthrough Pressure Difference vs. Pore Diameter
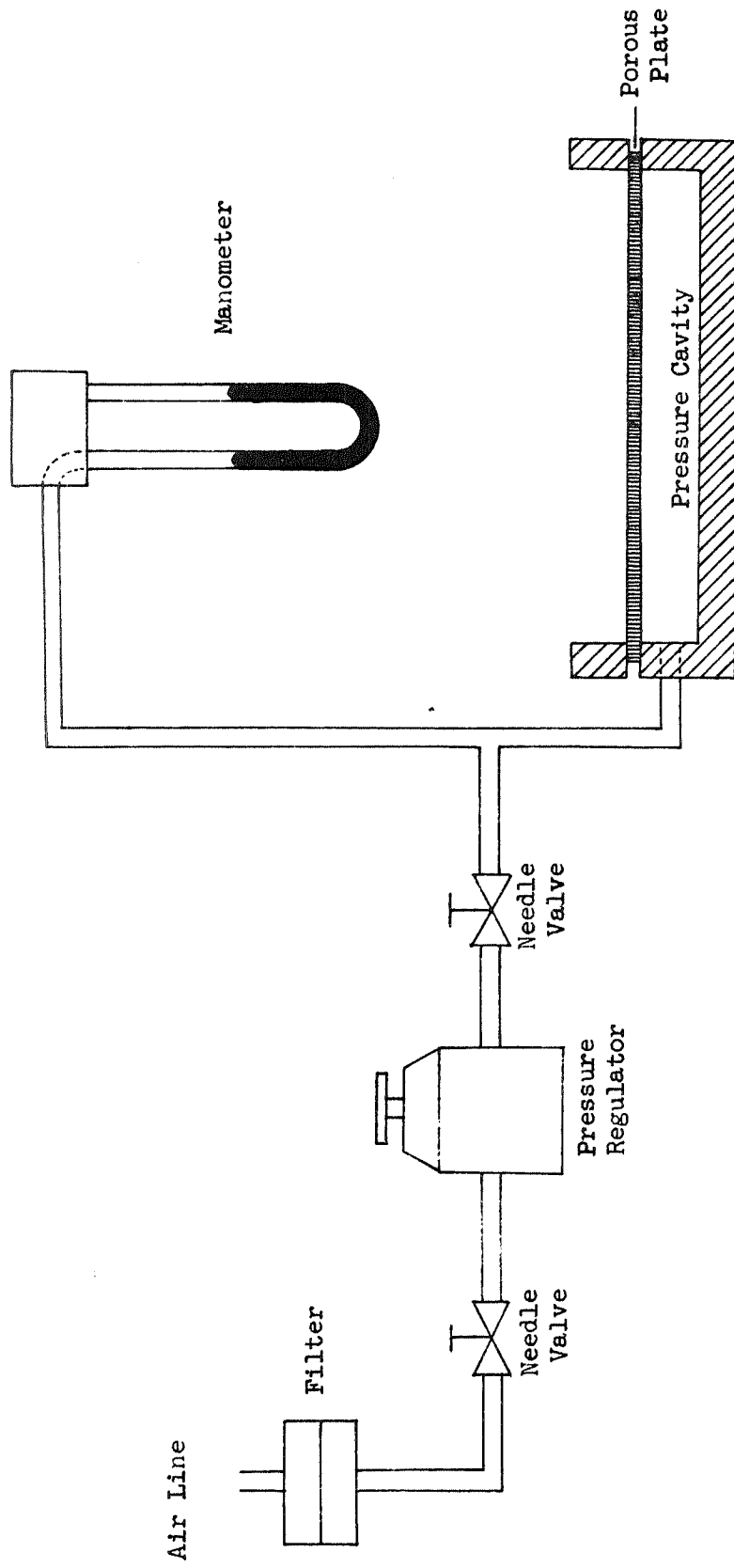
Figure 18

Schematic of the Bubble Test Apparatus
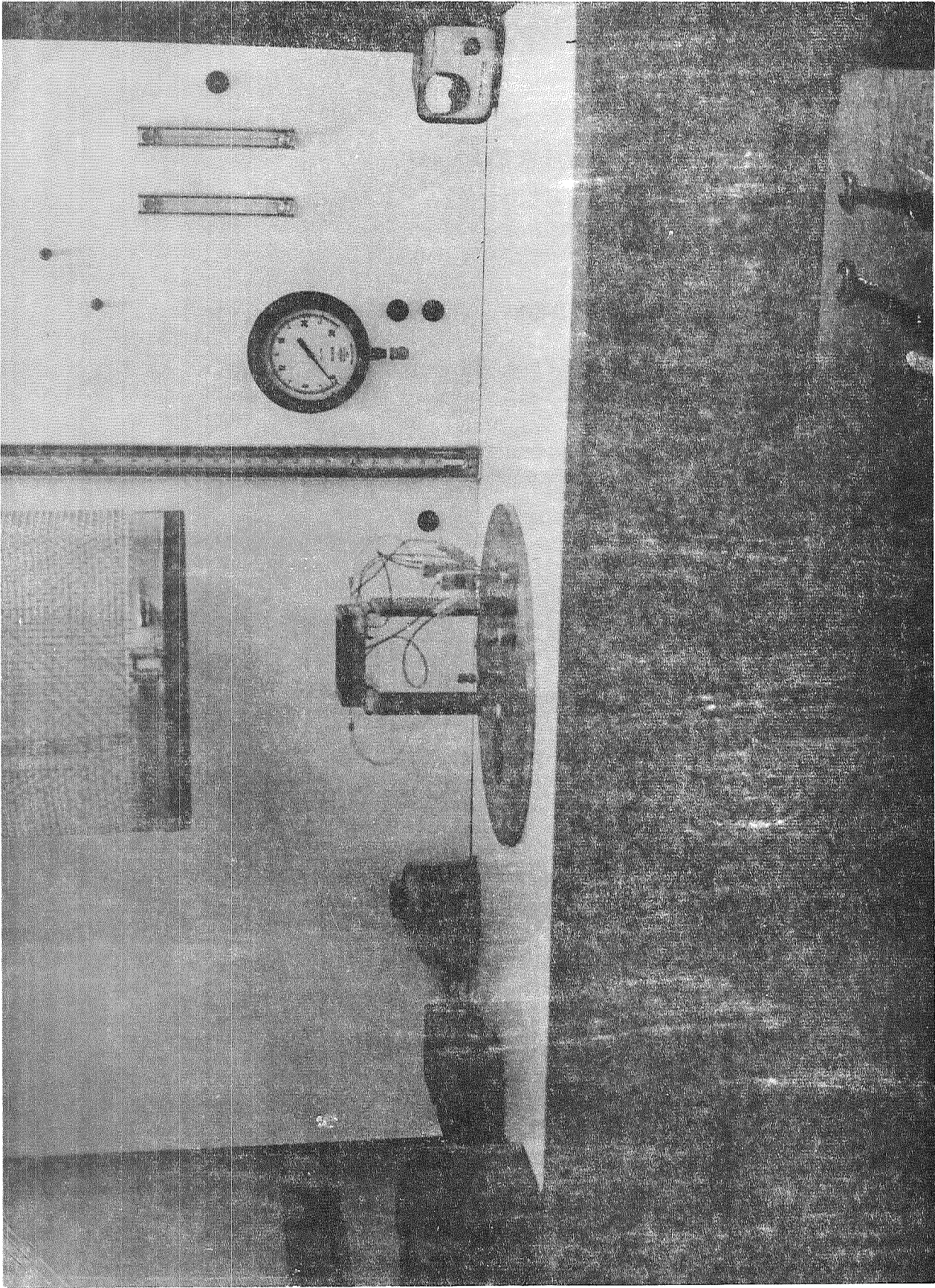
Figure 19

Complete Test Facility
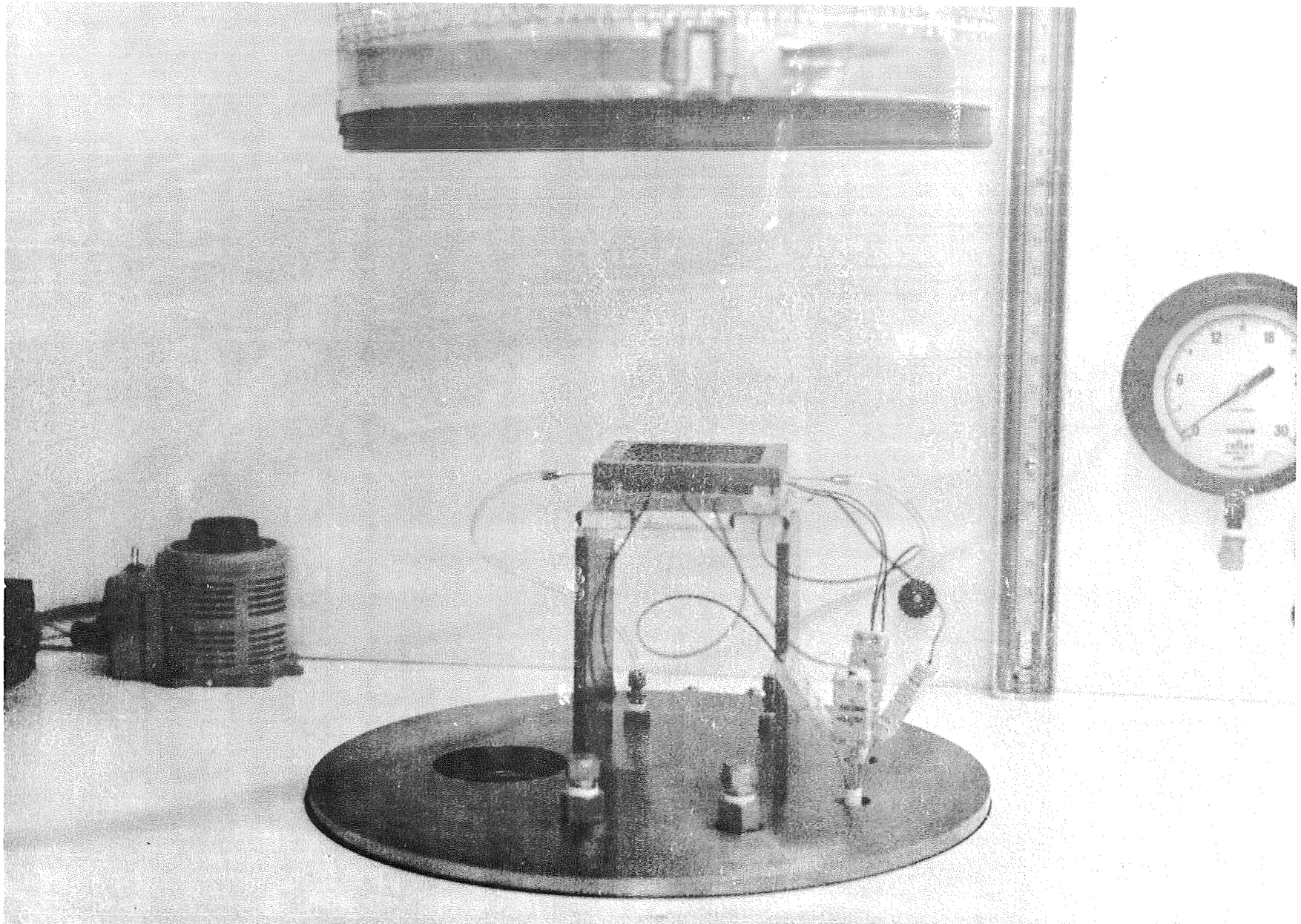
Figure 20

Electrically Heated Test Module Set Up In The Vacuum Chamber
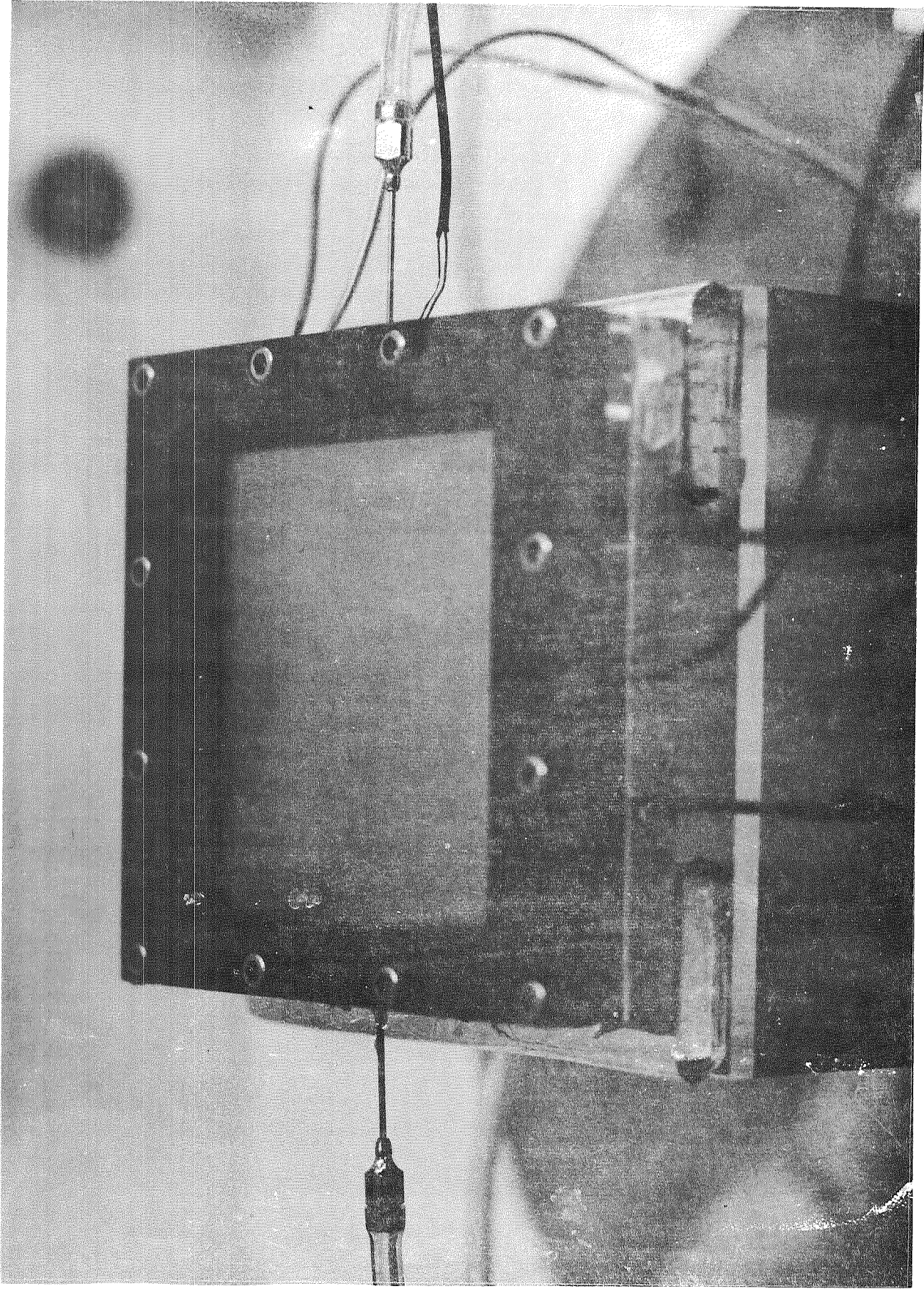
Figure 21

Electrically Heated Test Module
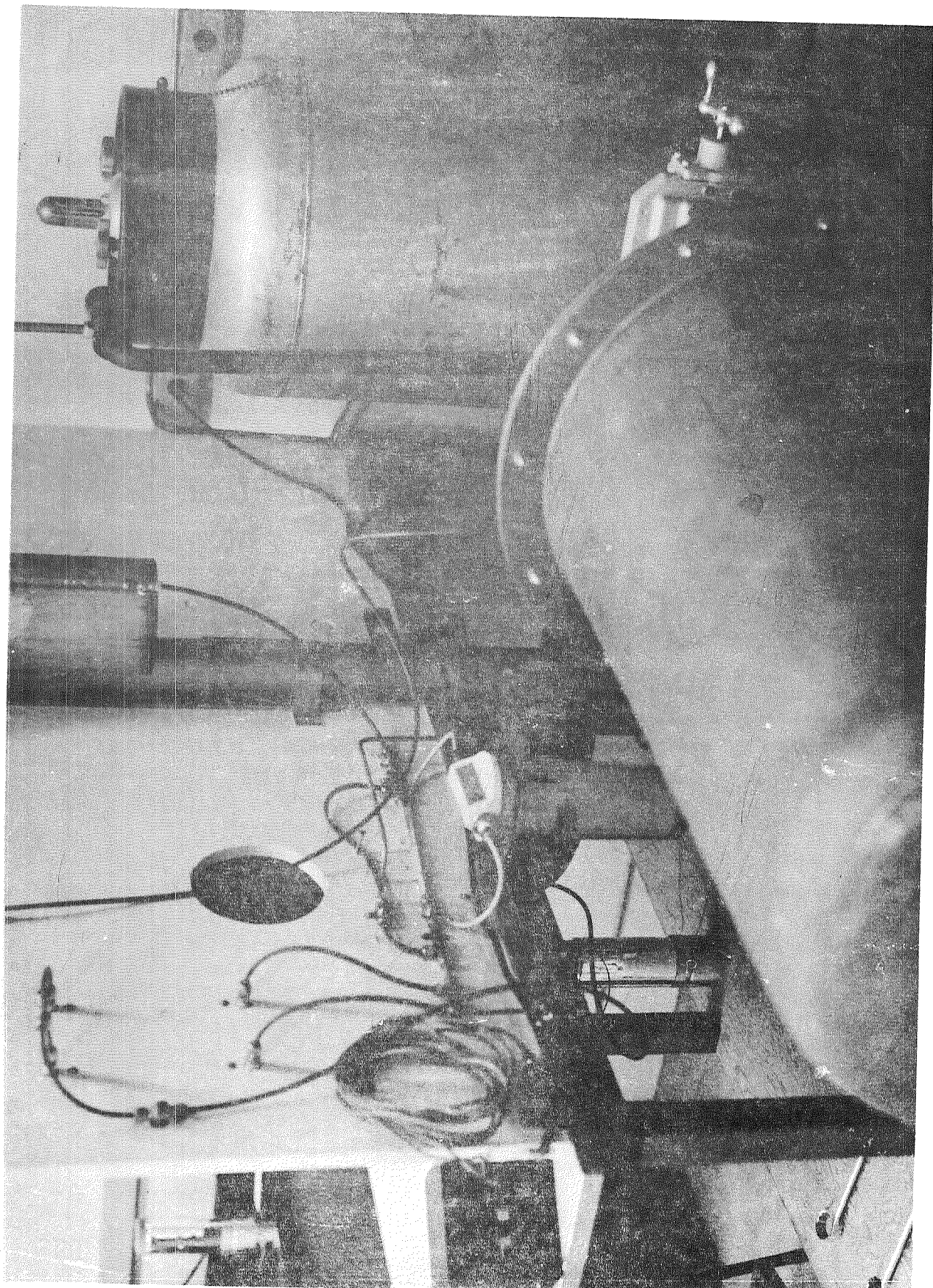
Figure 22

Water Feed System and Cold Trap
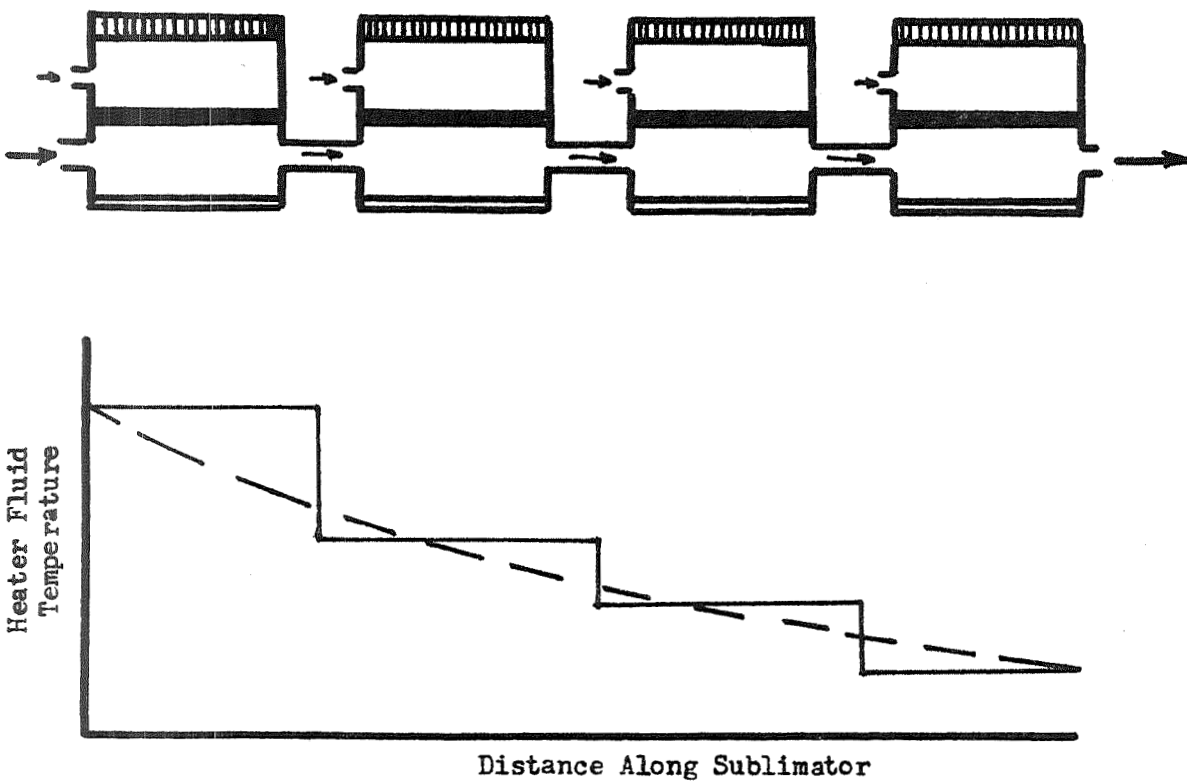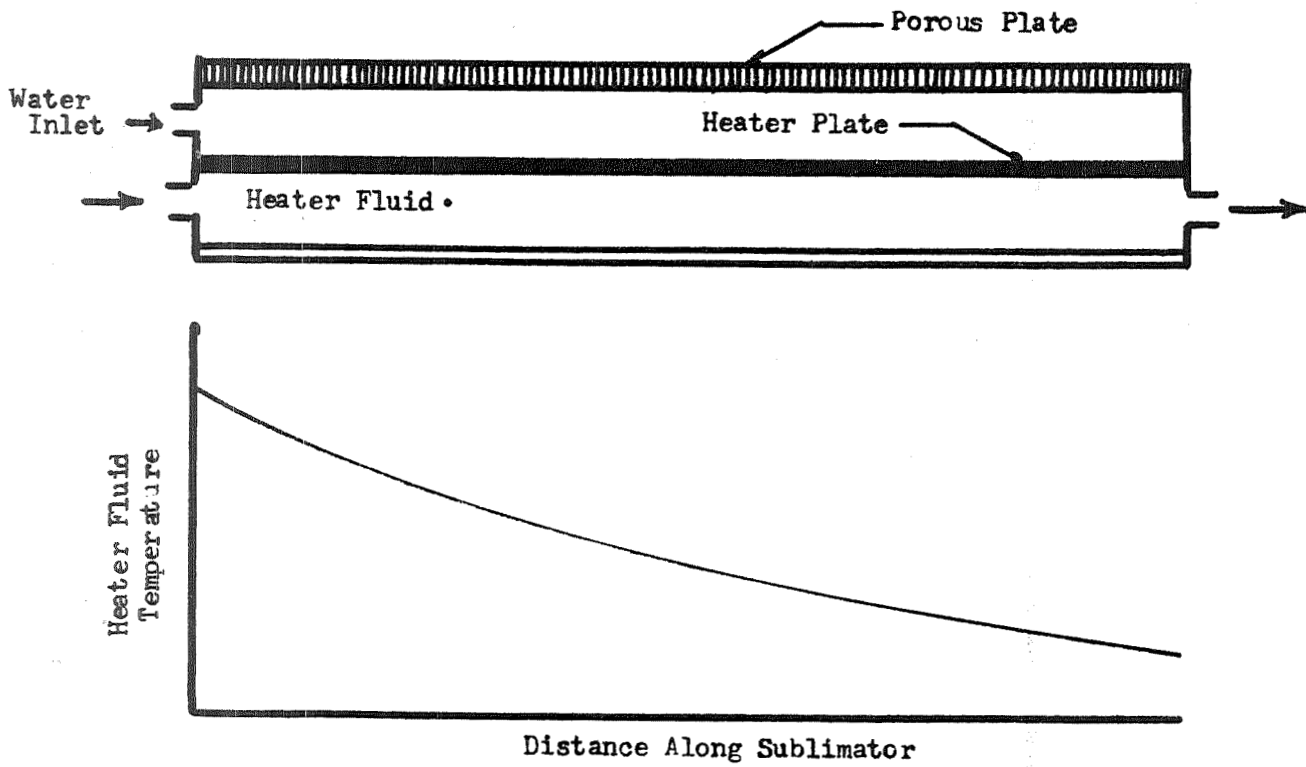
Figure 23

Model Representation of Fluid-Heated Sublimator Unit
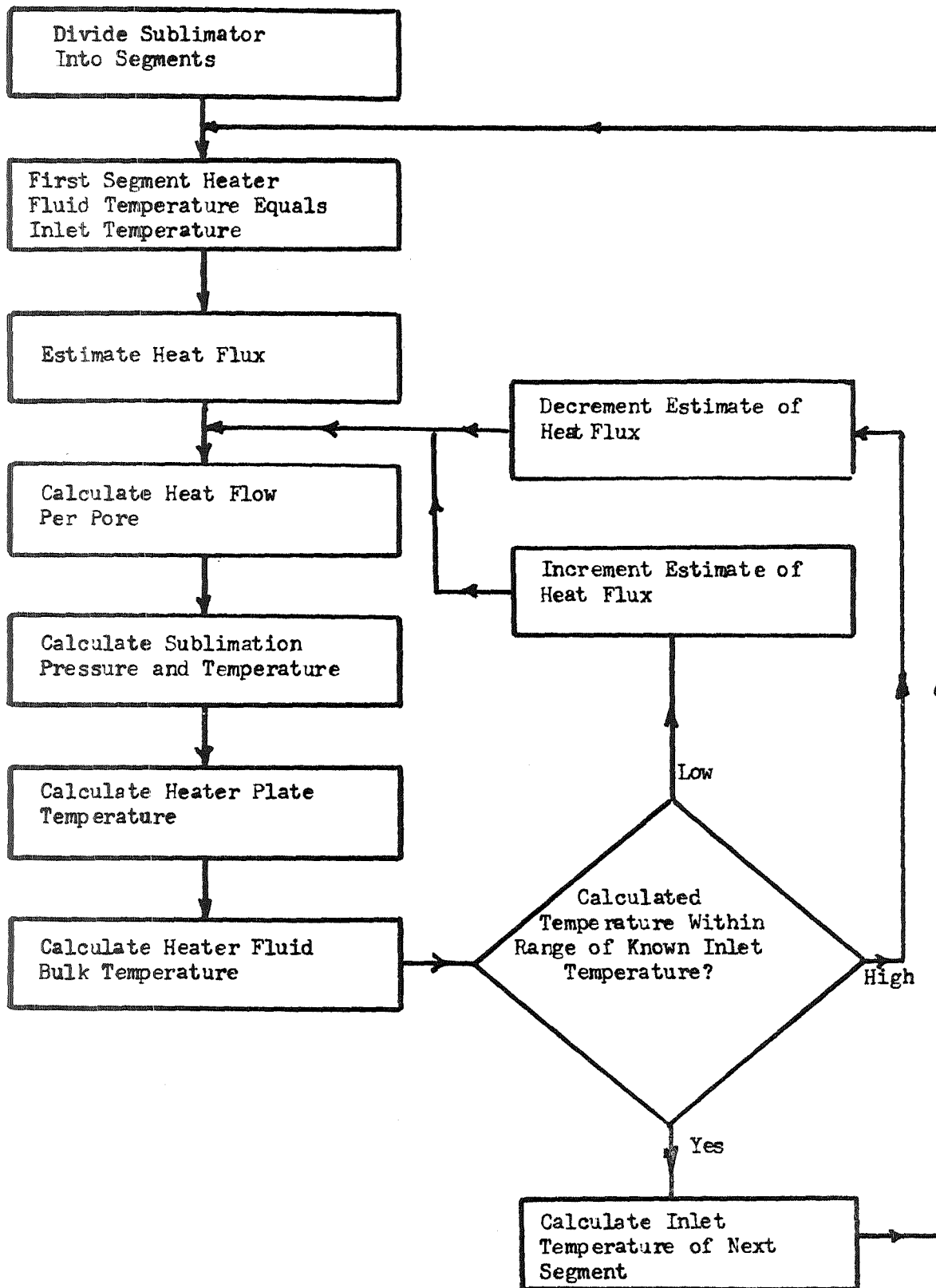
Figure 24

Performance Calculation Scheme for Fluid-Heated Unit

Figure 25

Schematic Diagram of Test Apparatus
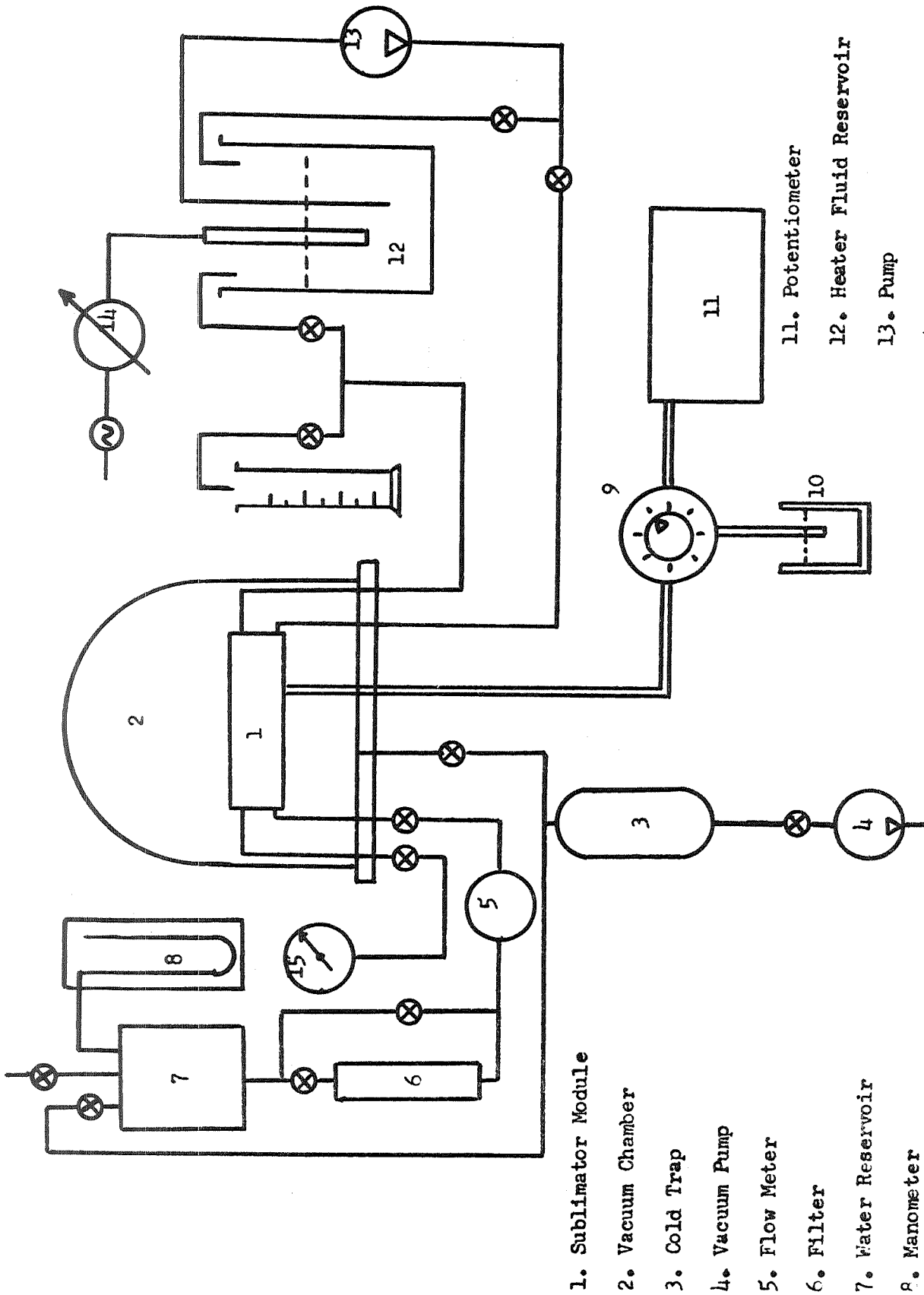
1. Sublimator Module

2. Vacuum Chamber

3. Cold Trap

4. Vacuum Pump

5. Flow Meter

6. Filter

7. Water Reservoir

8. Manometer

9. Thermocouple Switch

10. Reference Junction

11. Potentiometer

12. Heater Fluid Reservoir

13. Pump

14. Powerstat

15. Water Chamber Pressure Gage
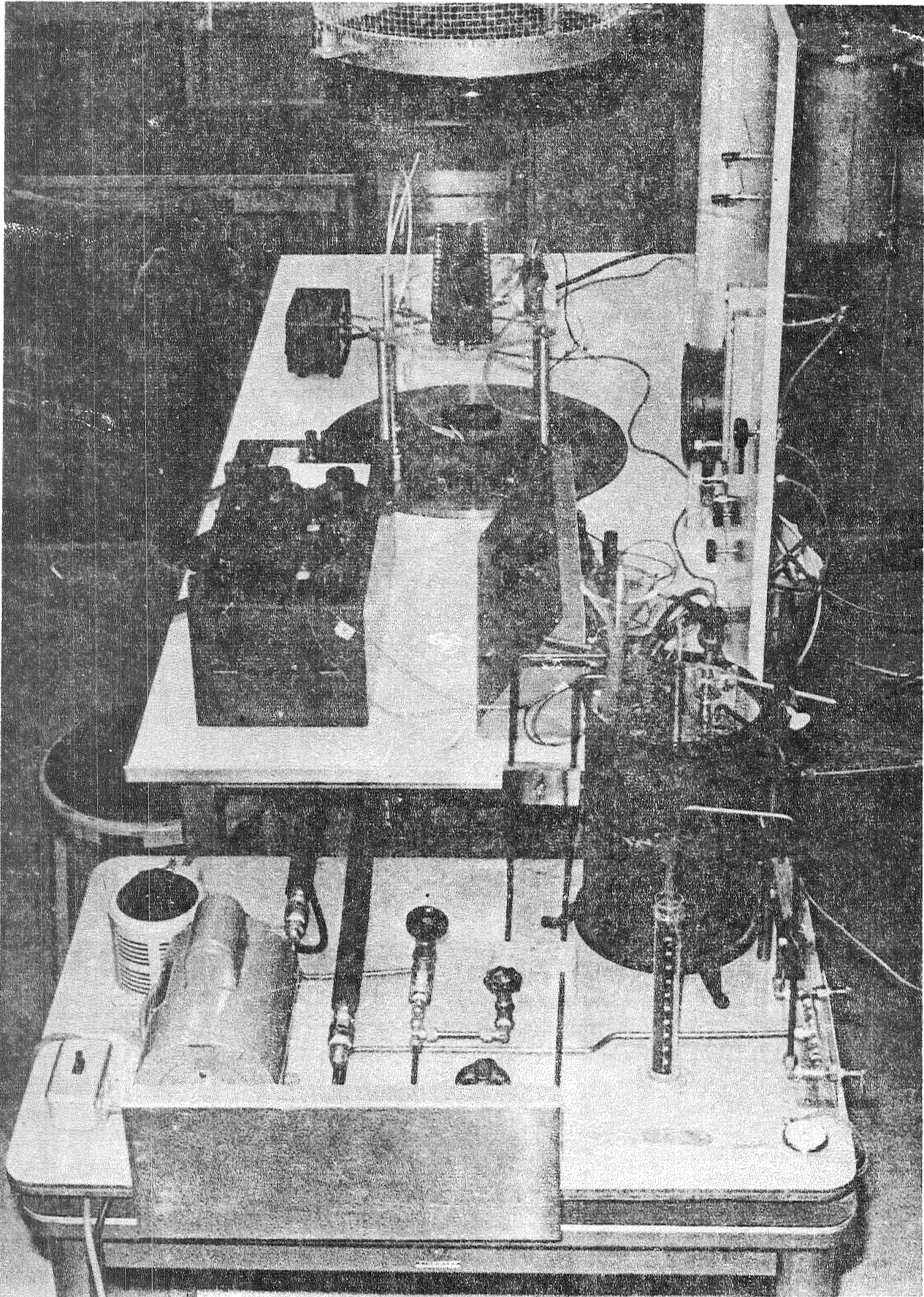
Figure 26

Photograph of Test Apparatus
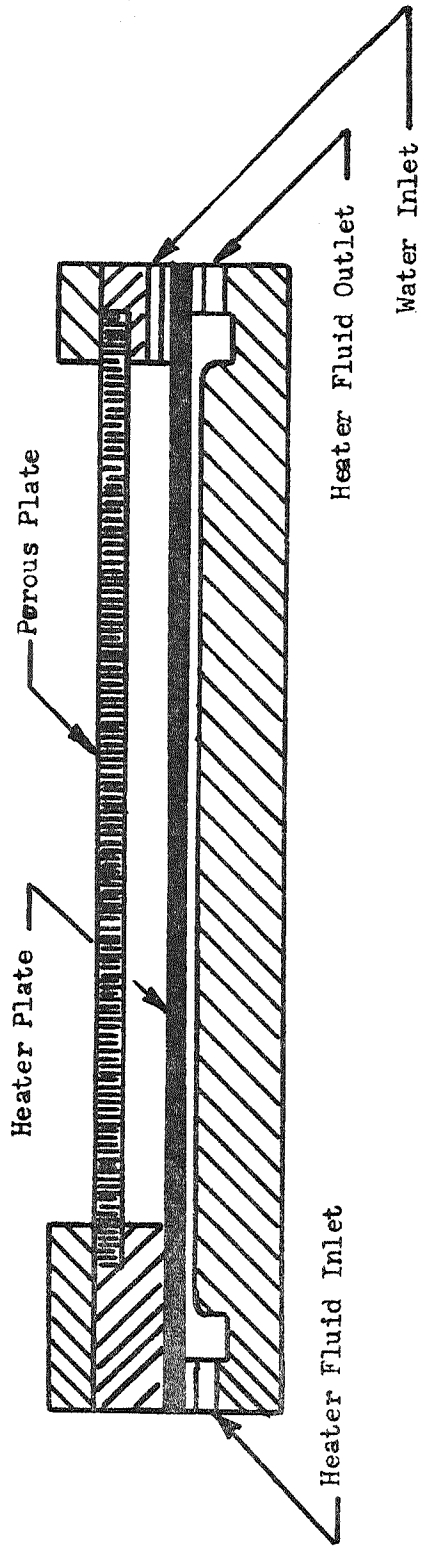
Figure 27

Schematic Diagram of Fluid-Heated Sublimator Unit
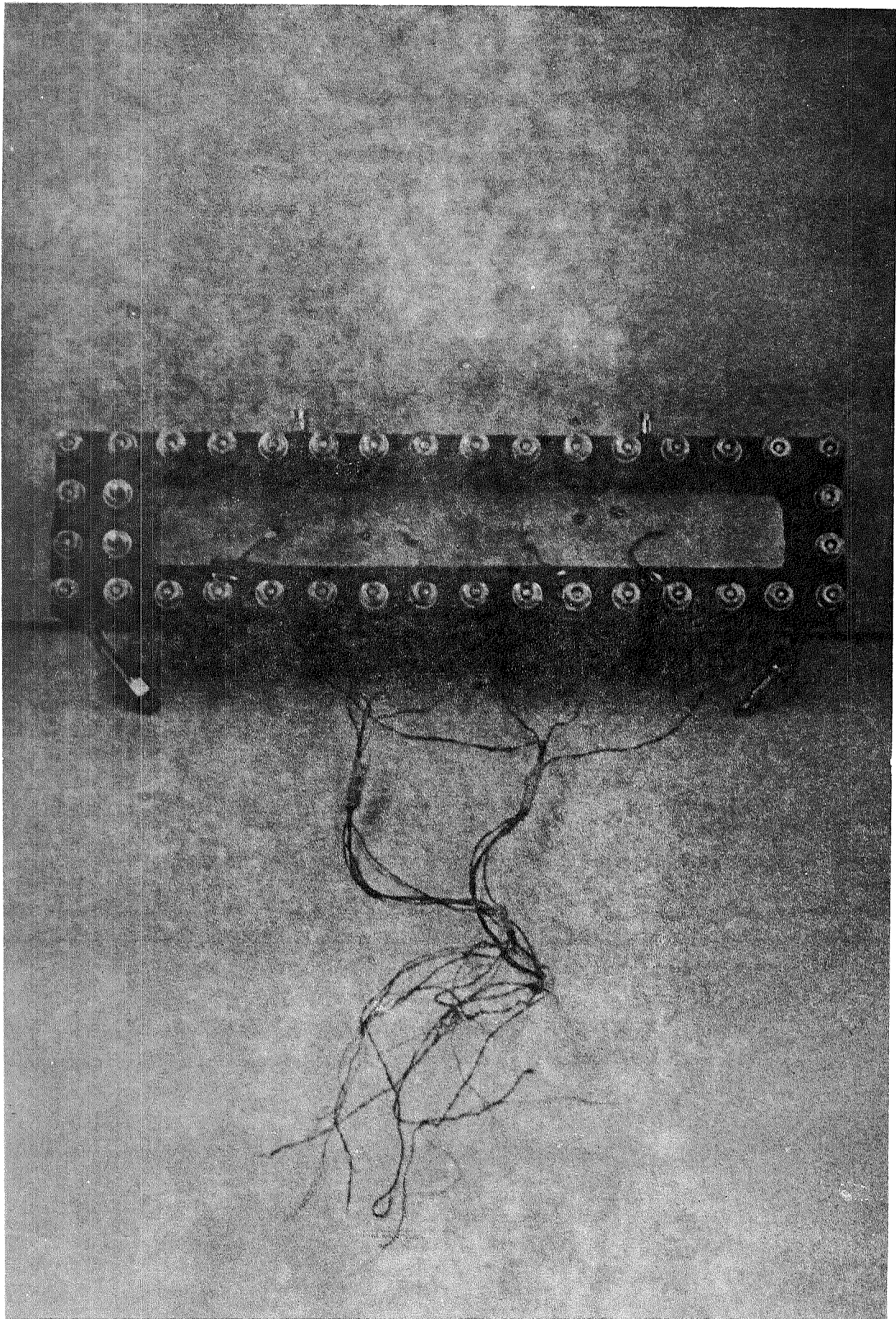
Figure 28
Photograph of Fluid-Heated Test Unit
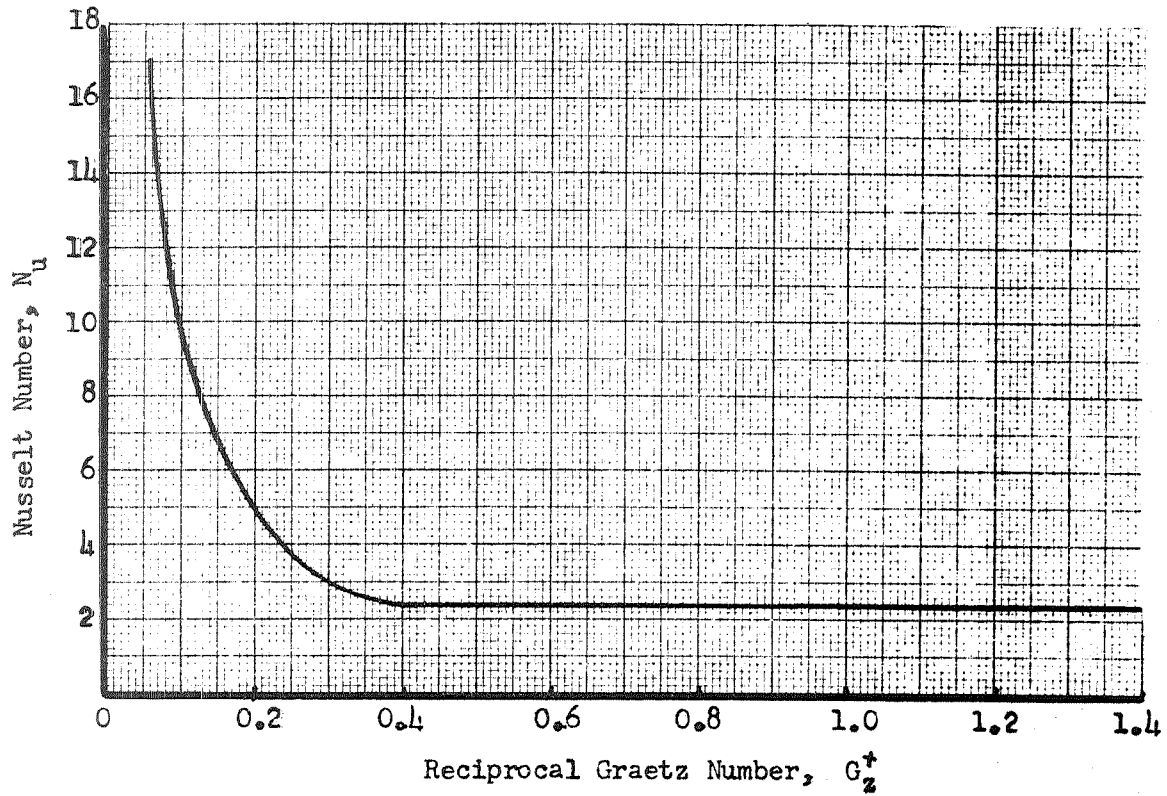
Figure 29

Heater Plate Heat Transfer Correlation
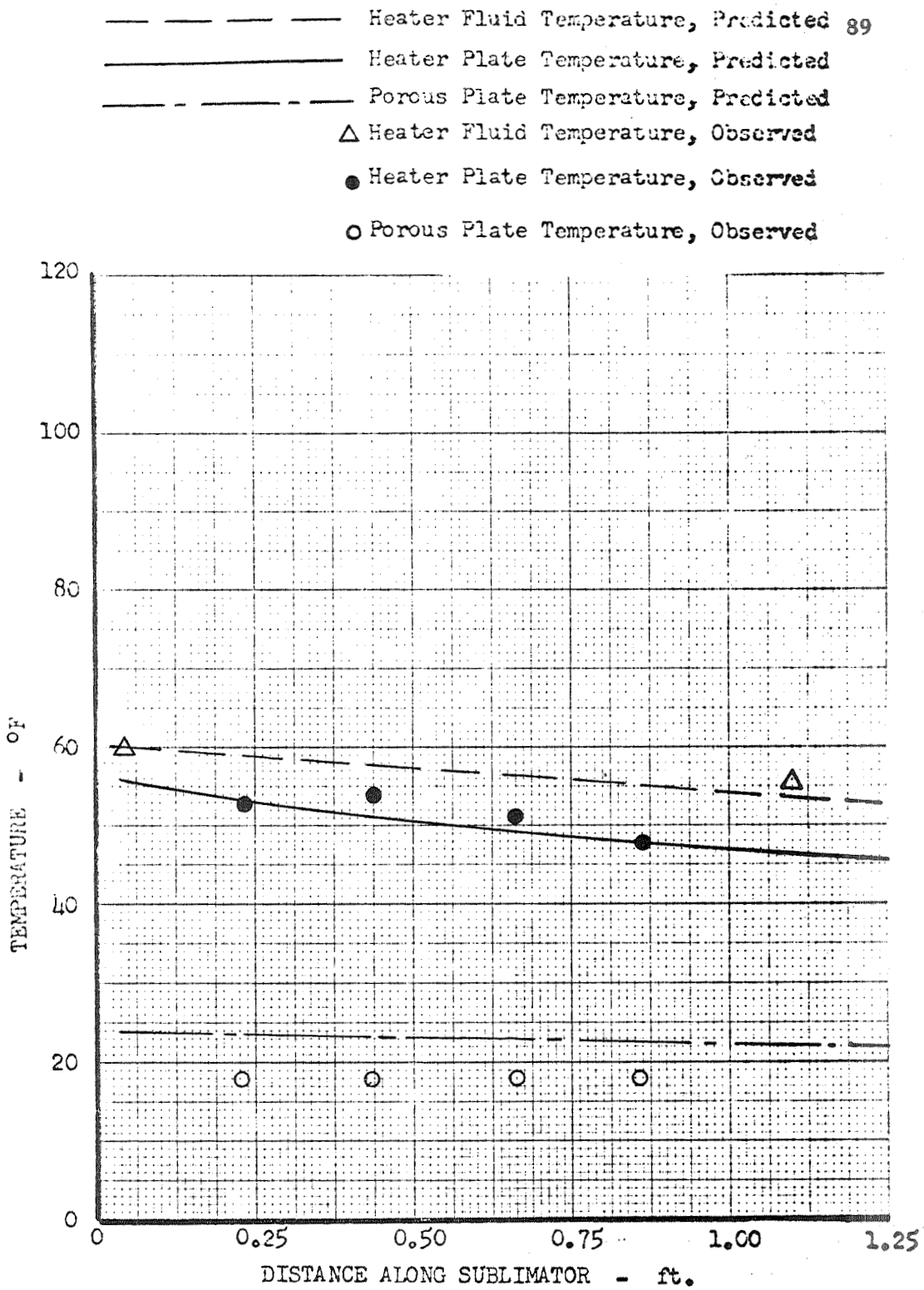
Figure 30
Test No. 1
Predicted and Observed Temperatures vs. Distance
for Fluid-Heated Units

Porous Plate: A
Heater Fluid: Water
Flow Rate   : 21.8 Lbm/Hr
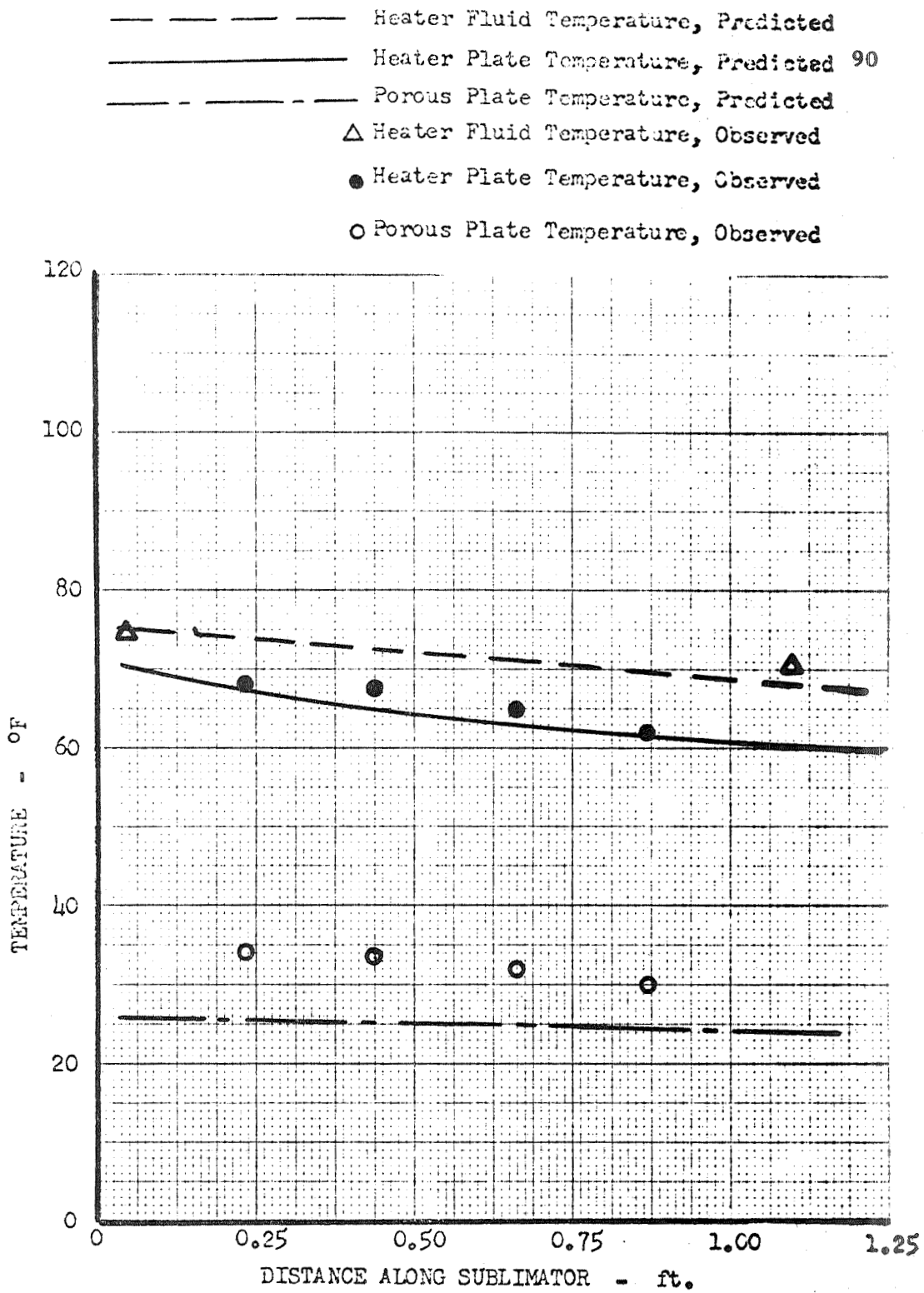
Figure 31
Test No. 2
Predicted and Observed Temperatures vs. Distance
for Fluid-Heated Units

Porous Plate: A
Heater Fluid: Water
Flow Rate : 22.2 Lbm/Hr
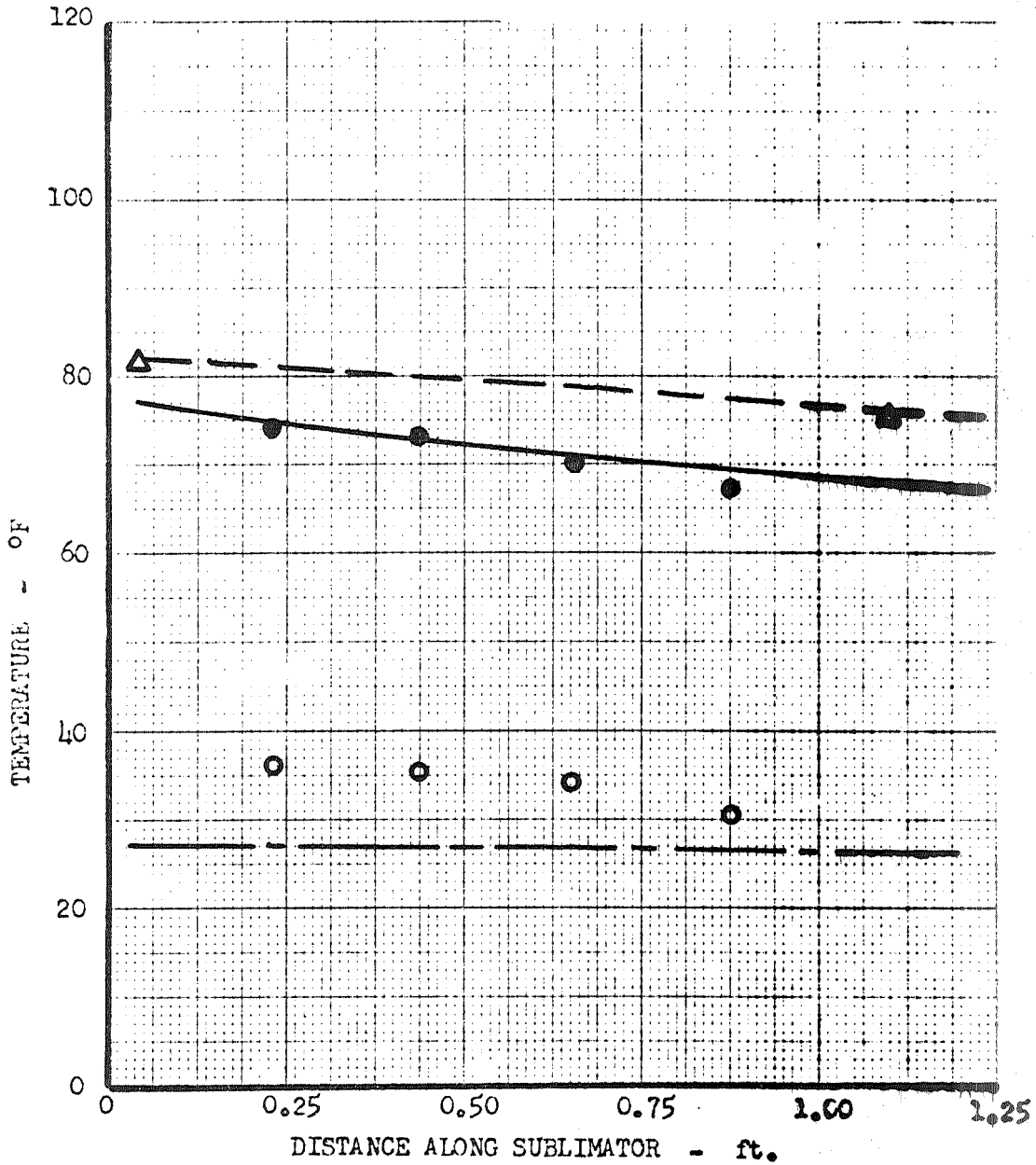
Figure 32
Test No. 3
Predicted and Observed Temperatures vs. Distance
for Fluid-Heated Units

Porous Plate: A
Heater Fluid: Water
Flow Rate   : 27.0 Lbm/Hr

— — — — Heater Fluid Temperature, Predicted

———————— Heater Plate Temperature, Predicted 92

— — — — Porous Plate Temperature, Predicted

△ Heater Fluid Temperature, Observed

● Heater Plate Temperature, Observed

○ Porous Plate Temperature, Observed


DISTANCE ALONG SUBLIMATOR — ft.
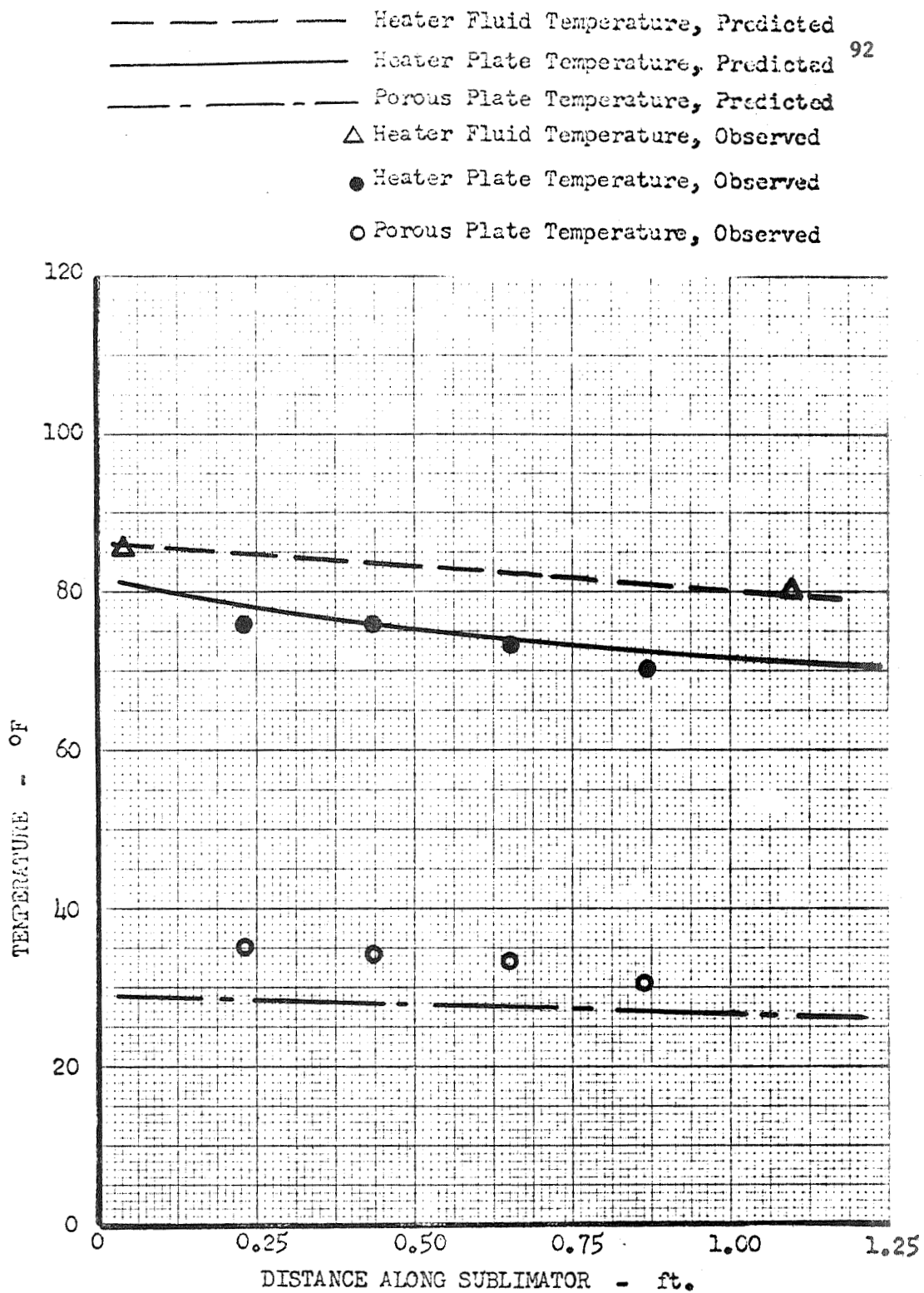
TEMPERATURE — °F

Figure 33
Test No. 4
Predicted and Observed Temperatures vs. Distance
for Fluid-Heated Units

Porous Plate: A
Heater Fluid: Water
Flow Rate   : 21.8 Lbm/Hr
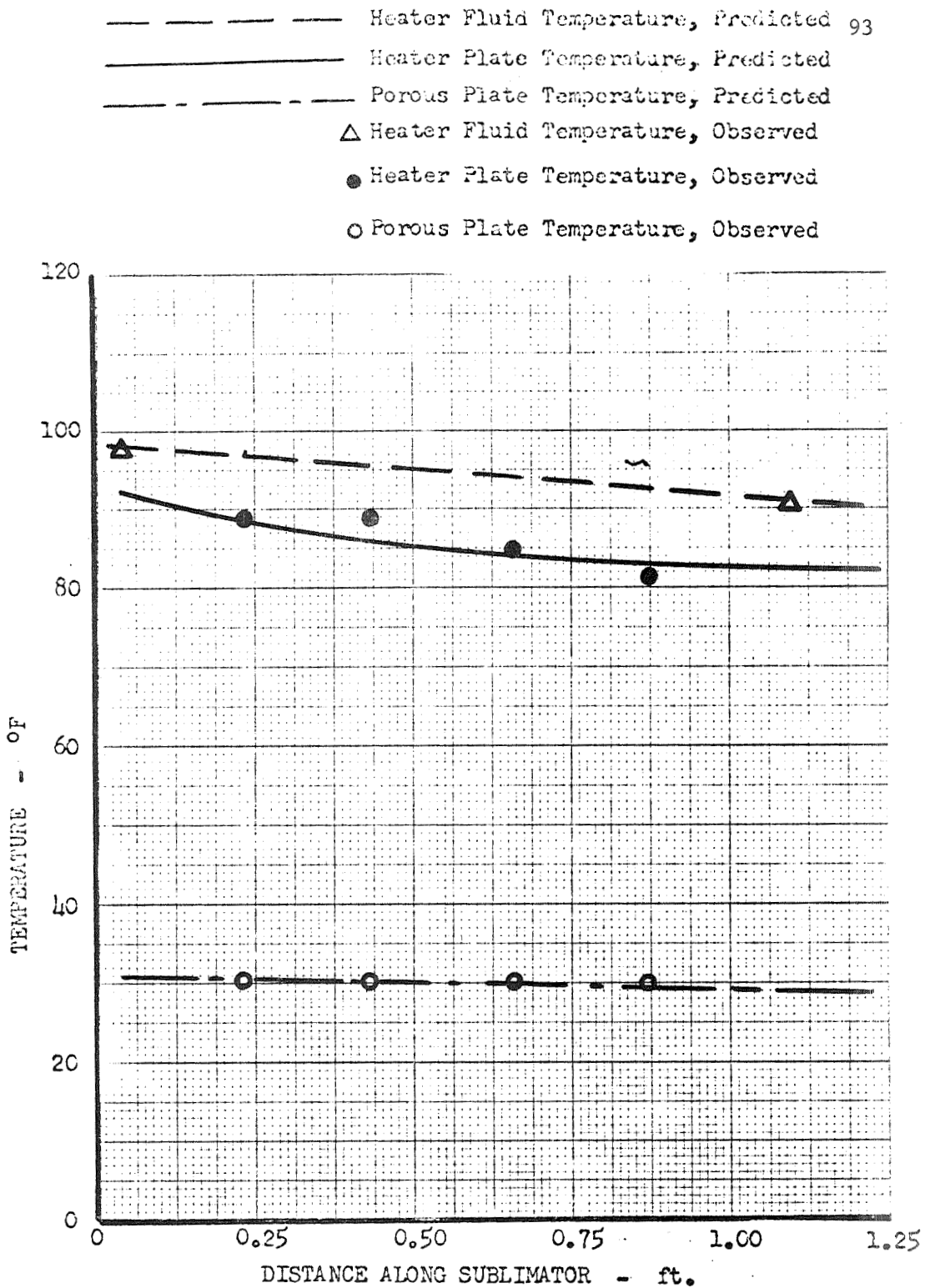
Figure 34
Test No. 5
Predicted and Observed Temperatures vs. Distance
for Fluid-Heated Units

Porous Plate: A
Heater Fluid: Water
Flow Rate   : 27.0 Lbm/Hr

— — — — — Heater Fluid Temperature, Predicted

———————— Heater Plate Temperature, Predicted

— — — — — — Porous Plate Temperature, Predicted

△ Heater Fluid Temperature, Observed

● Heater Plate Temperature, Observed

○ Porous Plate Temperature, Observed

DISTANCE ALONG SUBLIMATOR — ft.
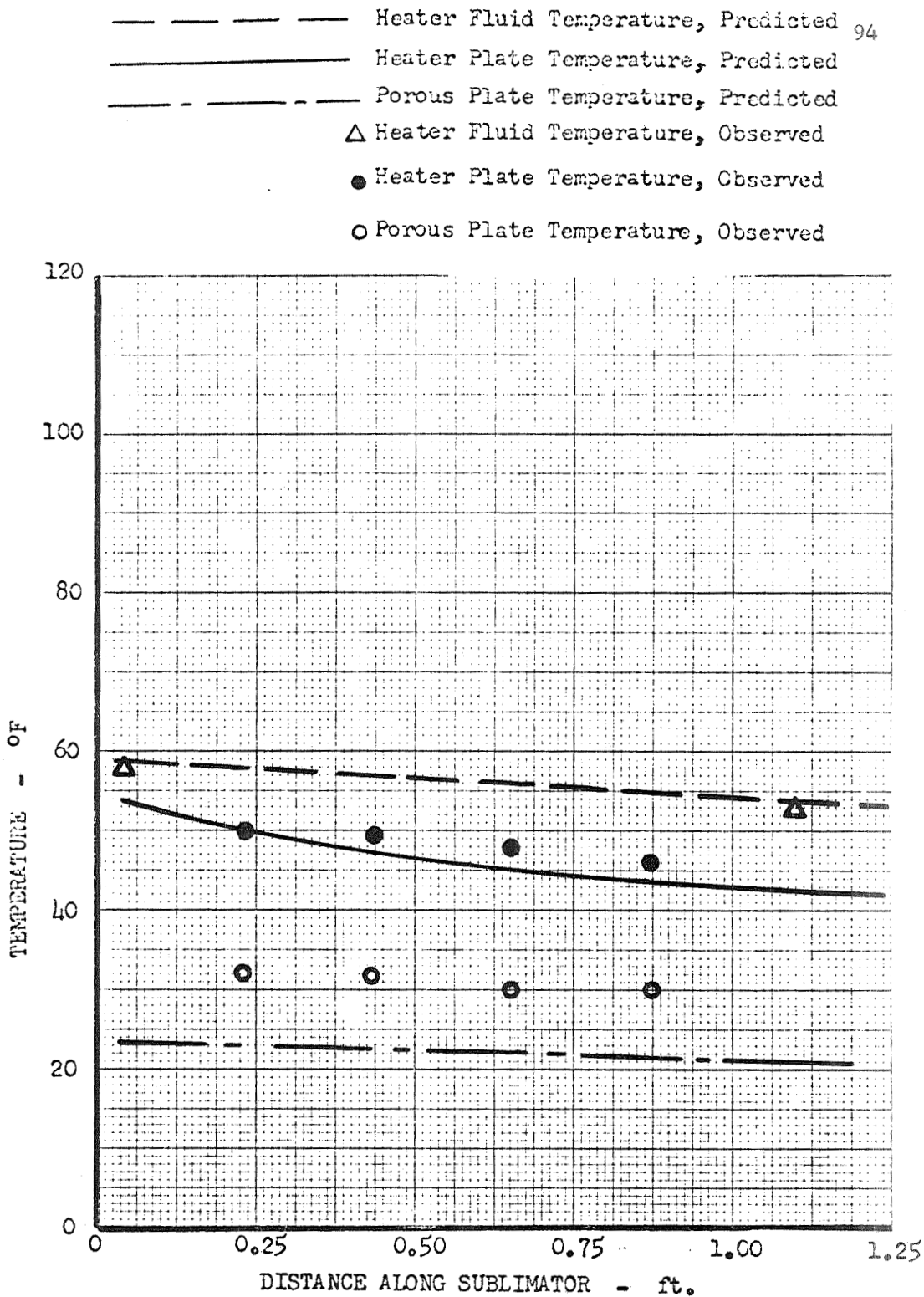
Figure 35
Test No. 6
Predicted and Observed Temperatures vs. Distance
for Fluid-Heated Units

Porous Plate: A
Heater Fluid: Water-Glycol
Flow Rate   : 29.0 Lbm/Hr
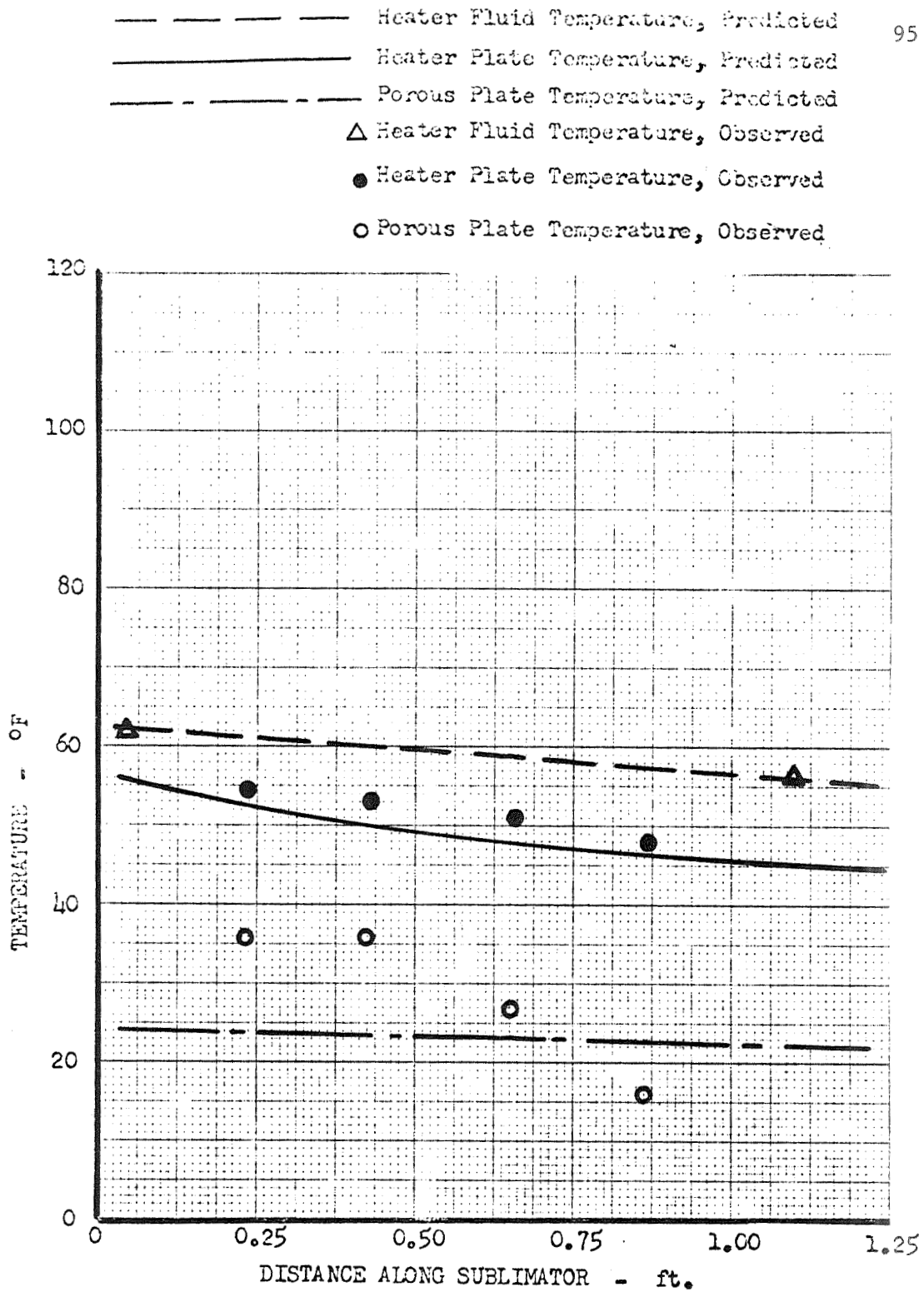
Figure 36
Test No. 7
Predicted and Observed Temperatures vs. Distance
for Fluid-Heated Units

Porous Plate: A
Heater Fluid: Water-Glycol
Flow Rate   : 26.2 Lbm/Hr
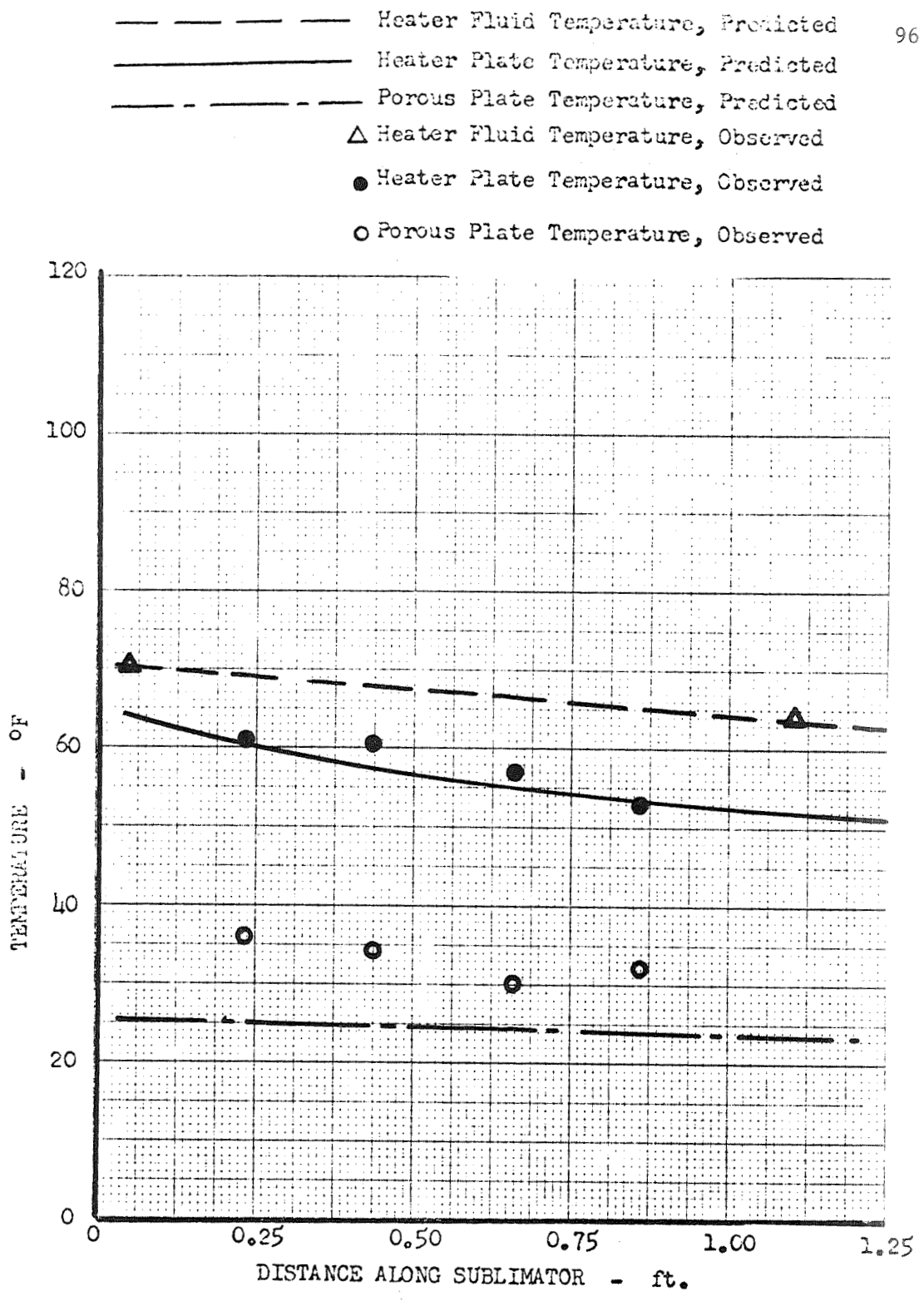
Figure 37
Test No. 8
Predicted and Observed Temperatures vs. Distance
for Fluid-Heated Units

Porous Plate: A
Heater Fluid: Water-Glycol
Flow Rate   : 25.6 Lbm/Hr
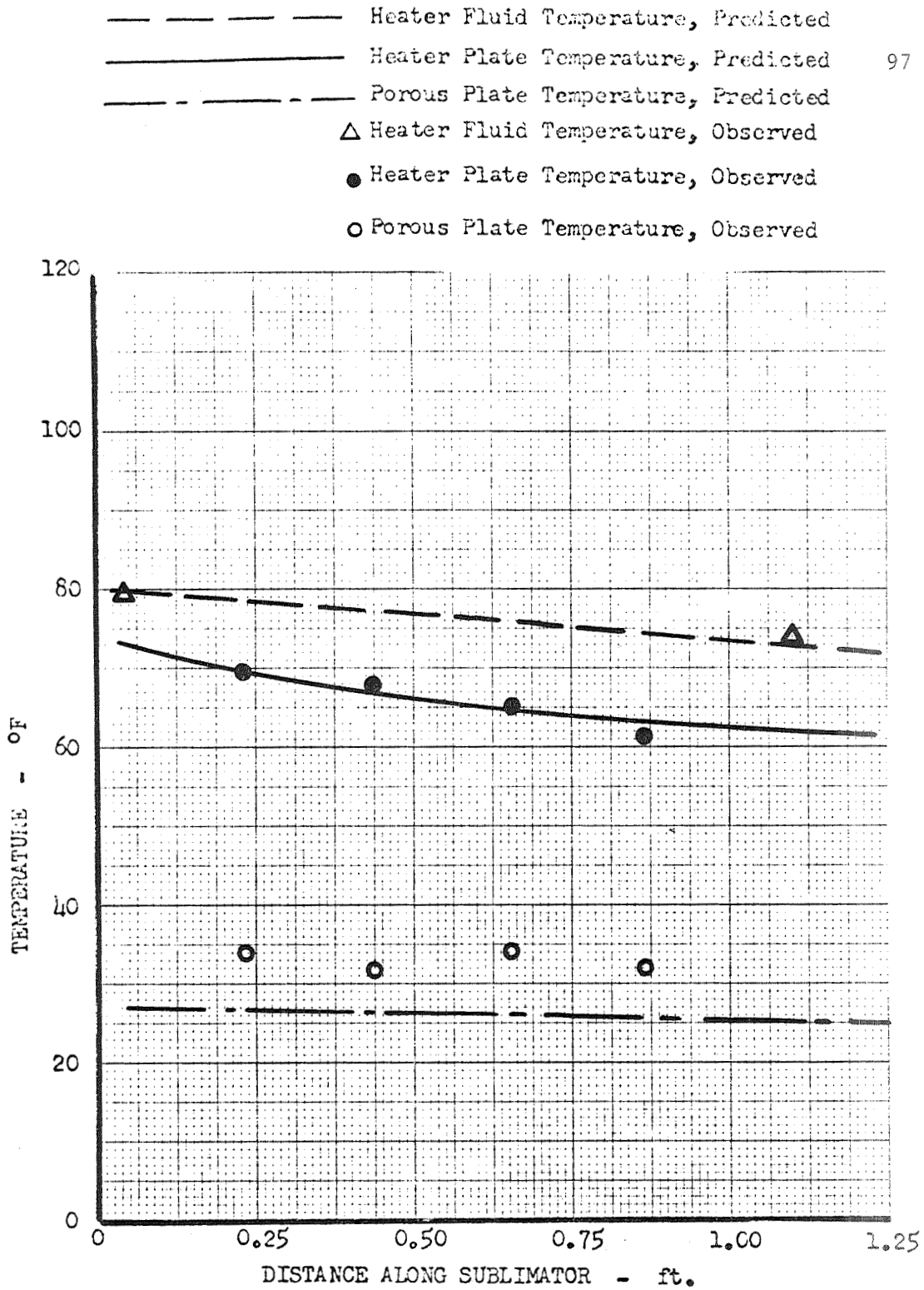
Figure 38
Test No. 9
Predicted and Observed Temperatures vs. Distance
for Fluid-Heated Units

Porous Plate: A
Heater Fluid: Water-Glycol
Flow Rate : 26.8 Lbm/hr
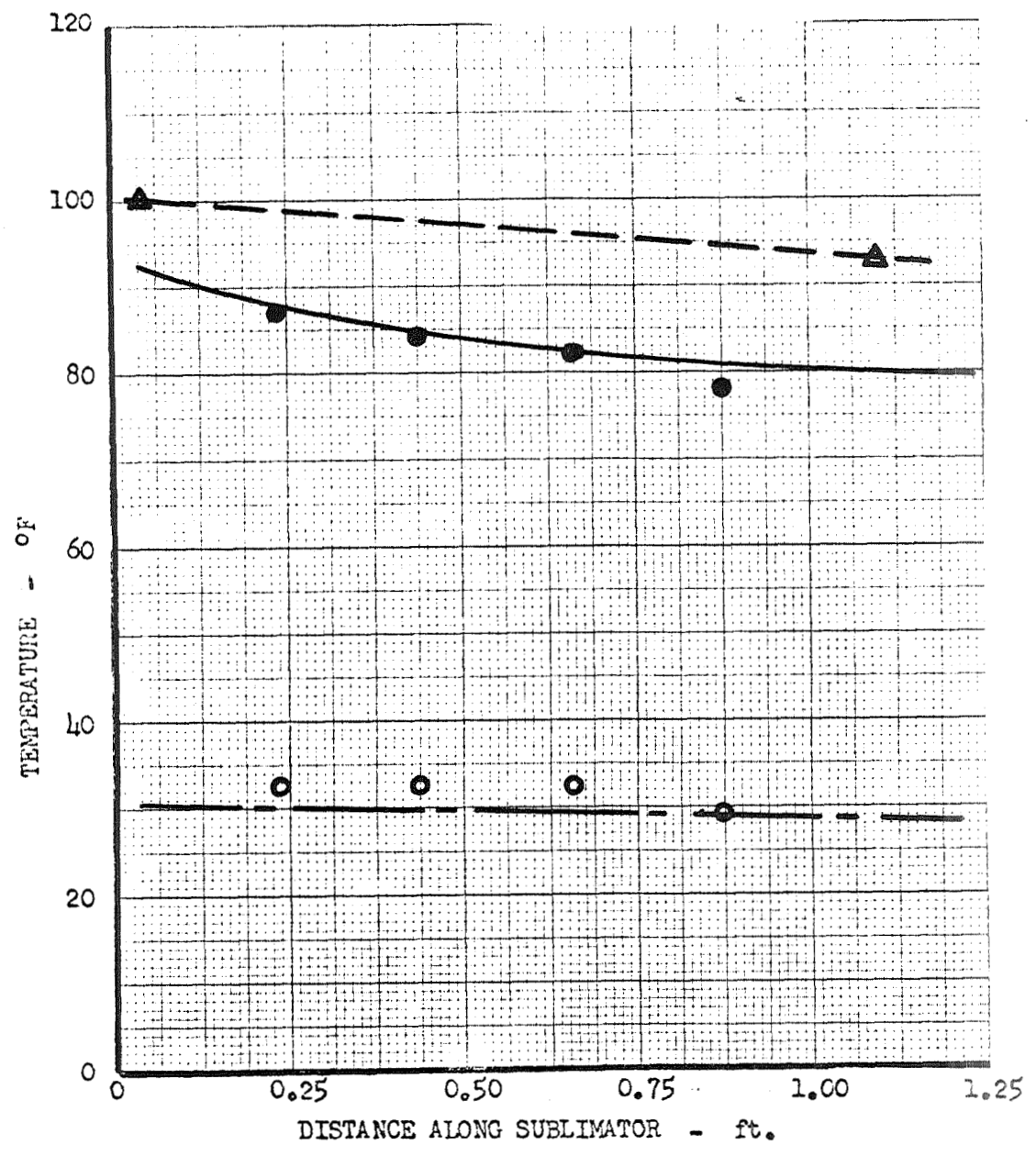
Figure 39
Test No. 10
Predicted and Observed Temperatures vs. Distance
for Fluid-Heated Units

Porous Plate: A
Heater Fluid: Water-Glycol
Flow Rate : 32.3 Lbm/HR
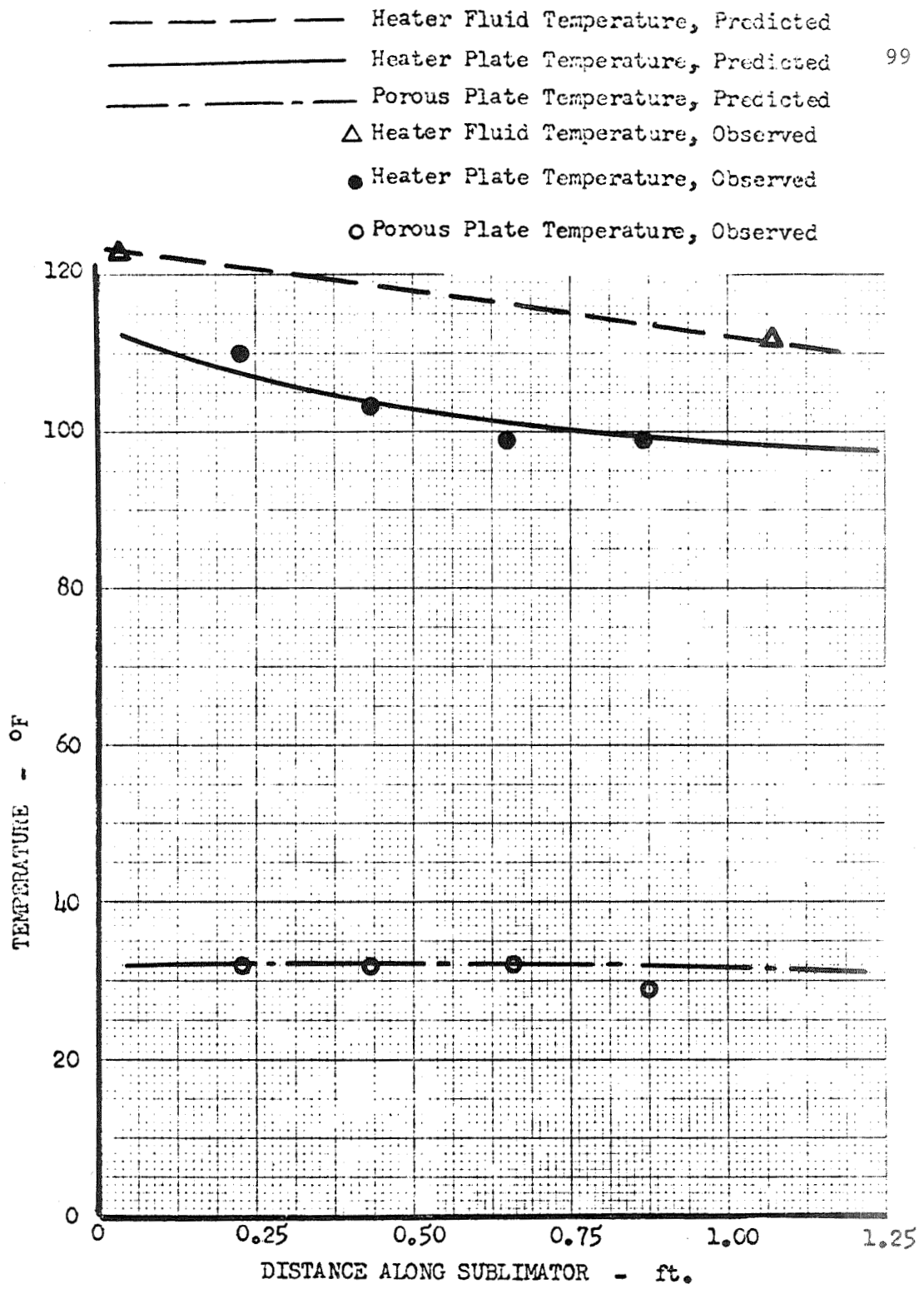
Figure 40
Test No. 11
Predicted and Observed Temperatures vs. Distance
for Fluid-Heated Units

Porous Plate: A
Heater Fluid: Water-Glycol
Flow Rate   : 29.0 Lbm/Hr
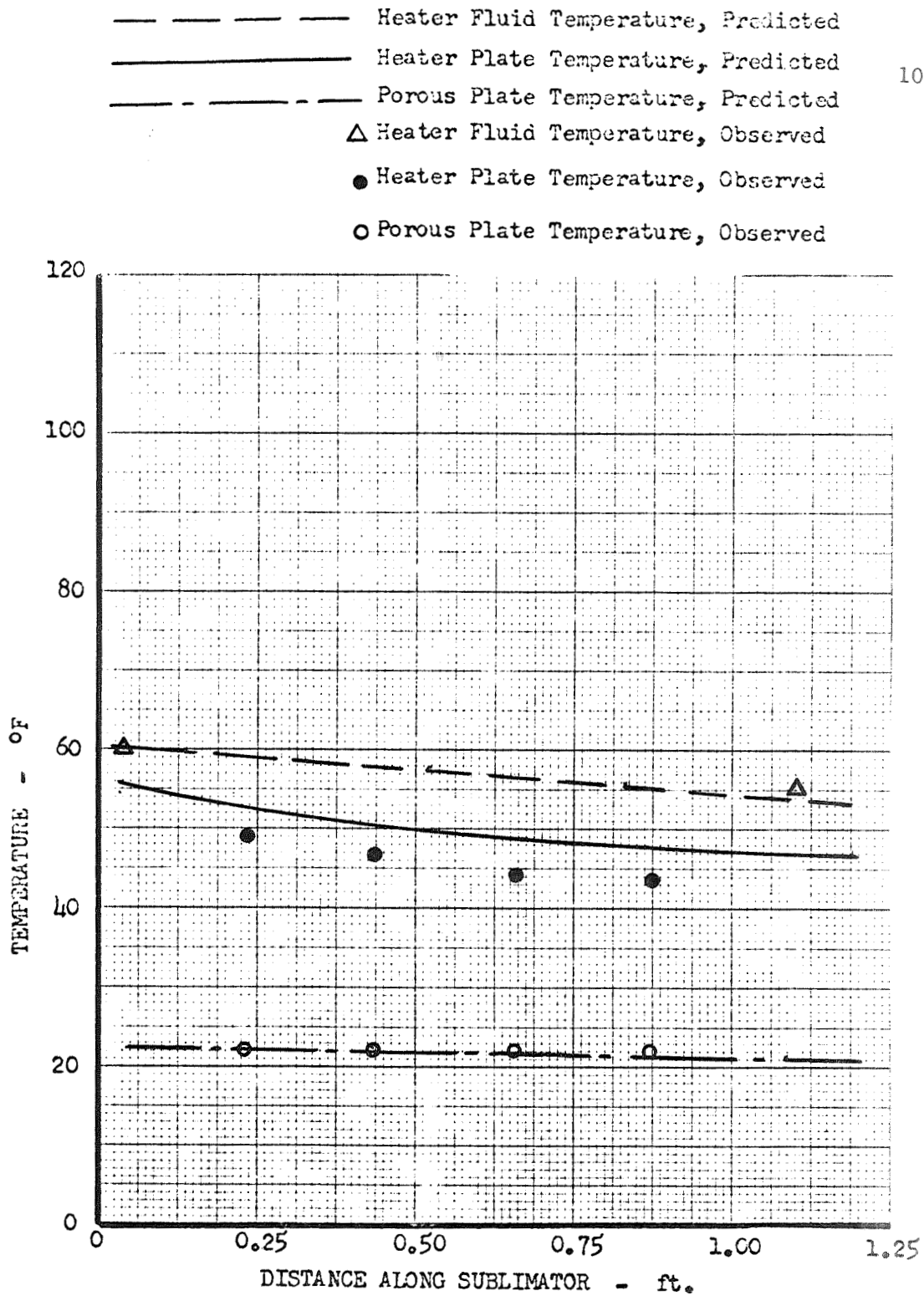
Figure 41
Test No. 12
Predicted and Observed Temperatures vs. Distance
for Fluid-Heated Units

Porous Plate: B
Heater Fluid: Water
Flow Rate   : 21.1 Lbm/Hr
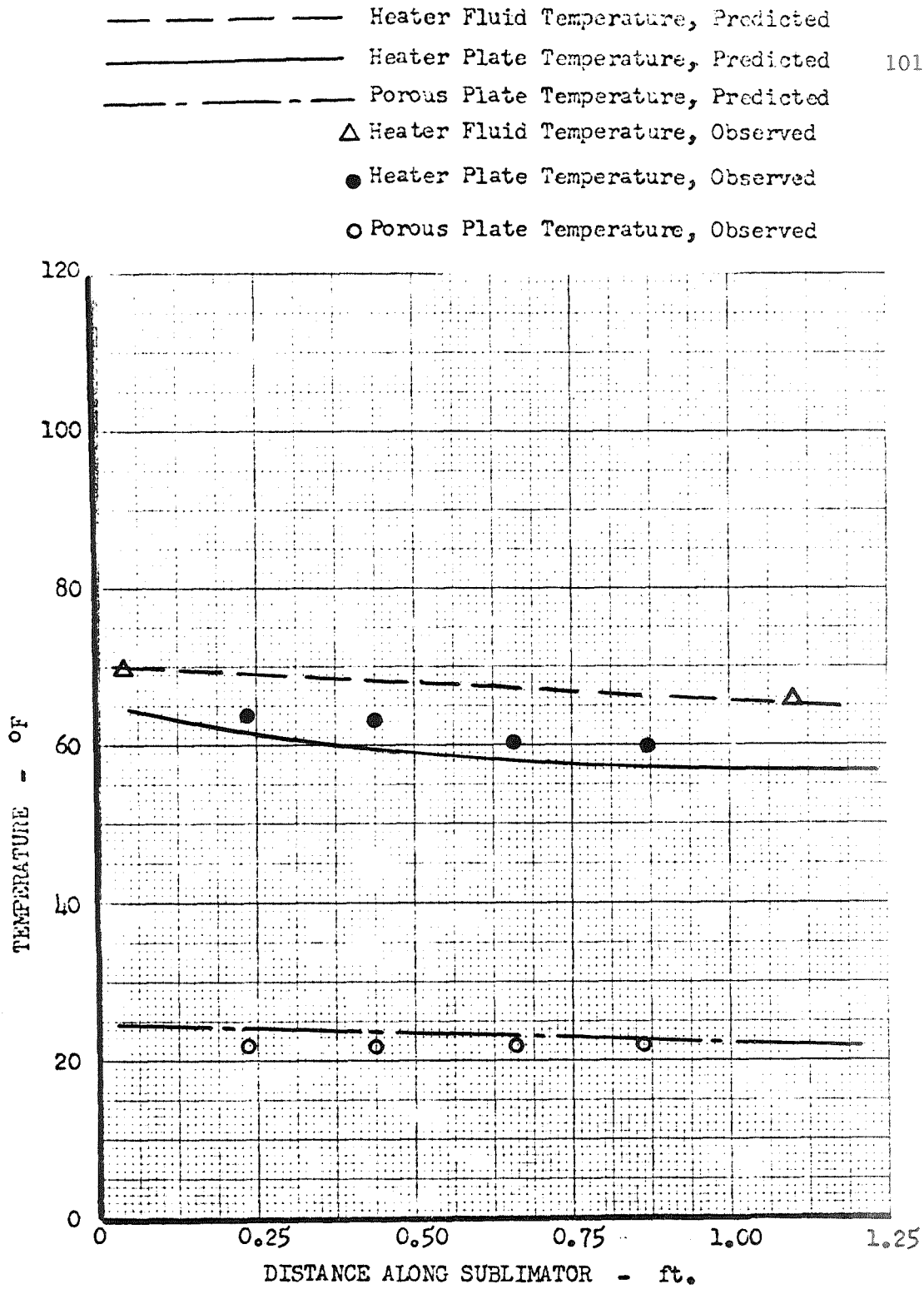
Figure 42
Test No. 13
Predicted and Observed Temperatures vs. Distance
for Fluid-Heated Units

Porous Plate: B
Heater Fluid: Water
Flow Rate   : 31.9 Lbm/Hr

— — — — Heater Fluid Temperature, Predicted

———————— Heater Plate Temperature, Predicted

— — — — Porous Plate Temperature, Predicted

△ Heater Fluid Temperature, Observed

● Heater Plate Temperature, Observed

○ Porous Plate Temperature, Observed
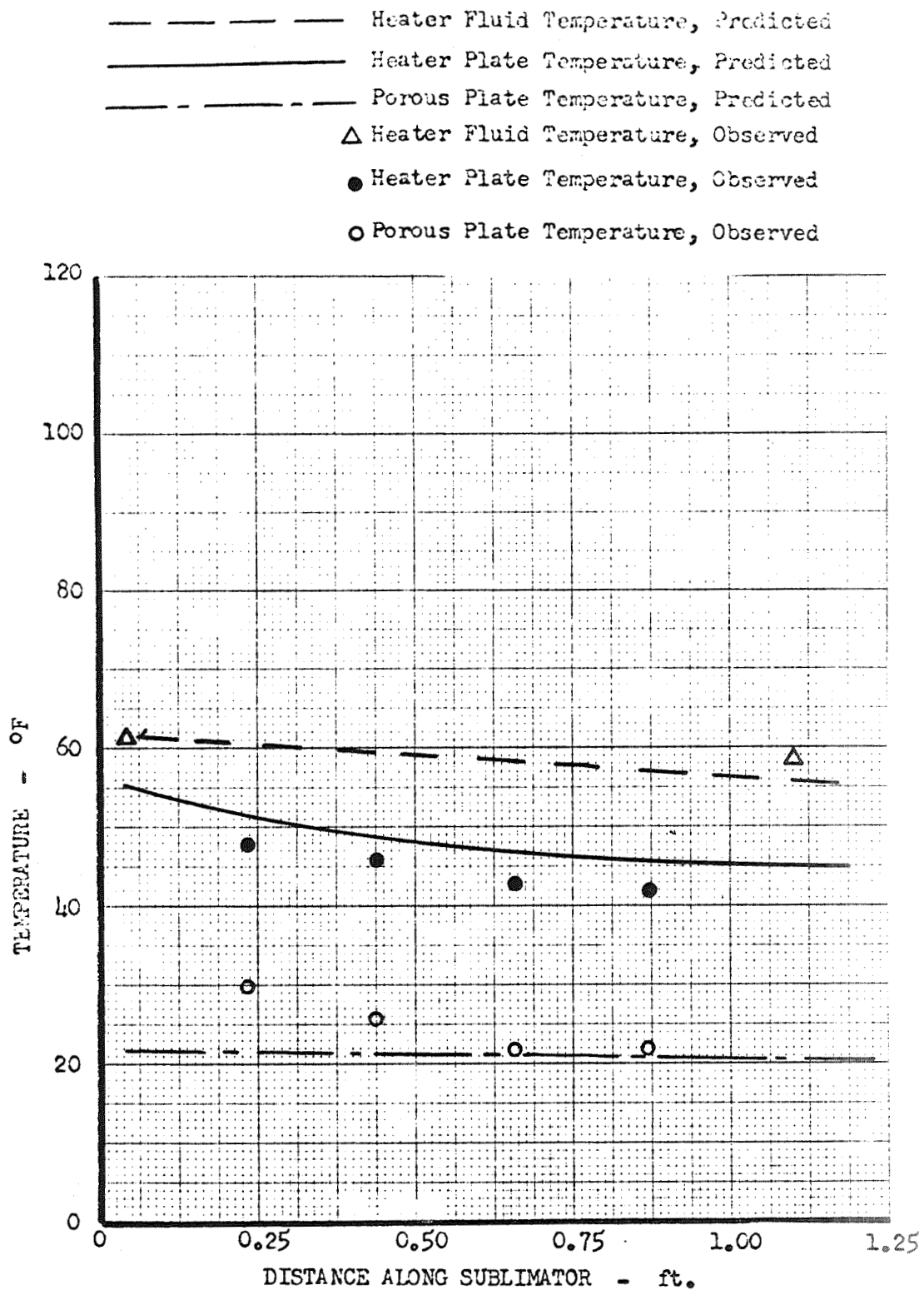
Figure 43
Test No. 14
Predicted and Observed Temperatures vs. Distance
for Fluid-Heated Units

Porous Plate: B
Heater Fluid: Water-Glycol
Flow Rate   : 43.5 Lbm/Hr
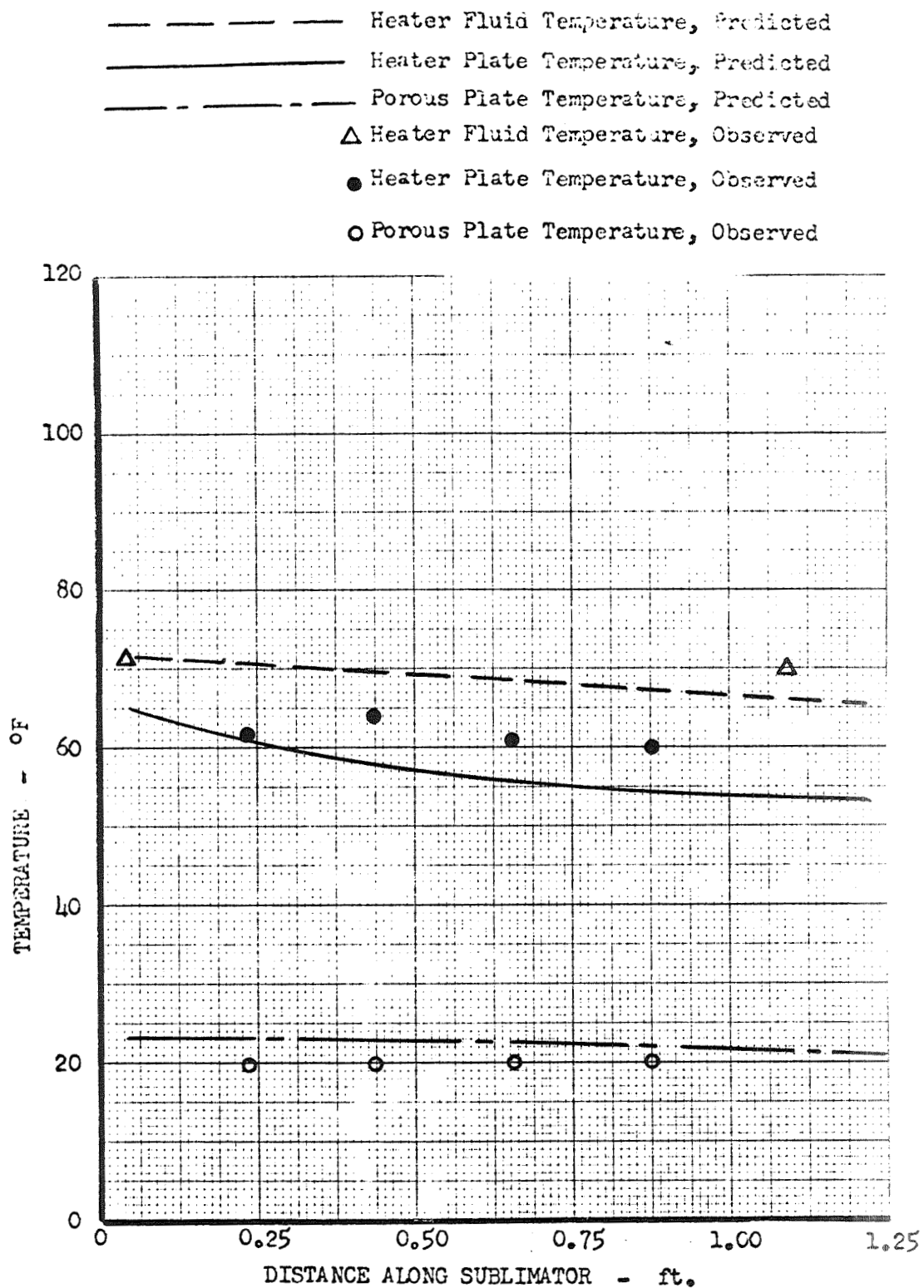
Figure 44
Test No. 15
Predicted and Observed Temperatures vs. Distance
for Fluid-Heated Units

Porous Plate: B
Heater Fluid: Glycol
Flow Rate : 34.8 Lbm/Hr

── ── ── ── Heater Fluid Temperature, Predicted

───────────── Heater Plate Temperature, Predicted

── ─ ── ─ ── Porous Plate Temperature, Predicted

△ Heater Fluid Temperature, Observed

● Heater Plate Temperature, Observed

○ Porous Plate Temperature, Observed
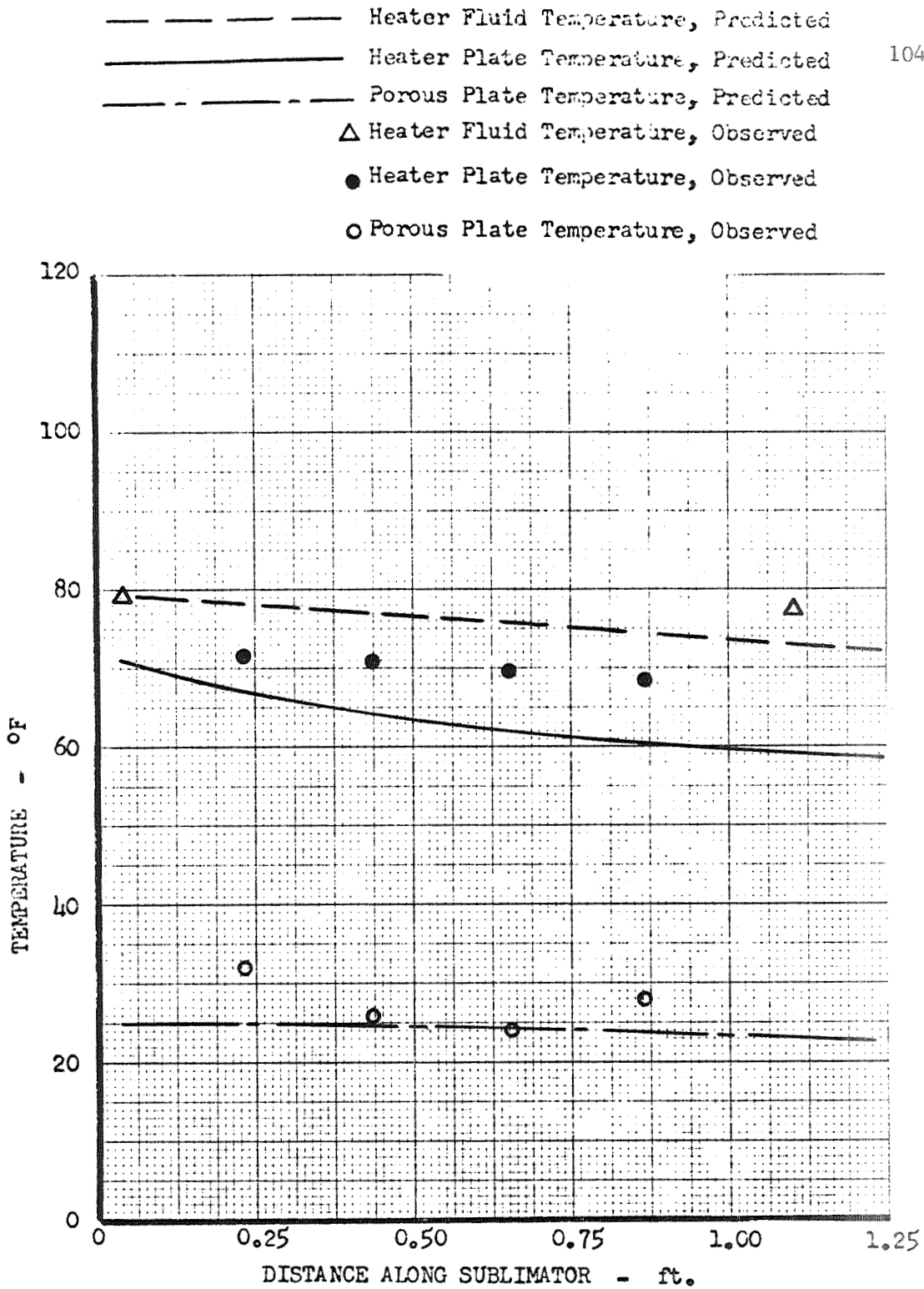
Figure 45
Test No. 16
Predicted and Observed Temperatures vs. Distance
for Fluid-Heated Units

Porous Plate: B
Heater Fluid: Water-Glycol
Flow Rate   : 32.2 Lbm/Hr
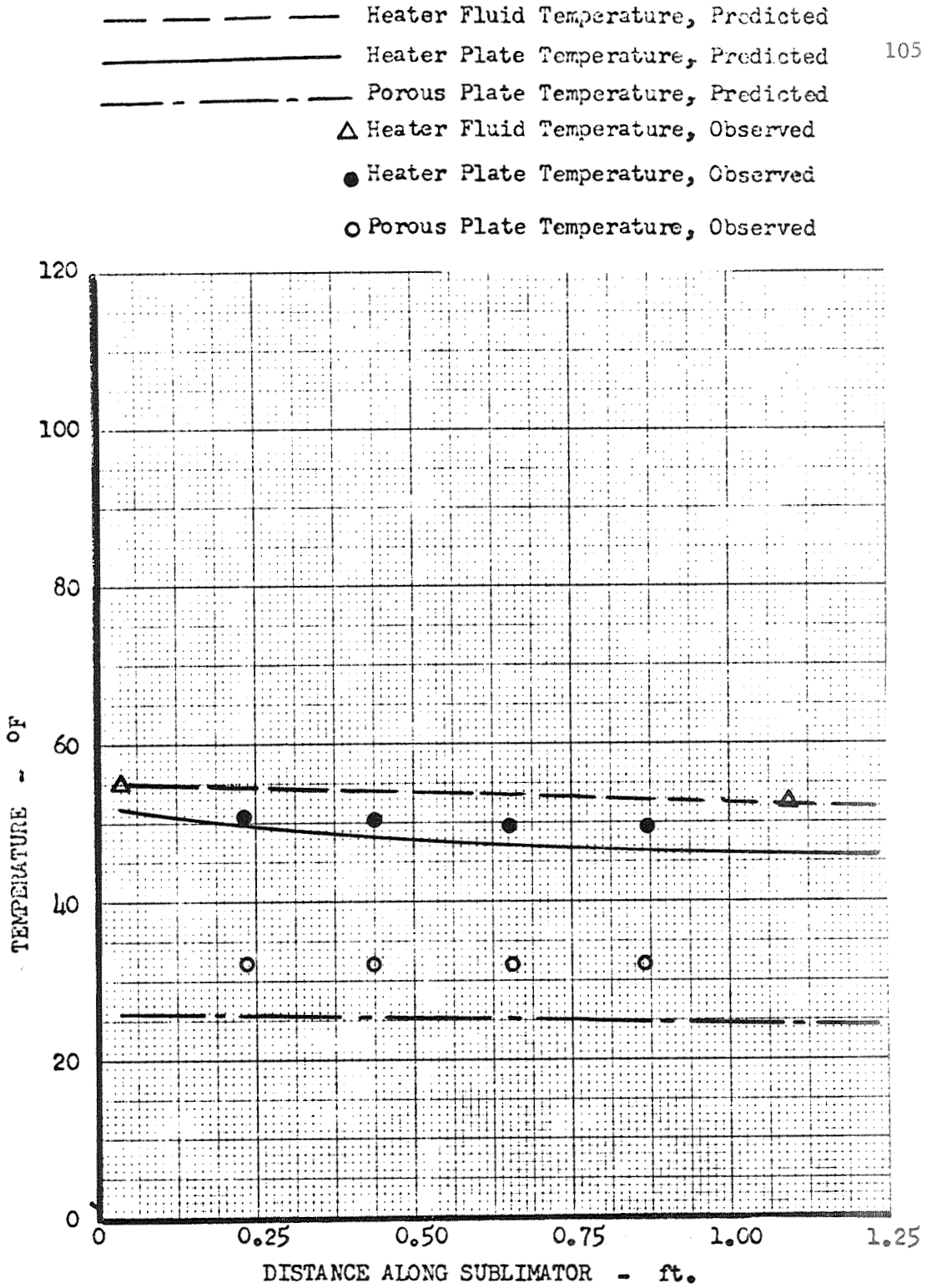
Figure 46
Test No. 17
Predicted and Observed Temperatures vs. Distance
for Fluid-Heated Units

Porous Plate: C
Heater Fluid: Water
Flow Rate   : 28.8 Lbm/Hr
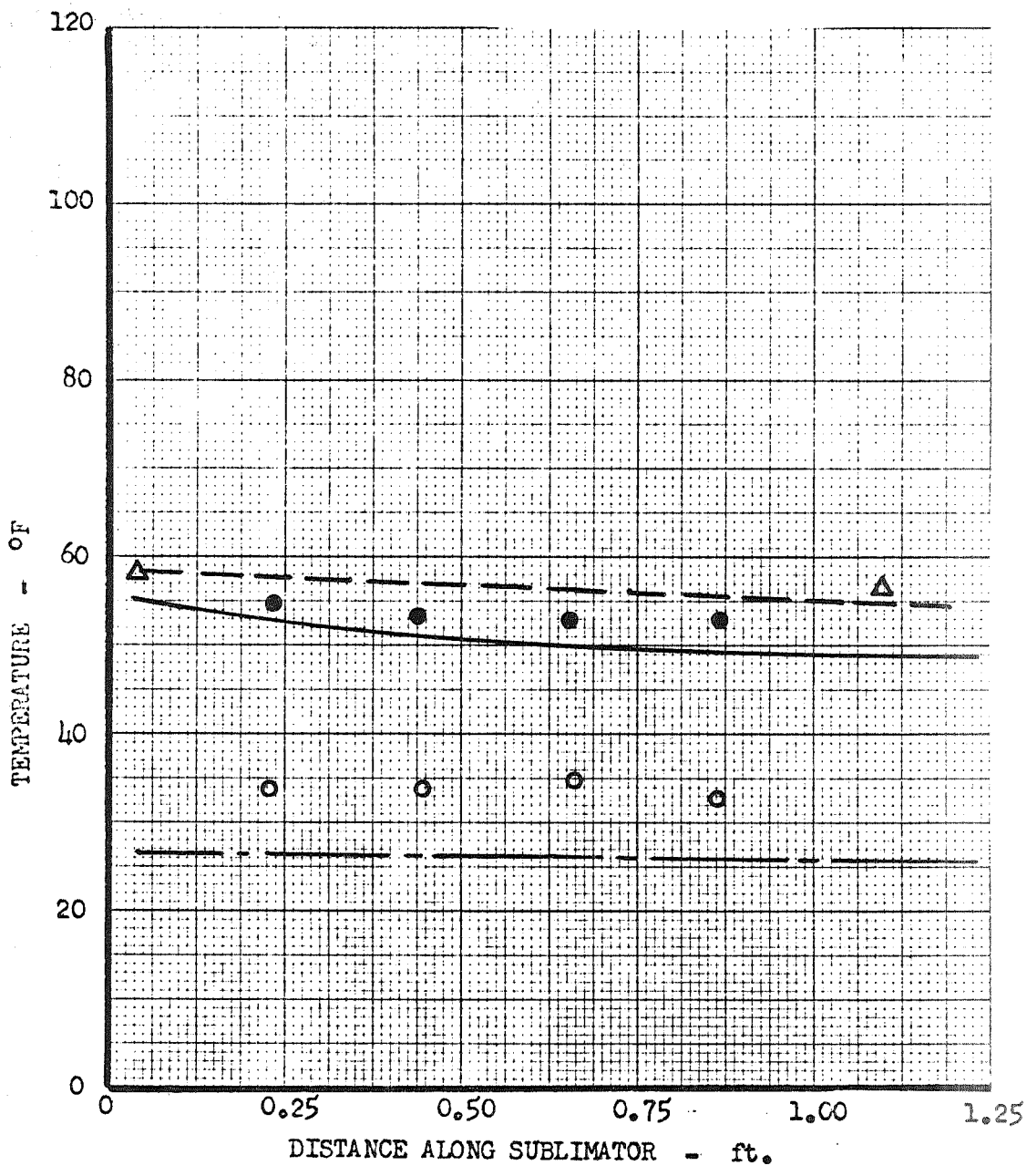
Figure 47
Test No. 18
Predicted and Observed Temperatures vs. Distance
for Fluid-Heated Units

Porous Plate: C
Heater Fluid: Water
Flow Rate   : 29.4 Lbm/Hr
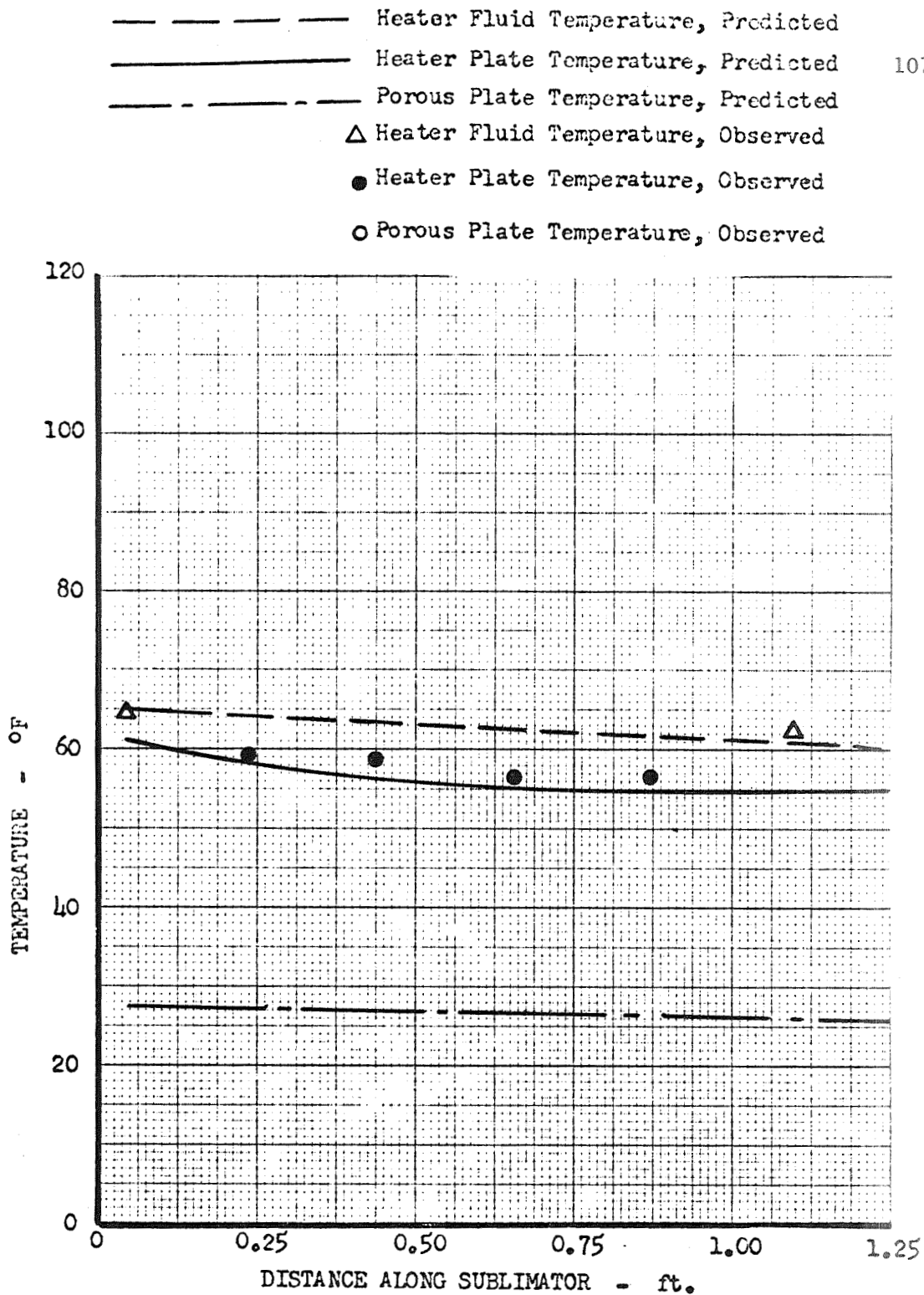
Figure 48
Test No. 19
Predicted and Observed Temperatures vs. Distance
for Fluid-Heated Units

Porous Plate: C
Heater Fluid: Water
Flow Rate   : 24.4 Lbm/Hr

— — — — — — Heater Fluid Temperature, Predicted
———————— Heater Plate Temperature, Predicted
— - — - — - Porous Plate Temperature, Predicted
△ Heater Fluid Temperature, Observed
● Heater Plate Temperature, Observed
○ Porous Plate Temperature, Observed
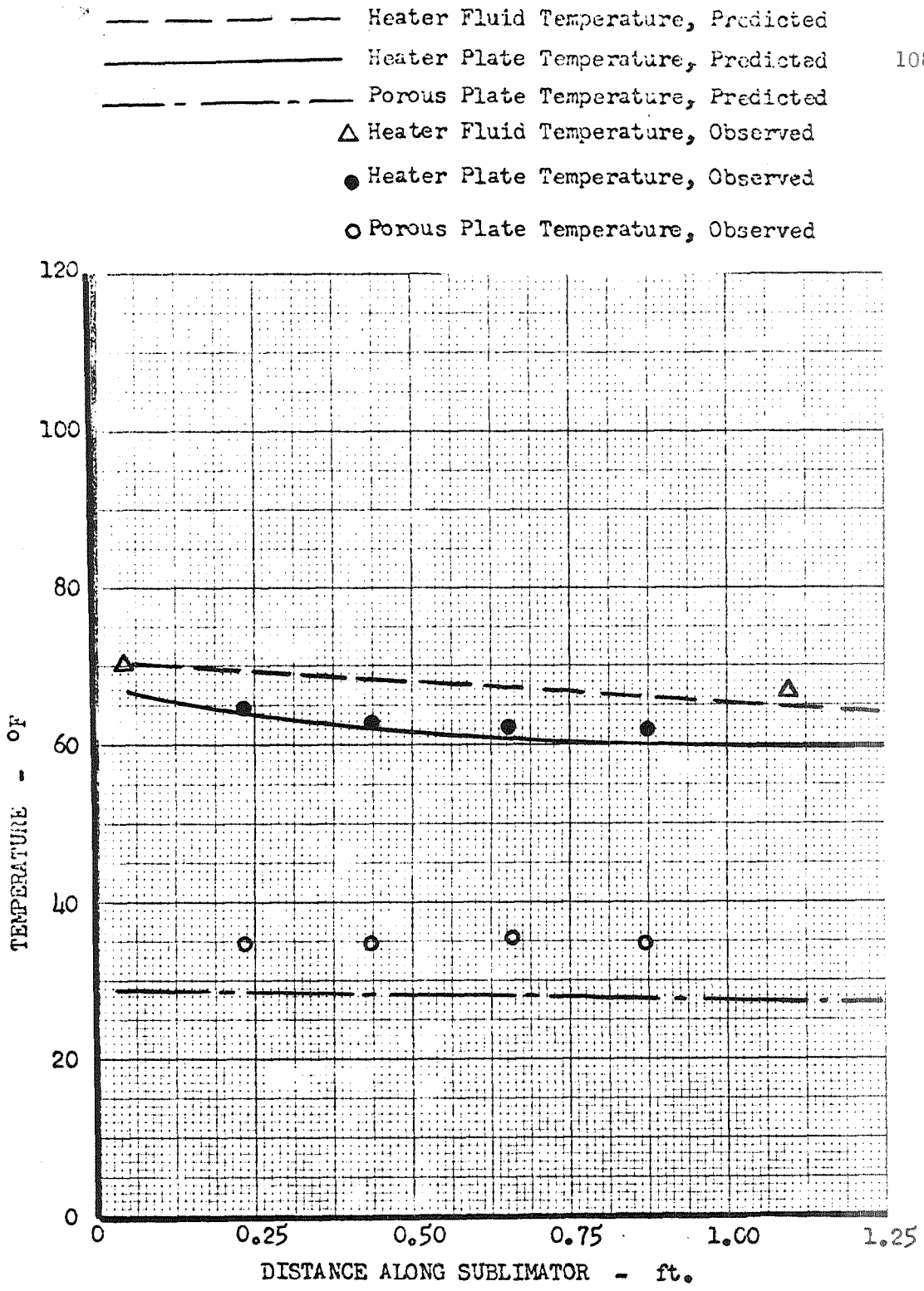
Figure 49
Test No. 20
Predicted and Observed Temperatures vs. Distance
for Fluid-Heated Units

Porous Plate: C
Heater Fluid: Water
Flow Rate   : 24.1 Lbm/Hr
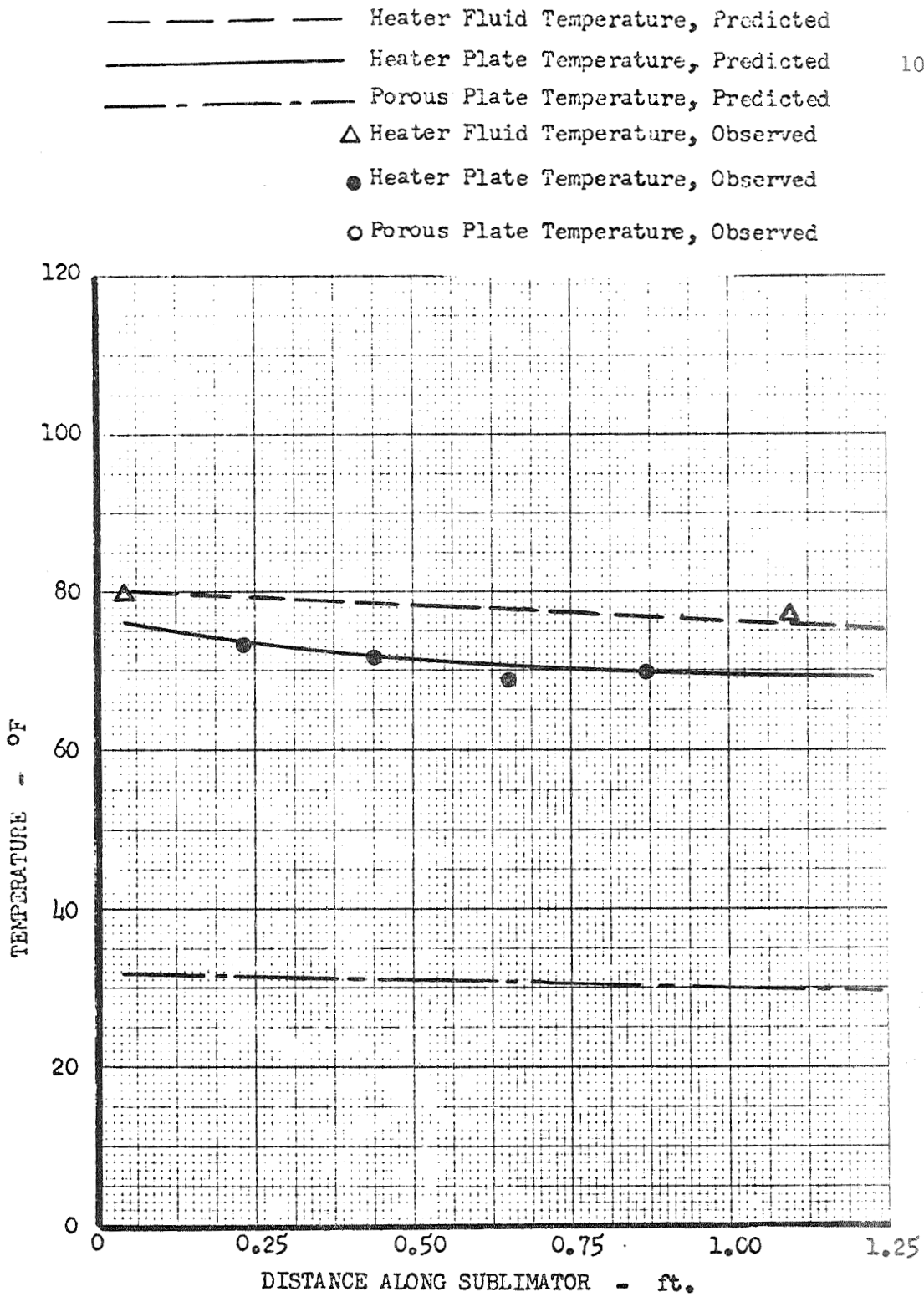
Figure 50
Test No. 21
Predicted and Observed Temperatures vs. Distance
for Fluid-Heated Units

Porous Plate: C
Heater Fluid: Water
Flow Rate   : 31.7 Lbm/Hr
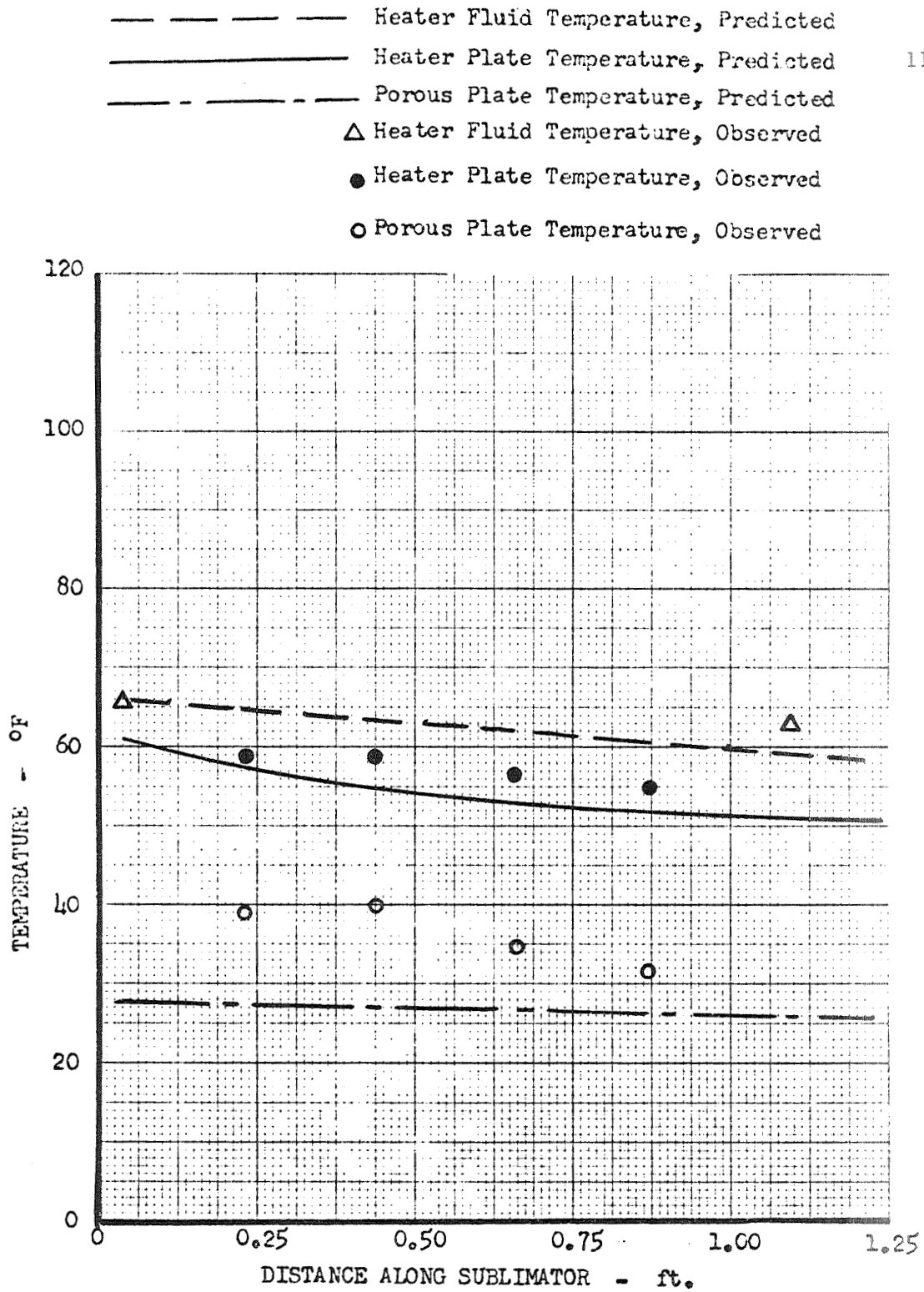
Figure 51
Test No. 22
Predicted and Observed Temperatures vs. Distance
for Fluid-Heated Units

Porous Plate: C
Heater Fluid: Water-Glycol
Flow Rate   : 33.5 Lbm/Hr
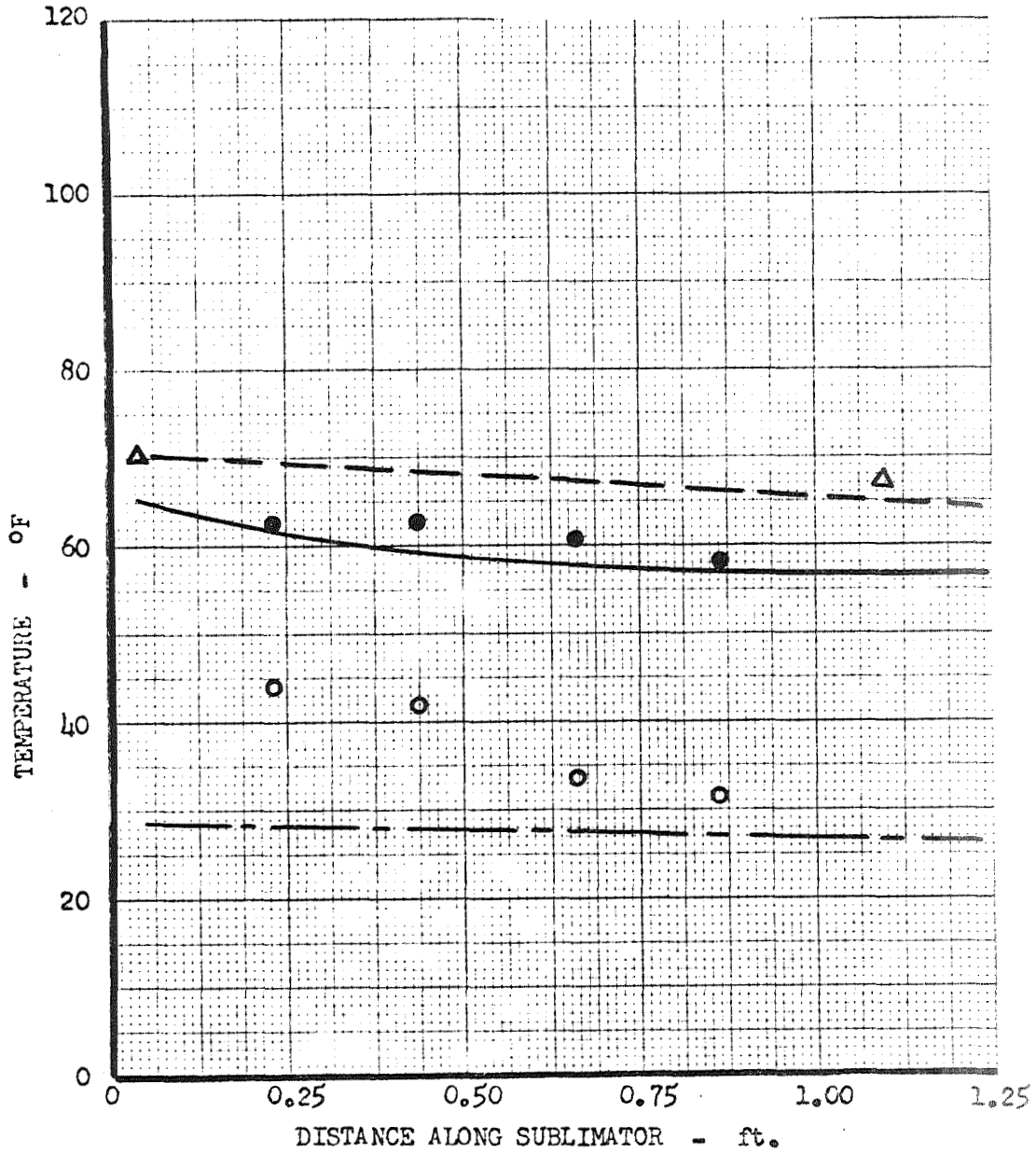
Figure 52
Test No. 23
Predicted and Observed Temperatures vs. Distance
for Fluid-Heated Units

Porous Plate: C
Heater Fluid: Water-Glycol
Flow Rate   : 33.5 Lbm/Hr
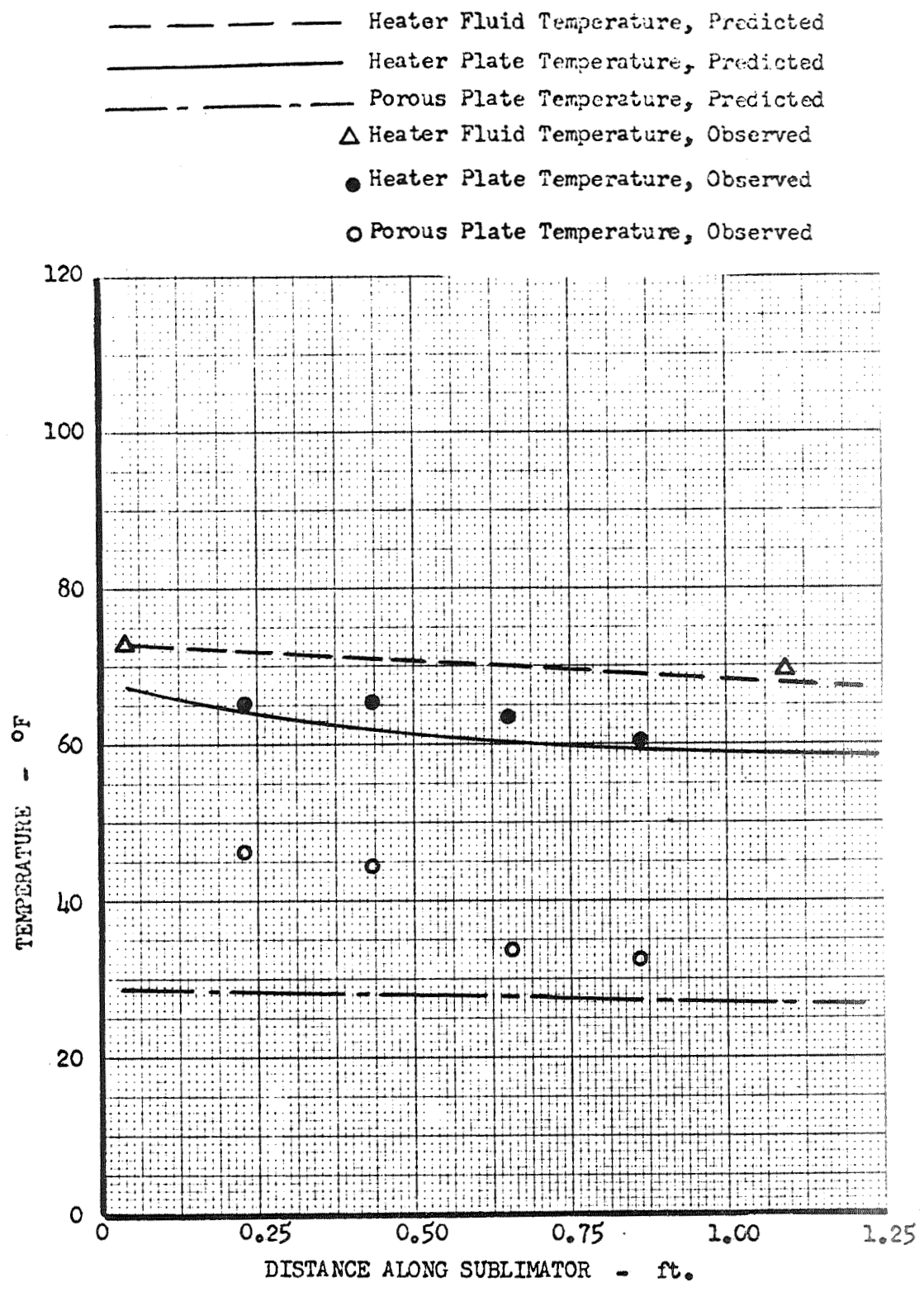
Figure 53
Test No. 24
Predicted and Observed Temperatures vs. Distance
for Fluid-Heated Units

Porous Plate: C
Heater Fluid: Water-Glycol
Flow Rate : 33.5 Lbm/Hr
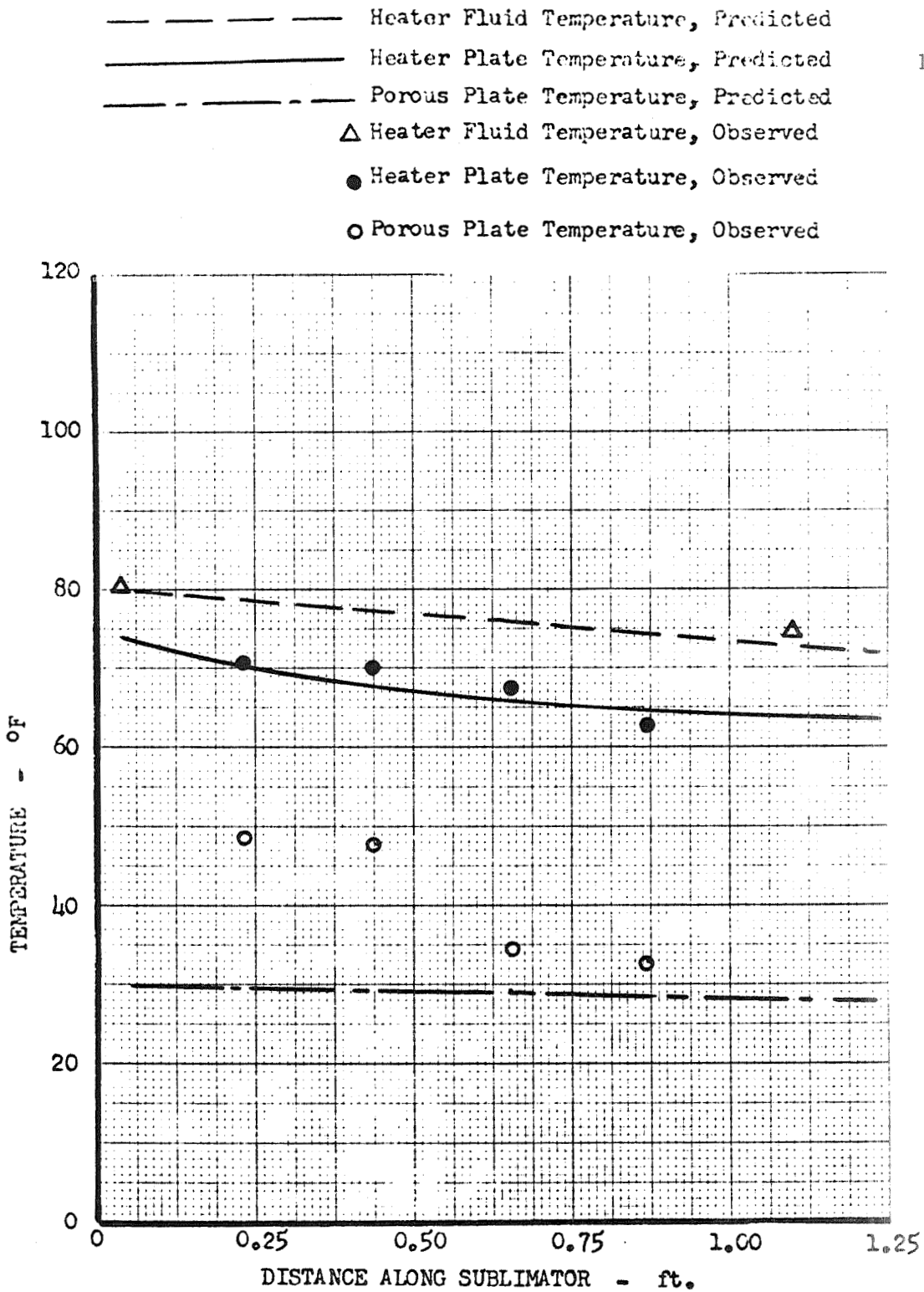
Figure 54
Test No. 25
Predicted and Observed Temperatures vs. Distance
for Fluid-Heated Units

Porous Plate: C
Heater Fluid: Water-Glycol
Flow Rate   : 22.2 Lbm/Hr
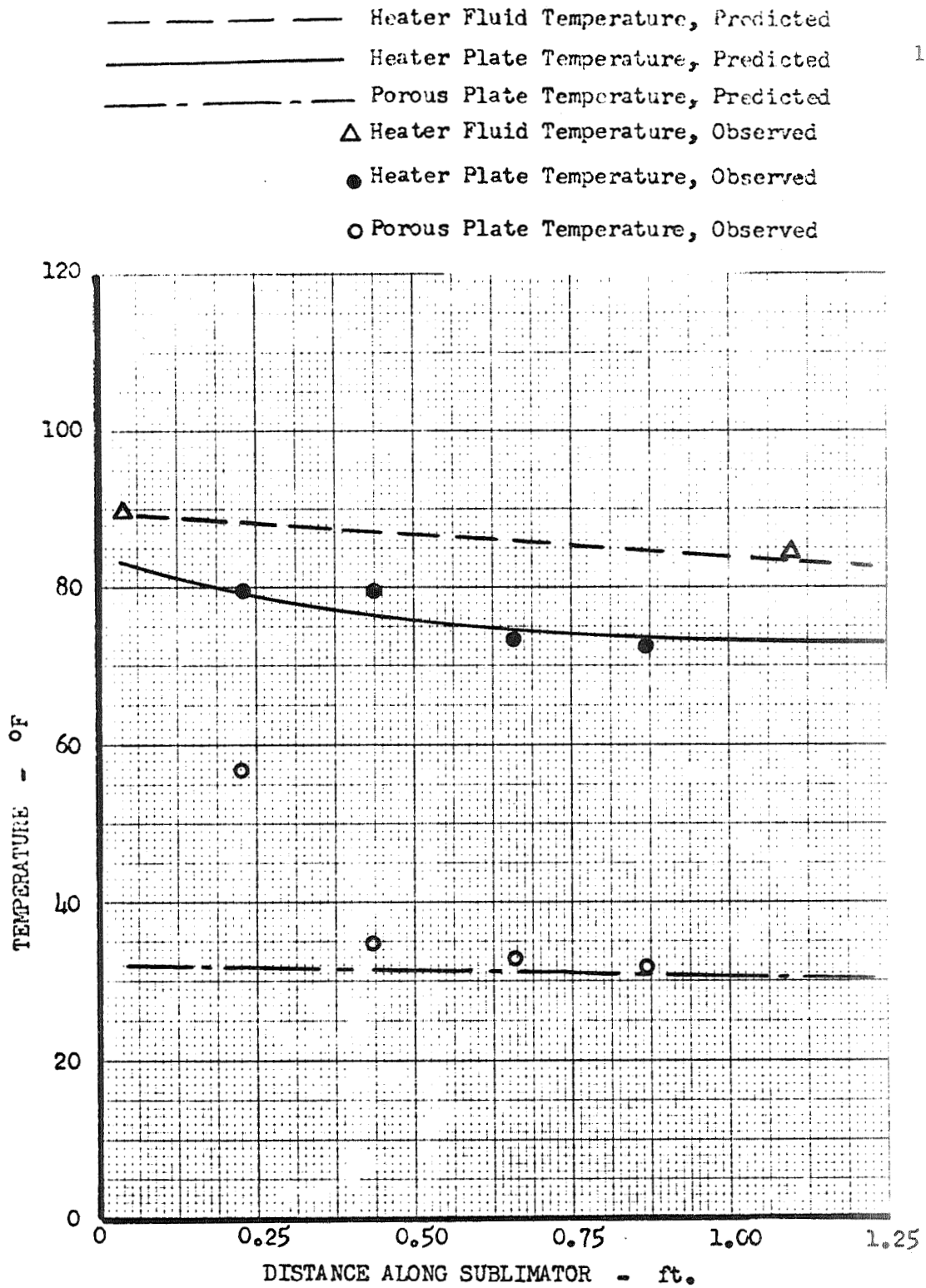
Figure 55
Test No. 26
Predicted and Observed Temperatures vs. Distance
for Fluid-Heated Units

Porous Plate: C
Heater Fluid: Water-Glycol
Flow Rate   : 32.2 Lbm/Hr
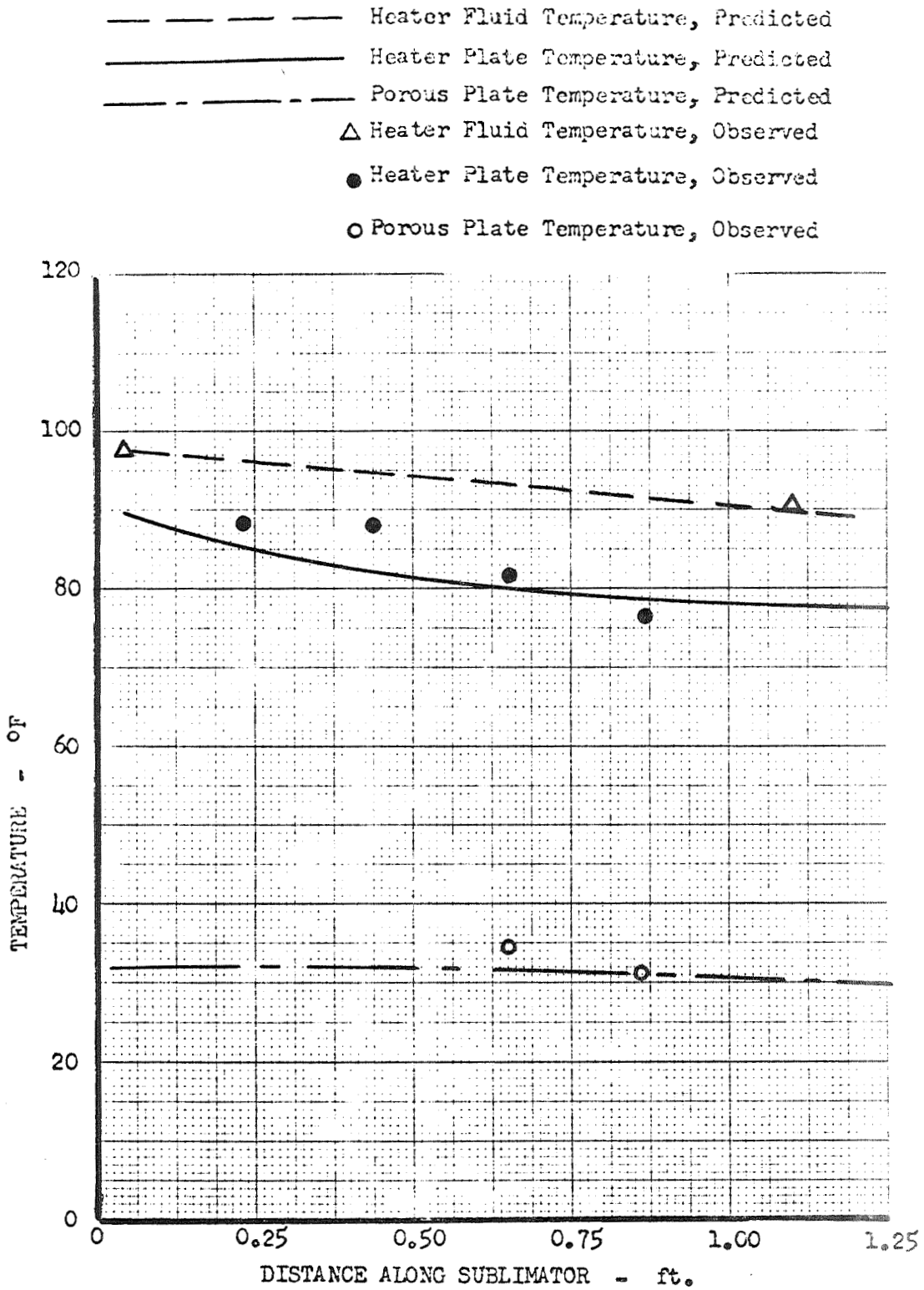
Figure 56
Test No. 27
Predicted and Observed Temperatures vs. Distance
for Fluid-Heated Units

Porous Plate: C
Heater Fluid: Water-Glycol
Flow Rate   : 27.2 Lbm/Hr
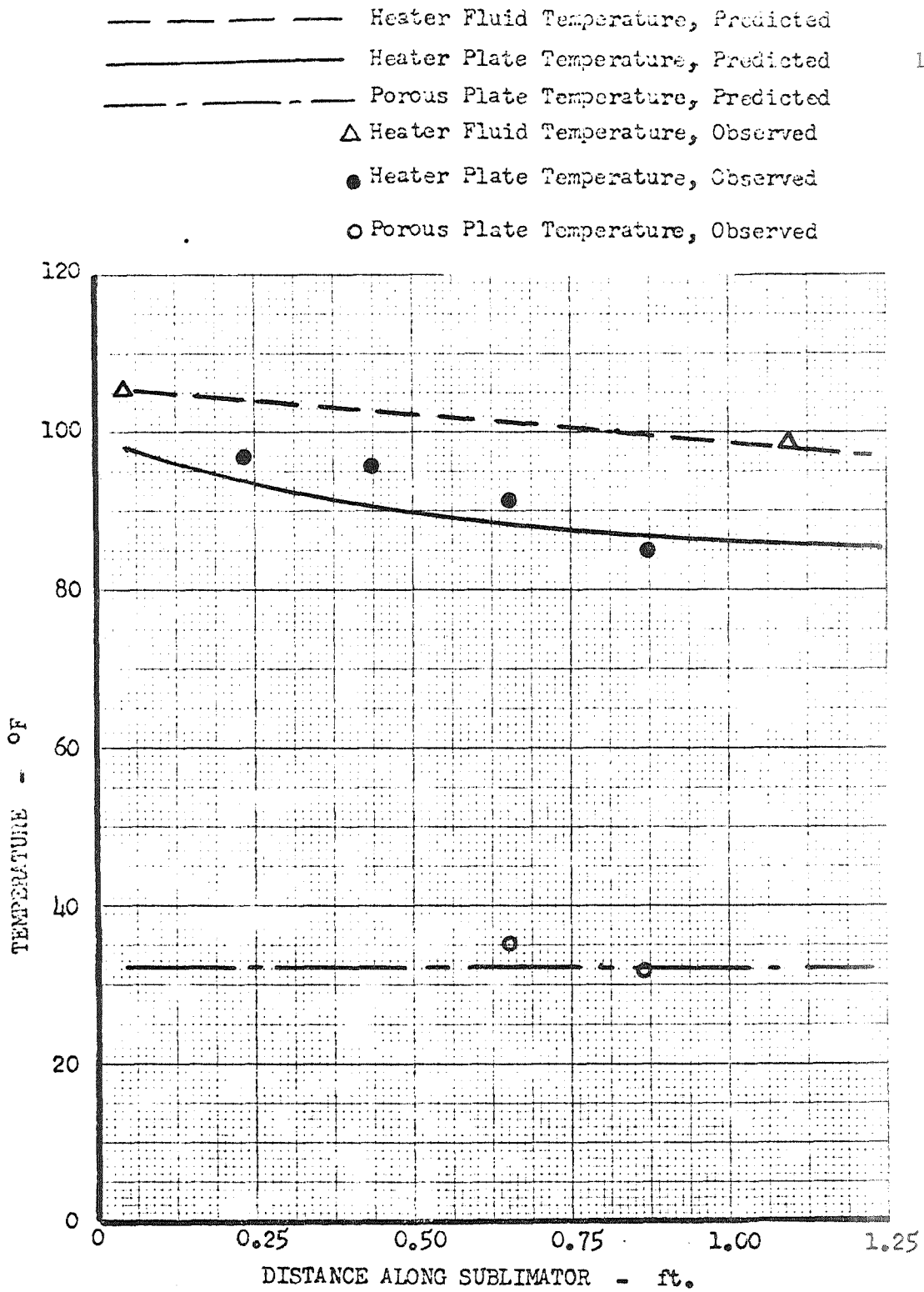
Figure 57
Test No. 28
Predicted and Observed Temperatures vs. Distance
for Fluid-Heated Units

Porous Plate: C
Heater Fluid: Water-Glycol
Flow Rate   : 29.0 Lbm/Hr

APPENDIX I

Bubble Point Test

This section presents the method used to determine the
size of the largest opening in a flat porous plate. Procedure
to gain information concerning the distribution of pore sizes
is also presented.

A schematic of the apparatus used is shown in Figure 18.

The inlet line carried dry shop air. This air was filter-
ed through a 0.45 micron absolute filter (Gleman # Green 6N).
Needle valves (Whitey #IVS4) were used in the line to control the
flow. A low range pressure regulator (Matheson model # 70) with
an out-put pressure range from 0-5 psi was used to regulate the
pressure in the test chamber.

The test chamber consisted of a square phenolic cavity
with a phenolic clamp which was used to hold the porous plate in
place. The pressure in the test sample was measured using a
mercury manometer.

The test procedure was initiated by soaking the plate
to be tested in alcohol for at least 15 minutes. The plate
was then removed from the alcohol and clamped in the test chamber.
A thin layer of alcohol, a few millimeters thick, was poured
on the top side of the plate. The pressure in the cavity was
then increased slowly using the pressure regulator.

The pressure at which the first bubble broke through
was recorded in mm Hg. This pressure can be related to the
diameter of the largest pore since it would release bubbles
first.

The test was continued by increasing the air pressure
until 50% of the plate surface was bubbling using the best
visual estimate. This pressure was recorded in mm Hg.

Because alcohol forms a contact angle of essentially
zero with nickel, the pressure differences which caused

breakthrough and 50% coverage can be related to the maximum pore size and median pore size. This is done using

$$\text{(I-1)} \qquad D = \frac{4\sigma}{\Delta P}$$

For alcohol, the value of surface tension σ is 1.292 X 10^{-4} lbs/in.

The data from the bubble tests on the plates is presented in Table 1.

APPENDIX II

Cyclic Sublimation Mode in a Perfect Insulator

The cyclic mechanism in each pore can be considered if the plate material is a perfect insulator. As stated in Section III, the cyclic sublimation mode occurs when the plate material is hydrophilic and the heat flow rate is such that no ice can exist behind the porous plate. Thus water can enter the pores, freeze, and then sublimate from the down stream end of the pores. The sublimation interface recedes in a pore and the vapor pressure at the interface increases. This process continues until all of the ice is sublimed or the vapor pressure goes above the triple point pressure. When this happens, the ice will melt and the water will enter the pore. Thus the cycle is completed and initiated again.

If the ice fills a large fraction of a pore, the sublimation part of the cucle will be large compared to the filling and freezing parts. The filling time will be short since the water must only flow into the pore. The melting time will be small compared to the sublimation time since the heat required to melt a given quantity of ice is one-seventh the heat required to sublimate it. Because of this, only the recession of the subli-mation interface will be analyzed. The equations governing the temperature as a function of time and position in a pore will be formulated. One pore will be analyzed with the idea that the total effect could be obtained by adding the influence of each pore with some appropriate phase angle included for each pore.

A side view of a pore during the sublimation part of the cycle is shown in Figure 4. In this figure, the scale of the diameter to length is greatly exaggerated. This pore can be modeled as a slab of material with freezing and sublimating interfaces. An equation must be written for each phase of the

slab; thus

$$(\text{II-1}) \quad \alpha_w \frac{\partial^2 T}{\partial x^2} = \frac{\partial T}{\partial t}, \quad 0 < x < f(t)$$

and

$$(\text{II-2}) \quad \alpha_I \frac{\partial^2 T}{\partial x^2} = \frac{\partial T}{\partial t}, \quad f(t) < x < S(t)$$

The boundary conditions are

$$(\text{II-3}) \quad q_o \Big/ \sum_i n_i \frac{\pi D_i^2}{4} = q_{am} = -k_w \frac{\partial T}{\partial x} \quad at \quad x = 0$$

and

$$(\text{II-4}) \quad T = T_s \quad at \quad x = S(t)$$

The energy relations at the interfaces are

$$(\text{II-5}) \quad k_w \frac{\partial T^-}{\partial x} - k_I \frac{\partial T^+}{\partial x} = -\rho_w \Delta H_f \frac{df}{dt} \quad at \quad x = f(t)$$

and

$$(\text{II-6}) \quad k_I \frac{\partial T}{\partial x} = \rho_I \Delta H_s \frac{dS}{dt} \quad at \quad x = S(t)$$

The temperature at the water ice interface is also known.

$$(\text{II-7}) \quad T = T_f \quad at \quad x = f(t)$$

In this formulation, it is assumed that no heat is trans-
ferred to the water-ice cylinder from the plate.

The temperature at the sublimation interface has to be
evaluated from the mass flow relationship using the free mole-
cular flow pressure drop relation from Equation (6).

The problem is terminated when $f(t) = S(t)$. This system
is complicated and a numerical approach has been undertaken.

It should be noted that some initial temperature distri-
bution must be provided before any solution can be obtained.

An explicit finite difference representation has been applied to a set of mesh points in the x, t plane where $\Delta x = h$, $\Delta t = K$ and (i,j) represents the point $x = ih$, $t = jk$.

Using the approximations

$$(\text{II-8}) \quad \left.\frac{\partial T}{\partial t}\right|_{i,j} = \frac{T(i,j+1) - T(i,j)}{K}$$

and

$$(\text{II-9}) \quad \left.\frac{\partial^2 T}{\partial x^2}\right|_{i,j} = \frac{T(i+1,j) - 2T(i,j) + T(i-1,j)}{h^2}$$

expressions for (II-1) and (II-2) become

$$(\text{II-10}) \quad T(i,j+1) = \alpha_w \frac{K}{h^2}\left[T(i+1,j) + T(i-1,j)\right] + \left(1 - 2\alpha_w \frac{K}{h^2}\right)T(i,j)$$

and
$$0 < x < f(t)$$

$$(\text{II-11}) \quad T(i,j+1) = \alpha_I \frac{K}{h^2}\left[T(i+1,j) + T(i-1,j)\right] + \left(1 - 2\alpha_I \frac{K}{h^2}\right)T(i,j)$$
$$f(t) < x < S(t)$$

The boundary conditions given by (II-3) becomes

$$(\text{II-12}) \quad T(1,j) - T(2,j) = q_{am}\frac{h}{k_w}$$

The calculation of $\frac{\partial^2 T}{\partial x^2}$ and $\frac{\partial T}{\partial t}$ at points adjacent to the water-ice interface and to the sublimation interface is done using an unequal interval finite difference approach given in Reference 3. This is an explicit method which makes computation very convenient.

Using this approach, (II-5) becomes

$$(\text{II-13}) \quad f(j+1) - f(j) = \frac{K}{h \rho_w \Delta H_f}\left[k_I\left(\frac{2v-5}{(2-v)(3-v)}T_f + \frac{3-v}{2-v}T(\ell+1,j) - \frac{2-v}{3-v}T(\ell+2,j)\right)\right.$$
$$\left. - k_w\left(\frac{v}{v+1}T(\ell-2,j) - \frac{v+1}{v}T(\ell-1,j) + \frac{2v+1}{v(v+1)}T_f\right)\right]$$

In this equation, ℓ is the x index of the last grid point before the interface is reached and N is such that vh is the distance from the $\ell-1$ grid point to the interface in the x direction.

This equation allows the position of the interface at a new time step to be calculated from the known quantities of the previous time step.

A similar expression can be written to replace (II-6), namely:

$$S(j+1) - S(j) = \frac{K k_I}{h \, \rho_I \, \Delta H_S} \left[\frac{w}{v+1} T(w-2, j) - \frac{v+1}{v} T(w-1, j) + \frac{2v+1}{v(v+1)} T_s(j) \right]$$

(II-14)

In this equation w is the x index of the last grid point before the right boundary is reached and v is such that vh is the distance from the $w-1$ grid point to the boundary in the x direction.

Using (II-14) and (6) we can write

(II-15) $$P_s(j+1) = P_a + \frac{3 \rho_I}{2 k_D} (S(j) - S(j+1))(a - S(j+1)) \sqrt{\frac{\pi R T_s(j)}{2 g_0}}$$

$T_s(j+1)$ can then be calculated using $P_s(j+1)$ and equilibrium pressure-temperature data for the sublimation of ice.

These equations allow the grid point temperatures and interface locations to be calculated from the data at the preceding time step. Thus for given initial conditions, it would seem that the system could be evaluated at later times by calculations on a digital computer.

These equations were programmed and run on the Burroughs 5500 computer at Rice University for various initial conditions. Oscillations in the sublimation temperature have occurred for all runs.

The use of an implicit boundary condition at the sublimation interface delayed the oscillation, but did not eliminate it. It is thought that an implicit formulation of the entire system might prevent the instability.

This approach was not taken, however, since it was seen that the model presented here does not represent the physical situation very well for the operation of a realistic sublimator.

Because of the large value of conductivity of the plate material, the individual pores cannot operate independently as discussed in Section III.

APPENDIX III

COMPUTER PROGRAM FOR FLUID-HEATED POROUS PLATE SUBLIMATOR

PERFORMANCE CALCULATION

```
      DIMENSION TL (10),PL (10)
      PUNCH100
100 FORMAT(18HPOROUS PLATE NO. 3)
      PUNCH99
 99 FORMAT(76H    I     Y     EMDOT    TIN      T      O
   C    TS    DELIC    H    XNGS     VX     TO)
      READ10,(TL(I),I=1, 10)
      READ11,(PL(I),I=1, 10)
 10 FORMAT(10F3.0)
 11 FORMAT(10F6.4)
C  GLYCOL PROPERTIES
      TIN=55.0
      EMDOT=28.8
      ROGLY=62.4
      ALPHA=.0056
      CONGL=.349
      CPGLY=1.0
      ENPOR=16E8
      DD=5.25E-15
      DELPP=.0060
      DIFF=.2
      BIT=.025
      N=15
C  GEOMETRIC PROPERTIES
      XTOT=1.2
      WIDTH=.167
      GLYTH=.0078
      TS=28.0
C  POROUS PLATE PROPERTIES
      T=TIN
      EN=N
      X-XTOT/EN
C  BASIC LOOP
      DO600I=1,N
C  ITERATION FOR PS
 50 J=0
 60 J=J+1
      IF(TL(J)-TS)301,302,303
301 GOTO60
302 TS=TL (J)
      P=PL(J)
      GOTO304
303 P=PL(J-1)+((TS-TL(J-1))/(TL(J)-TL(J-1)))*(PL(J)-PL(J-1))
```

COMPUTER PROGRAM FOR POROUS PLATE SUBLIMATOR

PERFORMANCE CALCULATION (CONTINUED)

```
304 Q=6.39*P*ENPOR/DELLP
    Q=Q*(10.0**6.0)
    DELIC=1.13*(32.0-TS)/Q
    TO=32.0+(.064*Q)-(3.1*(32.0-TS))
    XI=I
    Y=(XI-.5)*X
    VX=EMDOT/(ROGLY*GLYTH*WIDTH)
    XNGZ=(ALPHA*Y)/(VX&GLYTH*GLYTH)
    IF(XNGZ-.04)17,17,18
 17 XNUS=((VX*GLYTH*GLYTH)/(ALPHA*Y))**.333
    GOTO19
 18 XNUS=2.43
 19 H=(XNUS*CONGL)/GLYTH
    RP=1.0/H
    TSTAR=TO+(RP*Q)
    IF(ABS(TSTAR-T)-DIFF)401,401,402
402 IF(TSTAT-T)501,501,502
502 IF(TS-31.99)702,702,701
702 TS=TS+BIT
    GOTO50
501 TS=TS-BIT
    GOTO50
701 TS=32.0
    Q=T-32.0)/RP+.064)
    TO=T-RP*Q
    P=.0001
830 DELIC=1.13*(32.0-TS/Q
401 PUNCH41,I,Y,EMDOT,TIN,T,Q,TS,DELIC,H,XNGZ,VX,TO
 41 FORMAT(I4,F7.3,F5.1,2F7.1,F8.2,F6.2,F6.4,F7.5,F8.2,
    CF7.1)
    T=T-((Q*WIDTH*X)/(EMDOT*CPGLY))
600 CONTINUE
    STOP
    END
0.05.010.15.20.25.30.32.
 .0105 .0240 .0309 .0396 .0505 .0641 .0808 .0886
```